THE CONCENTRATION, TRANSPORT AND FATE OF NITROGEN OXIDES IN THE HIGHVELD ATMOSPHERE

by

Refilwe Faith Kai-Sikhakhane
(741786)

A thesis submitted in fulfilment of the requirements for the degree Doctor of Philosophy in the School of Animal, Plant and Environmental Sciences, the Faculty of Science, University of the Witwatersrand, Johannesburg

Supervisor: Prof. Mary Scholes
Co-supervisor: Prof. Stuart Piketh

Braamfontein
May 2025

DECLARATION

I declare that this thesis is my own, unaided work. It is being submitted for the Degree of Doctor of Philosophy at the University of the Witwatersrand, Johannesburg, South Africa. It has not been submitted before for any other degree or examination at any other university.

Refilwe Faith Kai-Sikhakhane

05 day of May 2025 at Johannesburg, Gauteng

ABSTRACT

The Highveld region of South Africa is a major source of emissions from large industries, including electricity utility power stations, petrochemical plants, and smelting industries. This study investigates the sources, concentrations, and transport of nitrogen dioxide (NO_2) emissions in Wakkerstroom, a town located downwind of major NO_2 emission sources in the Mpumalanga Highveld. Near-surface and tropospheric vertical column NO_2 concentrations were measured using ground-based Pandora-2s and TROPOMI-Sentinel-5P satellite instruments. The Pandora-derived diurnal NO_2 concentrations at Wakkerstroom ranged between 0.2 ppb, with a standard deviation of ± 0.04 ppb and 7.5 ppb, with a standard deviation of 5.7 ppb, with the highest concentrations recorded in September. Air quality monitors near power stations measured peak weekly averaged concentrations in winter (27.6 ppb) and summer (31.5 ppb) of 2020. The annual mean Pandora-derived tropospheric vertical column (TVC) NO_2 concentrations were 5.1 x 10^{-5} mol/m^2 with a standard deviation of 9.0 x 10^{-5} mol/m^2 in 2020 and 5.03 × 10^{-5} mol/m^2 with a standard deviation of 9.40 × 10^{-5} mol/m^2 in 2021, while TROPOMI measured 21% and 40% higher concentrations, respectively. Theil-Sen regression analyses showed that TROPOMI overestimates Pandora-derived TVC-NO_2 concentrations by over 50%. Backward trajectory analyses revealed that air mass transport from the east of Wakkerstroom, passing over eSwatini and southern Mozambique, contributed significantly to the observed NO_2 concentrations due to biomass burning. The findings of this study highlight the complex dynamics of NO_2 pollution in the Highveld region, revealing the influence of both local and regional sources on Wakkerstroom's concentrations. This research emphasises the fundamental role of continuous long-term ground-based data of pollutants in heavily polluted areas like the Highveld, which is characterised by unique synoptic meteorological patterns. Such data serves to bridge the information gaps to corroborate and augment high-spatial resolution satellite observations. Consequently, it helps to confirm the reliability and use of satellite data as a proxy for larger geographical areas with scarce ground-based instruments.

DEDICATION

This body of work is dedicated to:

Professor Robert J. Scholes

(1957 – 2021)

ACKNOWLEDGEMENTS

Completing this PhD has been a transformative journey, one that would not have been possible without the support, guidance, and encouragement of many remarkable individuals and institutions. I am deeply grateful to everyone who has played a role in making this achievement a reality.

- To my supervisor, Prof. Mary Scholes, thank you for your unwavering support, patience and belief in my potential. Thank you for giving me the opportunity to pursue this journey and continuously encouraging me to strive for excellence. Your guidance has been instrumental in shaping my growth, not only as a researcher but also as an individual. Your dedication and generosity, which went far beyond academic mentorship, have made a lasting impact on my academic and personal life, and I will always be deeply thankful for your role in helping me achieve this milestone.
- To my supervisor, Prof. Stuart Piketh, thank you for adopting me as one of your students. Thank you for welcoming me into the Climate Research Group (CRG). Your patience, guidance, and unwavering commitment throughout this PhD journey have been pivotal in shaping its success. Your support and kindness, extending well beyond academic mentorship, have profoundly influenced both my academic and personal growth. I am forever grateful for the role you played in helping me reach this milestone.
- To my supervisor, the late Prof. Robert Scholes, thank you for the instrumental role he played in developing the study proposal that guided this PhD journey to completion. Your legacy will continue to live on.
- To my advisor, Prof. Rebecca Garland, thank you for all your guidance and support. Thank you for the valuable time you spent reading my drafts and providing feedback.
- To Dr Henno Havenga, thank you for always being available to explain one concept or another.
- To Dr Caradee Wright, thank you for the chats and encouragement.
- To Dr Stephen Broccardo, thank you for the Pandora Therapy sessions. Thank you for setting aside time every fortnight to discuss the Pandora instrument and data with me.
- To Prof. Michel Verstraete, thank you for your prompt feedback when reading my drafts and for the time you spent reading and editing my work.

- Thank you to the NRF for funding provided to Prof. Mary Scholes through her DST-NRF research chair in System Dynamics. This funding has provided bursary support and research expenses.
- Thank you to the Climate Research Group for funding that provided bursary support and academic travelling expenses.
- Last but not least, thank you to my friends and family for all the support, encouragement and check-ins. This one is for you and you and you! We did it!

Ke Kgabo! Ke Mokgatlha! Ke legadimana ntweng! Ha ke ja ha ke gadimi!. Ke leitibolo laga Lorna le Osepeleng! Setlogolo sa Bakgatla! Ke makgakga ke mabela! Ke ipela ka thuto!

KGABO!

A E NAMELE EJE BOREKHU!

“I can do all this through him who gives me strength.”
Philippians 4:13

Table of Contents

LIST OF FIGURES

LIST OF TABLES

LIST OF ABBREVIATIONS

a.g.l	above ground level
a.s.l	above sea level
AMF	Air Mass Factor
CINDI	Campaign of Nitrogen Dioxide Measuring Instruments
DISCOVER-AQ	Deriving Information on Surface Conditions from Column and Vertically Resolved Observations Relevant to Air Quality
DOAS	Differential Optical Absorption Spectroscopy
DS	Direct Sun
GOME	Global Ozone Monitoring Experiment
hPa	hactor pascals
KORUS-AQ	Korea-United States Air Quality
MAX-DOAS	Multi-Axis Differential Optical Absorption Spectroscopy
MP	Mpumalanga
N	Nitrogen
NO	Nitric Oxide
NO_2	Nitrogen dioxide
NO_x	Nitrogen Oxides
OMI	Ozone Monitoring Instrument
PAN	Peroxyacetyl Nitrate
ppb	parts per billion
RNS	Reactive Nitrogen Species
SCD	Slant Column Density
SZA	Solar Zenith Angle
TROPOMI	TROPOspheric Monitoring Instrument
TVC	Tropospheric Vertical Column
UT	Upper Troposphere
VOC	Volatile Organic Compounds

Chapter 1

This Chapter discusses the background, rationale, aims and objectives of the study. It also outlines the structure of the thesis.

1 Introduction

1.1 Background and Rationale of the Study

The Highveld, an extensive geographical area, is located in South Africa's north-eastern region. It covers the majority of the Free State and Gauteng provinces, as well as significant portions of the surrounding provinces, including the Eastern Cape, Northern Cape, North-West, Limpopo, and Mpumalanga (Figure 1.1). This plateau, situated at an elevation typically ranging from 1500 m to 2100 m above sea level (a.s.l), is known for its distinctive grassland ecosystem and temperate climate (Mucina and Rutherford, 2006). It has an abundance of raw materials, particularly coal and gold, which fueled its development into a robust mining sector. The region's geological composition, which includes rich mineral deposits, has played a crucial role in shaping its economic significance (Maull, 1986; Burns and Collins, 2013).

The Highveld has served as the industrial heartland of South Africa for many years (Keegan, 1983). This region hosts a significant portion of the country's manufacturing and processing industries, ranging from steel production and automotive manufacturing to petrochemical refineries (Maregele, 2014). The Highveld is also home to 12 coal-fired power stations (https://www.eskom.co.za/eskom-divisions/gx/coal-fired-power-stations/ last accessed 3 October 2024). This concentration of industrial activity has led to the emergence of major urban centres, including the Gauteng-Tshwane metro, which serves as an economic hub for South Africa and the entire southern African region (Rogerson, 1996). The Highveld's economic output and infrastructure make it a critical component of South Africa's overall economic strategy and development plans. This industrial and economic development, however, has environmental repercussions, notably in the form of elevated nitrogen dioxide (NO_2) and other pollutant emissions.

Numerous studies, including those by Josipovic *et al.* (2010), Lourens *et al.* (2012), Conradie *et al.* (2016) and Duncan *et al.* (2016) have identified the Highveld as one of the top global regions for the emission of nitrogen oxides (NO_x), particularly NO_2, as a result of the urban

concentration in Gauteng and the energy-generation and petrochemical plants based in Mpumalanga, which also hosts the majority (10) of the coal-fired power stations in the Highveld (https://www.eskom.co.za/eskom-divisions/gx/coal-fired-power-stations/ accessed 3 October 2024). Nitrogen oxides are primarily emitted as NO (nitric oxide), which rapidly converts to NO_2 in the presence of oxygen. Despite these findings, limited research has been conducted on the spatial and temporal variability of NO_2 concentrations in the Highveld, particularly in areas which are affected by both local and transported pollutants.

Local NO_x sources are diverse, comprising both natural and anthropogenic contributors. Natural contributors include soil microbial processes and lightning (Chameides *et al.*, 1977; Ojelede *et al.*, 2008). Lightning-created NO_x, whose natural global concentration remains uncertain, is more prevalent in the upper troposphere, with particularly high levels in elevated areas of South Africa, such as the Highveld (Ojelede *et al.*, 2008). However, the concern is mainly about the multifaceted anthropogenic contributors, which include a combination of emissions from industrial, transport and biomass-burning activities. These anthropogenic emissions, particularly emissions from tall-stack power stations, are major contributors to NO_x loading in the troposphere (Lourens *et al.*, 2012). Consequently, there is a persistent presence of NO_x, particularly NO_2, in the Highveld atmosphere.

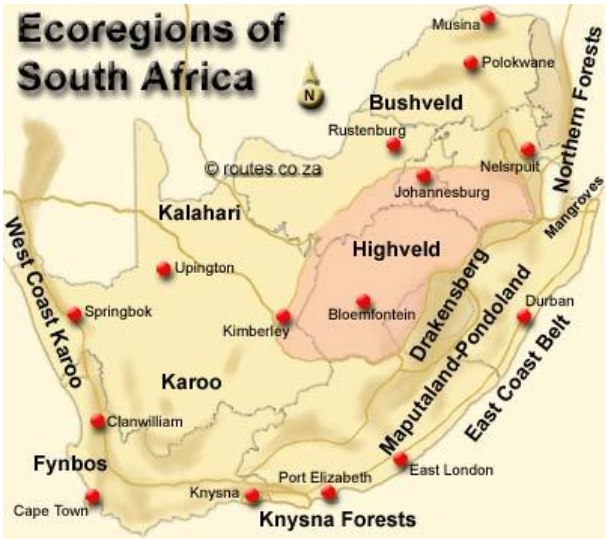

Figure 1.1: Map of South Africa showing the Highveld area (shaded in pink). https://thegainlineblog.wordpress.com/2013/10/03/trc-2013-the-importance-of-the-highveld/

The rate at which NO_x and other pollutant trace gases are emitted into the global atmosphere has increased over the years (Martins *et al.*, 2007; Shaw and Van Heyst, 2022). This increase is projected to continue in the future, mainly due to the increasing demand for resources such

as electricity and food (https://ourworldindata.org/environmental-impacts-of-food?insight=emissions-from-food-alone-would-take-us-past-15c-or-2c-this-century#key-insights last accessed 3 October 2024). Exposure to high levels of NO_2 has been linked to a range of adverse health effects, including respiratory and cardiovascular problems, as well as premature mortality (WHO, 2003; Wright *et al.*, 2011; Anenberg *et al.*, 2022). In addition, its presence indirectly exacerbates global climate change through its role in the production of tropospheric Ozone (O_3) (Dickerson, 1984; Zhang *et al.*, 2020). Increased atmospheric NO_x concentrations translate to elevated deposition of nitrogen compounds, predominantly in the form of NO_2 and nitrate (NO_3^-) (Collett, Piketh and Ross, 2010). This elevated deposition of nitrogen compounds can lead to soil acidification in terrestrial and eutrophication in aquatic ecosystems, potentially altering biodiversity and ecosystem functioning. Furthermore, the interaction between NO_x and other atmospheric pollutants can result in the formation of secondary pollutants, such as particulate matter (PM), which have additional adverse impacts on human health and the environment (Anenberg *et al.*, 2022).

The key to understanding the multifaceted impacts of elevated atmospheric NO_x lies in accurately measuring its concentrations and understanding the various sources. These accurate long-term measurements can reveal trends in air quality and help evaluate the success of implemented mitigation measures in highly polluted regions such as the industrialised Highveld (Laakso *et al.*, 2012). Additionally, understanding the transport of NO_2 emissions is essential for addressing air quality issues on a broader scale, as pollution from neighbouring areas can significantly impact local NO_2 concentrations.

A significant challenge with monitoring local atmospheric NO_2 concentrations in many regions of the Southern Hemisphere, such as the Highveld, is the lack of comprehensive NO_2 data (Laakso *et al.*, 2012). The lack thereof is caused by the absence of instrumentation in certain regions (Verhoelst *et al.*, 2021). This data scarcity hampers efforts to accurately assess the variability in the NO_2 concentrations and its impacts on human health and the environment in these areas. Satellite observations from instruments such as the TROPOMI have attempted to fill this gap and are capable of pointing out global NO_2 emission hotspots, but they often lack the temporal frequency needed for detailed local-scale analyses (Lourens *et al.*, 2012; Griffin *et al.*, 2019; Verhoelst *et al.*, 2021). The temporal frequency of the TROPOspheric Monitoring Instrument (TROPOMI) is daily, and local-scale analyses benefit from measurements taken

more frequently; the higher the temporal frequency, the better the analyses. Local-scale analyses contribute to the understanding of the heterogeneity of NO_2 concentrations, particularly in highly polluted areas such as the Highveld (Lourens *et al.*, 2012). Addressing this issue requires investment in ground-based monitoring networks and capacity building to ensure consistent and reliable data collection across underrepresented regions.

Ground-based instruments such as the Pandora offer a comprehensive temporal resolution to resolve the local diurnal NO_2 concentrations of an area. Pandora instruments provide continuous measurements throughout the day, giving the ability to track variations in NO_2 levels from morning to night. The high-frequency sampling capability of Pandora instruments enables the detection of short-term fluctuations in NO_2 concentrations, which can be crucial for understanding local air quality dynamics. This detailed temporal information can be particularly valuable for identifying local pollution sources and studying the impact of meteorological conditions on NO_2 distribution (Boersma *et al.*, 2007). Additionally, the data collected by Pandora instruments can be used to evaluate and complement satellite observations, enhancing our overall understanding of atmospheric NO_2 dynamics.

Pandora instruments possess the capability to capture the vertical distribution of NO_2 in the troposphere, a feature that distinguishes them from satellite-based instruments like TROPOMI. By employing multi-axis differential optical absorption spectroscopy (MAX-DOAS) techniques, Pandora can measure NO_2 concentrations at different elevation angles, providing information about the vertical structure of NO_2 in the lower atmosphere. While Pandora's measurements are confined to the lower troposphere, OMI and, recently, TROPOMI data have been used to show vertical profiles of NO_2 by employing the cloud-slicing technique (Choi *et al.*, 2014; Marais *et al.*, 2018). This technique takes advantage of the presence of clouds at different altitudes to infer the vertical distribution of NO_2. By analysing TROPOMI measurements taken at various cloud heights, the vertical profile of NO_2 concentrations can be reconstructed from the surface up to higher altitudes in the troposphere.

The combination of Pandora's detailed lower tropospheric measurements and TROPOMI's broader vertical profiling capabilities through cloud-slicing can provide a more comprehensive understanding of NO_2 distribution in the atmosphere. Vertical profiling of NO_2 concentrations in highly industrialised areas such as the Highveld will contribute to the improved accuracy of satellite retrievals and air quality models. Source attribution is enhanced, as understanding the vertical distribution aids in identifying pollution sources at different altitudes, such as ground-

level emissions and elevated industrial plumes. Vertical profiles can reveal information about the transport of NO_2 between different atmospheric layers and provide insights into the chemical and photochemical processes occurring at different altitudes.

Understanding the vertical distribution of NO_2 in polluted areas, in addition to the horizontal distribution captured by TROPOMI, is essential. Vertical profiles help in more accurately assessing human exposure to NO_2, as abundance can vary significantly with altitude in urban areas and the Highveld, which has persistent stable layers (Cosijn, 1996). Ground-based vertical profiles provide essential validation data for satellite observations, improving the overall accuracy of global NO_2 monitoring. By combining the horizontal distribution data from TROPOMI with the vertical profiling capabilities of instruments like Pandora and the cloud-slicing technique, researchers can develop a more comprehensive three-dimensional understanding of NO_2 pollution in urban and industrial areas.

Given the significant implications of NO_2 emissions on both environmental health and air quality in the Highveld, this study sought to bridge the current knowledge gap by providing data and an in-depth analysis of NO_2 concentrations in Wakkerstroom. The following section outlines the contributions this research aimed to make towards understanding NO_2 dynamics in the region.

1.2 Contributions to Science

Exploring the near-surface NO_2 concentrations in the Highveld hotspot in the presence and context of background NO_2 derived from other ground-based sensors showed that the main contributor to the measured concentrations in Wakkerstroom is biomass burning from eSwatini and the south of Mozambique. Even though Wakkerstroom is downwind from coal-fired power stations, the biomass burning during spring from the mentioned neighbouring countries significantly affected the NO_2 concentration loading of the air masses transported to Wakkerstroom.

The comparison of the tropospheric vertical column NO_2 concentrations from the Pandora-2s and the TROPOMI instruments shows that even though the Pandora-2s instrument measures NO_2 in the lower troposphere, unlike the TROPOMI instrument that measures in the total tropospheric column, the two data sets are spatially and temporally complementary and thus the globally available TROPOMI NO_2 concentration data can be used as a proxy for tropospheric and boundary layer NO_2 concentrations over the Highveld of South Africa.

1.3 Aim and Objectives

1.3.1 Aim

This study aimed to determine the spatio-temporal NO_2 concentration distribution in the major source region of the Highveld in South Africa.

1.3.2 Objectives

a) Assess the near-surface nitrogen dioxide concentrations at Wakkerstroom, Mpumalanga, using a ground-based upward-looking Pandora instrument and establish the observed seasonal cycle.
b) To compare and contrast the Pandora-2s- and TROPOMI satellite-derived tropospheric vertical column nitrogen dioxide concentrations at Wakkerstroom and establish the observed seasonal cycle.
c) To confirm the major transportation pathways during the highest concentration period of nitrogen dioxide in Wakkerstroom.

1.4 Research Questions

a) What are the Pandora-derived near-surface NO_2 concentrations at Wakkerstroom, and how do these compare to ground-based measurements from *in situ* air quality monitoring sites at the nearby power utility facilities and Elandsfontien?
b) How do the Pandora-derived nitrogen dioxide concentration vertical column data in Wakkerstroom compare to the TROPOMI-derived data, and what is the seasonal cycle of NO_2 in Wakkerstroom, as revealed by the Pandora-and TROPOMI-derived tropospheric vertical column data?
c) Is there a difference in the transportation pathways of the highest concentrations of nitrogen dioxide at Wakkerstroom when compared to the pathways in the Highveld region?

1.5 Structure of the Thesis

This thesis is presented in seven chapters. Chapters four and five are papers that have been published in international literature, and therefore, this thesis will include some unavoidable repetition.

The two published papers are as follows:

Paper one (Chapter 4)

Kai, R. F., Scholes, M. C., Piketh, S. J., and Scholes, R. J. Analysis of the first surface nitrogen dioxide concentration observations over the South African Highveld derived from the Pandora-2s instrument. *Clean Air Journal*. 2022, *32*(1), 1 – 11. https://dx.doi.org/10.17159/caj/2022/32/1.13242

Author Contributions

Conceptualisation: R.F.K., M.C.S., R.J.S. and S.J.P.; Methodology: R.F.K., M.C.S., S.J.P. and R.J.S.; Data Collection: R.F.K.; Data Analysis: R.F.K.; Interpretation, R.F.K.; Original Draft Preparation: R.F.K.; Review and Editing: R.F.K., M.C.S. and S.J.P.: Supervision: M.C.S., S.J.P., R.J.S.; Project Administration: R.F.K., M.C.S., R.J.S. and S.J.P.; Funding Acquisition: M.C.S. and R.J.S.

Paper two (Chapter 5)

Kai-Sikhakhane, R. F., Scholes, M. C., Piketh, S. J., van Geffen, J., Garland, R. M., Havenga, H., Scholes, R. J. Assessing Nitrogen Dioxide in the Highveld Troposphere: Pandora Insights and TROPOMI Sentinel-5P Evaluation. *Atmosphere*. 2024, *15*(10):1187. https://doi.org/10.3390/atmos15101187

Author Contributions

Conceptualisation: R.F.K, M.C.S., R.J.S., S.J.P., and R.M.G.; Methodology: R.F.K., M.C.S., S.J.P., R.M.G., and R.J.S.; Data Analysis: R.F.K.; Interpretation: R.F.K.; Original Draft Preparation: R.F.K.; Review and Editing: R.F.K., M.C.S., S.J.P., R.M.G., H.H., and J.v.G.; Visualisation: R.F.K.; Supervision: M.C.S., S.J.P., and R.M.G.; Project Administration: R.F.K., M.C.S., and S.J.P.; Funding Acquisition: M.C.S., R.J.S., and S.J.P.

Thesis structure

Chapter 1: This Chapter provides the introduction, including the background, rationale, aim and objectives of the study.

Chapter 2: This Chapter provides the literature review, which places this research in the context of the published literature.

Chapter 3: Methods and methodology, which includes a description of the study site as well as the two approaches used in this study.

Chapter 4: Paper 1, which addresses the first objective of the study. This chapter is introduced with a preface and is concluded with a postscript which details how this research provided input for the next chapter.

Chapter 5: Paper 2, which addresses the second and third objectives. This chapter is introduced with a preface and is concluded with a postscript which details how this research provided input for the next chapter.

Chapter 6: This Chapter provides a detailed discussion of the results of this study in the context of the published literature.

Chapter 7: This Chapter is the consolidated reference list of all of the publications cited in this thesis.

Chapter 2

2 LITERATURE REVIEW

Nitrogen (N) and nitrogen oxides (NO_x) are fundamental in atmospheric chemistry, influencing everything from the air we breathe to the climate we experience. This Chapter explores their discovery, chemistry, sources, measuring techniques and distribution in the atmosphere.

2.1 Nitrogen and Nitrogen Oxides

The discovery of nitrogen by Daniel Rutherford in 1772 marked a significant milestone in the understanding of atmospheric composition. Claude Louis Berthollet's investigations in 1785 provided insights into nitrogen's chemical properties and reactivity, and John Dalton's subsequent work in 1808 further elucidated the properties and behaviour of this essential element. These were followed by Jean-Baptiste Boussingault's extensive studies between 1836 and 1838, which were particularly influential as they explored nitrogen's role in plant nutrition and soil fertility. These initial investigations established a foundation for a more comprehensive understanding of the nitrogen cycle and its influence on ecosystems and the biosphere. Initial research concerning the biogeochemical significance of nitrogen provided the basis for contemporary atmospheric science, allowing for the study of the atmospheric composition.

The composition of Earth's lower atmosphere is a mixture of gases dominated by nitrogen and oxygen, with smaller amounts of other gases and particulate matter. Nitrogen, which accounts for approximately 78% of the atmosphere by volume, plays a crucial role in atmospheric chemistry and biological processes. While early research focused on the chemical properties and role of nitrogen in plant nutrition, subsequent studies expanded our understanding of atmospheric composition and the critical role of trace gases. This shift in focus led to the exploration of reactive nitrogen species (RNS) and their impacts on both the atmosphere and terrestrial ecosystems.

Despite its abundance in the atmosphere, nitrogen remains in an unreactive state (Smith, 1872). However, lightning, which operates through the Zel'dovich mechanism (Zeldovich, 1947), can activate and transform inert nitrogen into its reactive forms. Lightning activation involves the intense heat and energy of lightning strikes, which break the strong triple bond of nitrogen molecules, allowing them to combine with oxygen to form nitrogen oxides (Griffing, 1977).

The formation of NO_x through lightning occurs predominantly in the upper layers of the atmosphere, particularly in the stratosphere and upper troposphere (Levy, 1972; Ojelede *et al.*, 2008). This high-altitude production of NO_x has far-reaching implications for atmospheric composition and climate. This is because its presence at high altitudes can lead to the formation of O_3, a potent greenhouse gas, in the troposphere and stratosphere (Crutzen, 1973; Dickerson, 1984; Köhler *et al.*, 2008; Zhang *et al.*, 2020). The production of ozone can have significant effects on radiative forcing and global temperature patterns (Fuglestvedt *et al.*, 1999). Positive radiative forcing warms the earth, while negative radiative forcing results in the cooling of the earth.

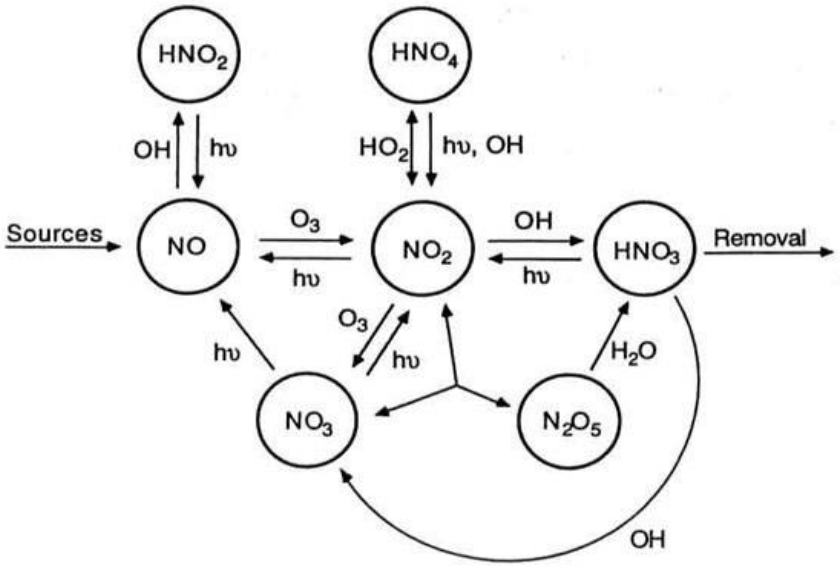

Figure 2.1: The principal tropospheric reactions of nitrogen oxides (Macalady, 1998**)**

In addition to NO_x, other RNS contribute to atmospheric chemistry (Figure 2.1). Numerous studies, including Levy (1972) and Crutzen (1970), have extensively explored the photochemistry of RNS and atmospheric transformations of NO_x, which are summarised in Figure 2.1. Peroxyacetyl nitrates (PANs) and volatile organic compounds (VOCs) were excluded from the figure illustration. Reactive nitrogen species, which are components of the nitrogen cycle, occur mainly as NO and undergo photochemical transformation into NO_2, a minor greenhouse gas (Zeldovich, 1947; Levy, 1972; Igbafe *et al.*, 2015). Nitrogen dioxide, a significant atmospheric component, undergoes photochemical dissociation upon exposure to light at < 430 nm, initiating the formation of photochemical smog (Haagen-Smit, 1964). Despite being a minor greenhouse gas, it serves as a critical tropospheric precursor to O_3 and is also a methane (CH_4) destroyer (Haagen-Smit, 1964; Crutzen, 1970; Levy, 1972). In the troposphere, NO_x is also

transformed into NO_3^- (nitrate) aerosols, contributing to slight radiation reflection (Levy, 1972). Nitric acid (HNO_3) is formed through the oxidation of NO_2 and is a major component of acid rain. Ammonia (NH_3), released from agricultural activities and natural sources, can neutralise acidic compounds in the atmosphere. Peroxyacetyl nitrate (PAN) is a secondary pollutant formed from the reaction of NO_x with volatile organic compounds (VOCs); it serves as a reservoir for NO_x and is capable of transporting reactive nitrogen over long distances. Nitrous oxide (N_2O) is a potent greenhouse gas that also contributes to stratospheric O_3 depletion.

These RNS interact with other atmospheric components, influencing air quality, climate, and ecosystem health. Their chemistry is interconnected with the cycles of other elements, particularly carbon and sulfur, creating a complex network of atmospheric processes. These interactions, in addition to the number and types of NO_x emission sources, rate of emissions, and transport of emissions from other regions (Logan *et al.*, 1981), are crucial for predicting the impacts of NO_2 emissions.

2.2 Sources of Nitrogen Oxides

Studies by Haagen-Smit (1964), Weiss and Craig (1976) and Logan (1983) have shown that sources of atmospheric NO_2 can be of natural or anthropogenic origin. Nitrogen oxide sources of natural origin are mainly from lightning, microbial soil activity, wildfires and oceans (microbial breakdown of nitrogen compounds in seawater) (Galloway *et al.*, 2004; Ito *et al.*, 2018). Meanwhile, anthropogenic sources are characterised by biomass burning, energy production, food production, and by-products of transport and industrial activity.

Sources of natural origin are dominated by lightning-produced NO_x, which was reported to account for ~ 25% of global atmospheric NO_x emissions (Logan, 1983). Lightning-produced NO_x is concentrated in the upper troposphere and the stratosphere, and NO_x from microbial soil activity, oceans, and sometimes wildfires are confined to the low troposphere. Ojelede *et al.* (2008) showed that ~ 9% of NO_x emissions reported to be from coal-fired power stations in the Highveld are actually lightning-produced. This finding highlights the importance of accurately distinguishing between natural and anthropogenic sources of NO_x, as misattribution of sources can lead to inaccurate emissions inventories.

Anthropogenic activities have become a major contributor to global atmospheric NO_x levels, accounting for over 50% of the total load (Haagen-Smit, 1964; Galloway *et al.*, 2004; Harlass

et al., 2024). This significant impact is primarily driven by the rapid industrialisation and urbanisation associated with population growth. The expansion of urban areas and industrial zones has led to a substantial increase in NO_x emissions from various sources, with vehicles and coal-fired power stations being particularly noteworthy contributors (Jaworski, Howarth and Hetling, 1997; Anttila, Tuovinen and Niemi, 2011; Shon, Kim and Song, 2011; Reidl-Leuthner *et al.*, 2015). These sources release large quantities of reactive nitrogen compounds into the atmosphere, exacerbating the overall NO_x burden (Lourens *et al.*, 2012). The growing human population has not only intensified industrial and urban emissions but has also indirectly increased NO_x levels through agricultural practices. As the demand for food production rises to meet the needs of an expanding population, there has been a corresponding increase in fertiliser applications. These fertilisers, rich in nitrogen compounds, contribute significantly to the overall NO_x load in the atmosphere when they volatilise or undergo chemical transformations due to soil microbes, which leads to the release of nitrogen oxide (Galloway *et al.*, 2004; Manahan, 2010; Guo *et al.*, 2020).

This interconnected relationship between population growth, industrialisation, urbanisation, and agricultural activity increase has led to a continuous upward trend in anthropogenic NO_x emissions, resulting in the deterioration of air quality, particularly in the Highveld and cities such as Johannesburg (Lourens *et al.*, 2012; Matandirotya and Burger, 2022). A study by Lourens *et al*. (2012) confirmed the presence of a second NO_2 emission hotspot over Johannesburg city in addition to the Highveld hotspot, further highlighting the importance of understanding the various sources which contribute to the measured elevated NO_2 concentrations.

Sources of anthropogenic NO_x emit these RNS into the atmosphere through point sources (single sources) or non-point sources (many various sources at once) at different altitudes (Lange, Richter and Burrows, 2022). Near-surface concentrations in the Highveld are dominated by emissions from biomass burning, agricultural activities, vehicle exhausts, and winter indoor fires (Adesina *et al.*, 2022). The seasonal nature of certain activities, such as biomass burning in spring and indoor fires in winter, leads to seasonal variations and peaks, which contribute significantly to the region's complex air quality challenges. The situation is further exacerbated during winter months, which are characterised by increased atmospheric stability and temperature inversions that can trap pollutants near the ground (Whiteman, Bian and Zhong, 1999). A case study in the Highveld reported elevated NO_x concentrations in the winter of 2005; the winter of 2005 had a biomass-burning peak during August, contributing to the measured near-

surface concentrations (Collett, Piketh and Ross, 2010). The Highveld region has a complex topography, which also contributes to the further trapping of NO_2 to the ground. The prevalence of these pollutants has far-reaching consequences, affecting not only human health but also local ecosystems and agricultural productivity.

Tropospheric column concentrations are mostly affected by emissions from coal-fired power plants, industrial activities, aircraft and transboundary transported emissions (Ross *et al.*, 2007; Collett, Piketh and Ross, 2010; Kollonige, Thompson, Josipovic, Tzortziou, Beukes, Burger, Martins, Zyl, *et al.*, 2018; Matandirotya and Burger, 2021). Energy-production NO_x emissions in the Highveld are released from tall stacks at around the 775 hPa level (Held, 1996) and have a relatively short lifetime. However, the NO_x lifetime, which typically ranges from 2 to 8 hours depending on the level of pollution, increases with altitude (Davis, Rutledge and Fuchs, 2019). Therefore, the measured atmospheric column concentrations can be a combination of various sources (Shah *et al.*, 2023).

The concentrations (of any emitted gas) observed at a location are also affected by the solar radiation (which drives transformations) (Igbafe *et al.*, 2015) and the dispersal of the emissions into, around or out of the region of emission (Ross *et al.*, 2007). This is why pollution is monitored at various sites (Lazar, Capatina and Simonescu, 2014; Kalbarczyk and Kalbarczyk, 2020). Solar radiation and the presence of hydrocarbons promote the transformation of NO. The dispersion of the emissions and their transformation products are affected by air mass transport, which can carry emissions over various terrains to neighbouring regions (Moller *et al.*, 2010; Yang *et al.*, 2020), where they are removed from the atmosphere through deposition. The deposition of emitted and transported gases depends largely on meteorological factors, such as temperature, wind speed, rainfall, and humidity (Crutzen, 1979). Increased atmospheric NO_x concentrations lead to higher N inputs into terrestrial and coastal ecosystems (Likens *et al.*, 1977) and negatively impact the health of exposed populations (Haagen-Smit, 1964; Molina and Molina, 2004; Anenberg *et al.*, 2022), such as those in the industrial Highveld area of South Africa.

Sustained elevated concentrations of reactive nitrogen compounds in the atmosphere can result in deposition rates sufficient to cause soil accumulation of NO_3^-. This may eventually lead to ecosystem nitrogen saturation, causing the leaching of nitrogen compounds and other displaced elements into rivers and groundwater (Likens *et al.*, 1977). Nitrogen saturation in ecosystems

leads to biodiversity loss and acidification in aquatic and terrestrial systems (Likens *et al.*, 1977).

2.3 Atmospheric Transport of NO_2 Emissions

The deposition site of NO_2 emissions depends on the transport of air masses, which is influenced by atmospheric conditions such as wind speed, vertical temperature gradient and solar radiation (Seinfeld, 1986). The long-range transport of these emissions can impact air quality and ecosystems in regions far from the original source. A study by West *et al*. (2009) showed that there is a strong inter-regional influence of NO_x from Europe to Africa due to the interactions of the transported NO_x with the emissions at the destination. As a result, the air quality in neighbouring regions can be shaped by high-altitude NO_x production, in which lightning-produced NO_x, a natural source, dominates. These reactions are influenced by the presence of solar radiation and other pollutants and affect the atmospheric lifetime of NO_2, which in turn impacts its transport range and transformation (Seinfeld, Pandis and Noone, 1998). Changes in solar radiation intensity and the rate of NO_2 emissions affect the diurnal NO_2 cycle and result in daily fluctuations, particularly in urban areas. NO_2 concentrations are shown to peak during morning and evening rush hours (Sillman, 1999; Lourens *et al.*, 2012). Seasonally, winter tends to have higher NO_2 levels due to reduced photolytic activity, which slows the degradation of NO_2, leading to longer atmospheric lifetimes of about one day (Lourens *et al.*, 2012; Matandirotya and Burger, 2021; Shah *et al.*, 2020).

The horizontal transport of trace gases is controlled by local thermo-topographic winds near the Earth's surface or by larger-scale circulation in synoptic flow fields (Tyson, 1969; Whiteman, 1990), while the vertical transport depends on the stable structure of the atmosphere (Tyson and Preston-Whyte, 2000). The advection and fate of the emissions depend mainly on the transport of air masses, which is dependent on meteorological factors such as temperature, wind, rainfall, and humidity in an area (Piketh and Walton, 2004; Saueprasearsit and Khummongkol, 2009; Conradie *et al.*, 2016). The circulation and recirculation patterns determine the amount and dispersion rate of emissions in the source region (Ross *et al.*, 2007; Ibebuchi, 2021). Long-range transport of NO_2 can significantly impact air quality and ecosystems in regions far from emission sources, affecting rural and even marine environments (Galloway *et al.*, 2003). These transported NO_2 plumes contribute to nitrogen deposition and can influence atmospheric chemistry far from their source, including the ocean they transverse due to nitrogen fertilisation (Wenig *et al.*, 2003).

NO_x compounds are emitted into the atmosphere, dispersed through transportation to other regions, and eventually removed from the system through its boundary layer adjacent to the Earth's surface as dry and wet deposition (Jaworski, Howarth and Hetling, 1997; Bergström and Jansson, 2006; Galy-Lacaux *et al.*, 2014; Conradie *et al.*, 2016). Climate change may alter atmospheric transport patterns by shifting wind dynamics, temperature, and atmospheric stability, which could influence the distribution and transport of NO_2. Changes in temperature and precipitation patterns could affect photochemical reaction rates (Jacob and Winner, 2009), potentially increasing NO_2 lifetimes and altering regional air quality.

South Africa lies beneath the descending arm of the Southern Hemisphere Hadley circulation, and therefore, its atmosphere is characterised by high stability and anticyclonic circulation (Tyson and Preston-Whyte, 2000). The high atmospheric stability contributes to limited vertical mixing as a result of inversion trapping and recirculation, especially during winter, which enhances the accumulation of emissions in the boundary layer and lower troposphere.
In the Highveld, atmospheric transport is dependent on the easterly and westerly circulation patterns of the hemisphere (Piketh and Walton, 2004). The transport pattern over the Highveld is such that it tends to disperse NO_2 and other secondary nitrogen compounds in summer but confines it to the source region during winter (Collett, Piketh and Ross, 2010; Shikwambana, Mhangara and Mbatha, 2020; Yang *et al.*, 2020). This, therefore, means that there is more deposition closer to the source region in winter than in summer seasons. Meteorological conditions in the Highveld, such as stable winter inversion layers, further trap pollutants near the surface, enhancing NO_2 accumulation. Seasonal wind patterns, including easterlies and westerlies, affect horizontal dispersion, while temperature inversions limit vertical mixing (Freiman and Piketh, 2003).

In addition, the concentration of NO_2, formed by the transformation of NO in the atmosphere, has been reported to increase as the distance between the monitoring site and the source of the emission increases (Freiman and Piketh, 2003; Lee, Kim and Lee, 2009). However, due to dilution, there is a limit to this increase in concentration.

The transport of airmasses over Southern Africa and the Highveld has been researched for many years (Tyson, Garstang and Swap, 1996; Sturman, Tyson and D'Abreton, 1997; Connors *et al.*, 1999; Tyson, 1997; Freiman and Piketh, 2003; Piketh and Walton, 2004; McGill *et al.*, 2020). The research shows that airmass transport over the Highveld atmosphere differs at different atmospheric heights. The lower troposphere is dominated by transport from the Indian

Ocean, while at higher altitudes, the Atlantic Ocean transport is more prominent. However, the recirculation of air masses over the Highveld does not vary significantly with height (Freiman and Piketh, 2003).

Studies in Europe and East Asia have demonstrated the transboundary transport of NO_2 by atmospheric circulation, impacting downwind regions. Nitrogen dioxide emitted in East Asia is often transported across the Pacific Ocean, affecting air quality in Western North America (Zhang *et al.*, 2007). Such transboundary transport highlights the global implications of regional NO_2 emissions.

2.4 Measuring Nitrogen Dioxide in the Atmosphere

Atmospheric NO_x measurements have been successfully achieved using ground-based (Guicherit, 1972) and remote sensing instruments (Burrows *et al.*, 1999; Herman *et al.*, 2009). Ground-based instruments initially used the chemiluminescence technique (Guicherit, 1972) to measure *in situ* surface trace gas concentrations (Vlemmix *et al.*, 2010). These measurements were reliable but were limited to surface concentrations. Advances in ground-based atmospheric NO_2 measurements led to the use of the differential optical absorption spectroscopy (DOAS) technique (Brewer, Mcelroy and Kerr, 1973; Noxon, 1975) that is currently employed in ground-based and satellite instruments to measure near-surface and vertical column trace gas concentrations. These ground-based measurement techniques have continued to evolve, with the development of multi-axis DOAS (MAX-DOAS) systems allowing for improved vertical profiling of atmospheric NO_2 (Dimitropoulou *et al.*, 2020). Remote sensing technologies, such as lidar and passive imaging spectrometers, have further expanded our capabilities for measuring NO_2 distributions over larger spatial scales (Veefkind *et al.*, 2012). These advancements have enabled a better understanding of the spatial and temporal variability of NO_2 concentrations in urban and rural environments.

The DOAS technique can identify individual gases simultaneously, at very low concentrations and in complex mixtures, by using their unique light absorption characteristics (Platt, Perner and Pätz, 1979). The system's spectrometer monitors the wavelength (ultraviolet/visible) absorption of trace gases in an optical path (Platt and Perner, 1983). A light source, usually radiation from the sun or an artificial source (Platt and Perner, 1983), travels through the atmosphere and interacts with various trace gases. Each gas has specific wavelengths at which it strongly absorbs light, such as NO_2, which absorbs solar radiation from 300 to 600 nm and

shows elevated absorption at 400 nm (Davidson *et al.*, 1988; Solomon *et al.*, 1999). As light passes through the atmosphere and reaches the DOAS instrument, the spectrometer records the scattered light spectrum, showing reductions in intensity at wavelengths absorbed by gases present in the path. Absorption paths are usually at a maximum of ~ 10 km to increase the sensitivity of the instrument to low gas concentrations. The optical path length is greater in cleaner environments and can be limited to a few hundred meters in highly polluted areas (Harris *et al.*, 1983). By comparing this observed spectrum to a reference spectrum (one with minimal or no absorbing gases), DOAS isolates the "differential" absorption features that uniquely correspond to each trace gas. This differential approach filters out broad-spectrum interferences, like aerosols and background scattering, allowing accurate identification of gases.

The trace gas slant column density (SCD), which is the total amount of trace gas along the light path through the atmosphere (Boersma, Brinksma and Eskes, 2004), is derived from the differential absorption features using Lambert-Beer's Law (Platt, 1994). The SCD is then divided by the estimated air mass factor (AMF) - the ratio of the line-of-sight slant column abundances (Ω_s) and the vertical column (Ω_v) of a specific trace gas - to obtain the trace gas concentration in the vertical column (Platt, 1994). The DOAS method uses a radiative transfer calculation for AMF estimation (Solomon, Schmeltekopf and Sanders, 1987). Scattered light measurements produce large AMFs, which decrease the influence of the reference spectrum and give a strong NO_2 signal, increasing sensitivity for small amounts of NO_2 (Platt, 1994). In satellite instruments, the estimated AMF value is affected by atmospheric parameters such as the assumed shape of the vertical NO_2 profile, aerosols, clouds, and the surface albedo, resulting in high uncertainty for the AMFs (Heland *et al.*, 2002). The reference spectrum for satellite instruments is usually direct from the sun, unlike ground-based DOAS instruments, which use diurnal measurements at low solar zenith angles as reference spectra (Platt, 1994; Leser, Hönninger and Platt, 2003).

Ground-based instruments also use the multi-axis (MAX) (Hönninger and Platt, 2002) or direct sun (DS) (Brewer, Mcelroy and Kerr, 1973) DOAS techniques to measure near-surface and atmospheric NO_2 concentrations. The MAX-DOAS method uses scattered light from zenith sky observations at several elevation angles between the horizon and zenith, and this allows for tropospheric vertical column NO_2 concentrations to be separated from the stratospheric concentrations (Hönninger and Platt, 2002; Hönninger, von Friedeburg and Platt, 2004). In MAX-DOAS instruments, the AMFs are affected by the elevation angles, aerosol load in the lower

troposphere and surface albedo (Hönninger, von Friedeburg and Platt, 2004). At low elevation angles, the zenith optical path in the troposphere is shorter than that in the stratosphere (Hönninger, von Friedeburg and Platt, 2004). The shorter optical path increases the sensitivity of absorbers (trace gases) in the boundary layer (Hönninger and Platt, 2002). MAX-DOAS instruments can produce quality, high-temporal-resolution measurements under snow conditions (Hönninger and Platt, 2002).

While the DOAS method relies on scattered light from a source (Noxon, 1975), the DS-DOAS method directly observes the sunlight (Cede *et al.*, 2006). The DS-DOAS method does not rely on the same radiative transfer calculations that DOAS does for AMF calculations since the direct solar irradiance is measured at a known solar zenith angle (SZA) (Cede *et al.*, 2006). The AMFs are calculated geometrically (Herman *et al.*, 2009). The effect of atmospheric parameters, which greatly affect the AMF estimates in DOAS techniques, is minimal in DS-DOAS measurements. Measuring NO_2 in DS mode produces small signals, leading to the underestimation of total column NO_2 concentrations, particularly in highly polluted areas (Cede *et al.*, 2006).

Satellite-based instruments have significantly extended the application of DOAS, enabling global NO_2 monitoring with comprehensive spatial resolution. Instruments like the Global Ozone Monitoring Experiment (GOME) on ESA's ERS-2 satellite (Burrows *et al.*, 1999), the Ozone Monitoring Instrument (OMI) on NASA's Aura satellite (Levelt *et al.*, 2006, 2018), and the TROPOspheric Monitoring Instrument (TROPOMI) on Sentinel-5P (Veefkind *et al.*, 2012) apply DOAS principles to capture NO_2 and other trace gases across the Earth's surface. TROPOMI is a nadir viewing instrument with capabilities to measure trace gases in the UV, VIS, near-infrared (NIR) and shortwave infrared (SWIR) spectral bands (Veefkind *et al.*, 2012). This means the satellite measures trace gases directly below it as it orbits the Earth. It has two-dimensional detectors that give it the capability to provide daily global coverage and a good signal-to-noise ratio. TROPOMI scans the earth for 1 second, and during that time, the satellite moves ~ 7 km. It has a daily overpass time of 13:30 h local solar time with an orbital height of ~ 824 km (Veefkind *et al.*, 2012). The high spatial resolution (5.5 km x 3.5 km) of TROPOMI allows for the observation of NO_2 concentrations at the city level (Prunet *et al.*, 2020) and better quantification of emission sources (Veefkind *et al.*, 2012). Satellite observations, while offering global coverage at high spatial resolution, have limitations such as low temporal resolution (Platt, 1994; Heland *et al.*, 2002).

There is a long history of atmospheric NO_2 concentration monitoring using remote-sensing instruments (Schaub *et al.*, 2006; Celarier *et al.*, 2008; Herman *et al.*, 2009; Ionov and Timofeev, 2009; Pinardi *et al.*, 2020; Verhoelst *et al.*, 2021). Measurements from ground-based instruments are used to validate the satellite-derived NO_2 measurements in missions such as the Cabauw Intercomparison Campaign of Nitrogen Dioxide Measuring Instruments (CINDI) (Roscoe *et al.*, 2010), Deriving Information on Surface Conditions from Column and Vertically Resolved Observations Relevant to Air Quality (DISCOVER-AQ) and Korea–United States Air Quality (KORUS-AQ) study missions (Choi *et al.*, 2020). Nitrogen dioxide measurements from ground-based instruments have been used to validate the satellite measurements. The majority of the validation studies use DS-DOAS (Cede *et al.*, 2006; Choi *et al.*, 2020; Pinardi *et al.*, 2020; Verhoelst *et al.*, 2021) measurements to validate satellite measurements because DS measurements have less uncertainty than MAX-DOAS-derived measurements. The DS measurements use geometrically determined AMFs to determine atmospheric NO_2 concentrations, while MAX-DOAS-derived measurements use estimated AMFs. The study by Verhoelst *et al.* (2021) showed that TROPOMI NO_2 measurements overestimated the measurements from ground-based networks by a bias of 50% in highly polluted areas such as the Mexico Universidad Nacional Autónoma de México (UNAM) sites. This discrepancy can be attributed to the local horizontal and vertical variations of NO_2 (Dimitropoulou *et al.*, 2020). Cloud coverage and aerosol interference (Heland *et al.*, 2002) also contribute to the observed satellite measurements. Obtaining global NO_2 concentration data with widespread geographical coverage and high temporal continuity using a satellite is still difficult (Guo *et al.*, 2022).

2.5 Distribution of Nitrogen Dioxide in the Highveld Atmosphere

Overall, the global distribution of NO_2 emissions is a function of their local production, transport and mixing in the atmosphere. A study by Brinksma *et al.* (2008) showed that NO_2 is highly heterogeneous, contributing to its uneven distribution in the atmosphere. The uneven distribution is due to variability in its sources and the atmospheric processes it undergoes (Kerr, Goldberg and Anenberg, 2021). This variability has also been seen in the Highveld, with maximum daily mean surface NO_2 concentrations varying between 130 ppb and 15.3 ppb in the same Highveld region (Rorich and Galpin, 1998). The Highveld region of South Africa, with its numerous coal-fired power plants and other industrial activities, continues to show particularly elevated NO_2 levels with hourly mixing ratios of ~ 100 ppb at a site close to a petrochemical plant (Lourens *et al.*, 2012). Other sites, also in close proximity to major sources of NO_2

emissions, such as coal-fired power stations and metallurgy plants, showed hourly mixing ratios lower than 40 ppb (Lourens *et al.*, 2012). The observed variability highlights the importance of understanding local sources and the atmospheric dynamics which affect the concentrations measured.

The majority of the NO_2 sources in the Highveld contribute significantly to near-surface NO_2, particularly evident in the Highveld region, where some industrial stacks and other emission sources such as biomass burning, wildfires and indoor fires for heating are often situated close to the surface (Collett, Piketh and Ross, 2010; Adesina *et al.*, 2020). Consequently, the NO_2 released from these sources has limited opportunity for dispersion before reaching populated areas due to their shorter lifetime at lower elevations (Davis, Rutledge and Fuchs, 2019).

The surface NO_2 concentrations in the Highveld also exhibit diurnal and seasonal variations, with elevated concentrations (~ 50 ppb to 95 ppb) in the morning from about 06:00 to 09:00 and in the afternoon to evening from about 17:00 to 21:00 (Rorich and Galpin, 1998; Lourens *et al.*, 2012) and during winter. These peak periods align with morning and evening rush hours in adjacent Johannesburg, suggesting a strong influence of transported vehicle emissions on NO_2 levels in the region. The afternoon to evening peak may also be influenced by the accumulation of pollutants due to a stable nocturnal boundary layer. The lower concentrations observed during midday may be attributed to increased atmospheric mixing and photochemical reactions (Balashov *et al.*, 2014). The seasonal variation showed peak concentrations in winter at sites located downwind from major point sources or with significant local sources (Lourens *et al.*, 2011). The winter elevated concentrations were approximately 10 ppb, measured in July (Lourens *et al.*, 2011). The winter months are characterised by temperature inversions, which trap emissions within the surface (Whiteman, Bian and Zhong, 1999).

The observed significant spatial and temporal variations of surface NO_2 concentrations in the Highveld highlight the various sources which contribute to the measured concentrations. Accurately measuring near-surface NO_2 concentrations is essential for understanding its spatio-temporal patterns and tracking emissions from sources like power plant plumes and vehicles. Khodayari *et al.* (2018) reported that uncertainties in NO_x emissions, whether from natural or anthropogenic sources, affect the accuracy of NO_2 monitoring. Precision in measuring NO_2 concentrations depends on the systems used and the transport of NO_2 from emission sources. Meteorological factors, such as cloud cover, solar radiation, and wind dispersion, also impact

the effectiveness of these measurements, making some highly dependent on ground-based systems (Ambus *et al.*, 2011; Galy-Lacaux *et al.*, 2014). However, inaccuracies in monitoring data and in the spatiotemporal patterns of NO_x emissions can obscure a clear understanding of their impacts. For example, a study monitoring atmospheric NO_2 over the Paris region showed that measurement accuracy decreased as anthropogenic emissions increased (Ionov and Timofeev, 2009). Calibration studies are therefore essential to ensure that monitoring data are reliable and accurate (Kollonige, Thompson, Josipovic *et al.*, 2018).

Satellite instruments, such as TROPOMI, offer broad spatial coverage for NO_2 monitoring but are less sensitive to near-surface levels and are often biased in highly polluted areas. In contrast, ground-based instruments, while limited in spatial coverage, provide more detailed vertical profiles, making an integrated approach essential for comprehensive monitoring. Literature suggests that using NO_2 measurements derived from the MAX-DOAS method can reduce bias between satellite and ground-based instruments (Roscoe *et al.*, 2010; Dimitropoulou *et al.*, 2020), adding value to trends calculated from satellite data and providing realistic uncertainty estimates.

Pandora MAX-DOAS-derived NO_2 measurements, with a spatial representation of up to 10 km depending on the elevation angle, provide a more precise spatial overview. Ground-based instruments such as the Pandora-2s can also map the atmospheric vertical distribution of NO_2 concentrations (Cede, 2021). However, these instruments are sparse in the Southern Hemisphere. Vertical profiles from Pandora-2s instruments in MAX-DOAS mode are limited to approximately 550 hPa, and the horizontal spatial resolution is similarly restricted to a maximum of 10 km. TROPOMI, while extensive in coverage, does not produce vertical profiles as an official product, highlighting the need for more comprehensive methods to capture complete vertical distribution profiles of pollutants like NO_2.

The cloud-slicing method enables vertical NO_2 profiling and measurement in the upper troposphere using satellite data, particularly TROPOMI, despite challenges posed by cloud cover, which obscures the Earth's surface and lower atmospheric layers (Cede *et al.*, 2006; Marais *et al.*, 2018). This technique employs radiance measurements at various wavelengths to differentiate between clear and cloudy atmospheric sections. It utilises cloud-top height data to estimate NO_2 concentrations at different altitudes, effectively minimising cloud cover's impact by dividing the atmosphere into vertical slices for analysis (Choi *et al.*, 2014; Marais *et al.*, 2018). Cloud-slicing has been validated against *in situ* aircraft observations, offering high-quality

tropospheric NO_2 data, especially valuable in regions with limited ground-based data (Liu *et al.*, 2014; Marais *et al.*, 2018). It is particularly beneficial for assessing NO_2 distribution in areas with persistent cloud cover, enhancing the accuracy of satellite-derived gas concentration data and reducing biases (Marais *et al.*, 2018). Despite its usefulness, cloud slicing has some challenges. The accuracy of NO_2 retrieval depends on the precision of cloud characterisations, such as cloud height, optical thickness, and the specific absorption and scattering properties of both the gas and clouds. Some clouds, particularly thick or highly variable ones, can still interfere with the signal, resulting in uncertainties in the measurements. However, cloud slicing remains a valuable tool in improving the accuracy of atmospheric gas concentration measurements, particularly in regions where cloud cover is prevalent.

This satellite-based approach leverages cloud-top height data to estimate NO_2 concentrations at different altitudes, offering critical insights into NO_2 distribution across various atmospheric layers (Liu *et al.*, 2014). Choi *et al.* (2014) reported the first global estimates of tropospheric NO_2 abundances using cloud-slicing, marking a significant step forward in obtaining vertical profiles of NO_2 from satellite data.

Accurately determining the AMF for satellite observations requires consideration of several atmospheric parameters, including vertical NO_2 profiles, aerosols, clouds, and surface albedo. Even under clear-sky conditions, the uncertainty in the satellite AMF for polluted regions can be high (Heland *et al.*, 2002). A thorough understanding of the spatial and temporal variations of air pollutants is essential for modelling their transport, especially in areas where rapid fluctuations in pollutant concentrations occur. Disparities in measured NO_2 concentrations remain, and as a result, NO_x levels in the upper troposphere (above 500 hPa) are often misrepresented in models (Marais *et al.*, 2018).

Ground-based and satellite data integration has become particularly valuable in air quality studies, where these two data sources complement each other to reveal pollution patterns and trends. The DS-DOAS systems, for instance, are instrumental in assessing NO_2 concentrations. Satellite measurements offer spatially resolved insights, and ground-based instruments refine vertical profiles with high temporal resolution data (e.g., MAX-DOAS for vertical profiling). This combined approach could enhance our understanding of NO_2's role in atmospheric chemistry and pollution transport.

Chapter 3

This Chapter discusses the methods and data used to address the objectives and research questions in the study.

3 Methods and Methodology

3.1 Study Sites

Wakkerstroom (27°21'17.7"S, 30°08'37.8"E), situated in Mpumalanga province, South Africa (Figure 3.1), covers an area of 87.68 km^2 and has an approximate population of 8500. With a minimum elevation of about 1730 m above sea level, the town lies relatively close to 12 coal-fired power stations, located within a range of 48 to 214 km, which serve as significant sources of nitrogen oxide (NO_x) emissions. Positioned downwind of most of these power stations, Wakkerstroom is nearest to Camden and Majuba, with Camden lying to the northeast and Majuba to the north-west. Situated in the heart of the Highveld, the Elandsfontein site serves to measure the consolidated plume from several major NO_x sources. The monitoring stations at Kendal and Majuba are strategically positioned downwind of their namesake power plants to capture peak ground-level concentrations (Thomas and Scorgie, 2006). The Kendal monitoring station is approximately 30 km to the southwest of Emalahleni, where coal is commonly used for domestic purposes in low-income neighbourhoods (Matimolane, 2019). Additionally, NO_x emissions from agricultural activities in nearby townships and surrounding farmlands contribute to the region's atmospheric pollution (Lynch *et al.*, 2021). Due to this dense concentration of power stations, the Highveld has been recognised as a major NO_2 pollution hotspot on a subcontinental scale.

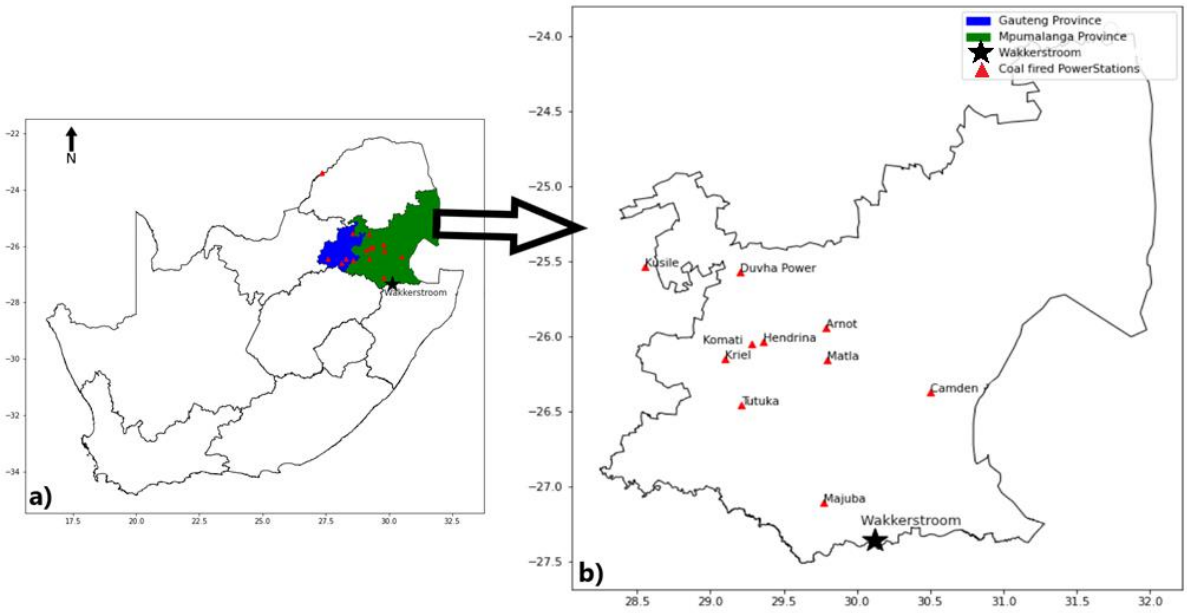

Figure 3.1: The map of South Africa highlights a) the Mpumalanga (MP) and Gauteng provinces and b) the Mpumalanga province in greater detail, showcasing the coal-fired power stations located in the Highveld region alongside Wakkerstroom.

3.2 Instruments

3.2.1 Pandora Instrument

The Pandora 2s instrument, installed in Wakkerstroom, forms part of the global ground-based Pandora sun photometer network (Pandora Global Network-PGN). The PGN, launched initially as the Pandora project, was initiated in 2006. The Pandora instrument is a compact and affordable device designed for high-precision measurements. It operates as a dual ultraviolet (UV) and visible (VIS) spectrometer, covering spectral ranges of 270 – 530nm and 400 – 900nm, with resolutions of 0.6nm for UV and 1.1 nm for VIS. The Pandora 2s is equipped with an azimuth and elevation tracker controlled by a microprocessor (https://sciglob.com/wp-content/uploads/2023/12/Pandora2S_datasheet-1.pdf), enabling it to be pointed in any direction. This functionality allows the instrument to perform integrated column direct sun/moon (DS) and multi-axis sky-scanned (MAX) DOAS observations of various trace gases, including O_3, NO_2, SO_2, and CH_2O (Herman *et al.*, 2009).

Both observation modes employ the differential optical absorption spectroscopy (DOAS) technique to detect the unique spectral signatures of trace gases. These gases absorb solar radiation at specific wavelengths within the ultraviolet to the visible spectrum, creating identifiable spec-

tral patterns (Abad *et al.*, 2019). The DS mode points directly at the sun to measure these signatures, with variations in the solar zenith angle (SZA) as the sun's position shifts. This mode provides total column amounts of trace gases. In contrast, the MAX-DOAS mode captures near-surface and tropospheric column concentrations and provides vertical atmospheric profiles of selected trace gases (Cede *et al.*, 2021). This study focused on near-surface and tropospheric vertical column data.

The MAX-DOAS technique involves scanning the sky at various elevations and azimuth angles, enabling the near-simultaneous detection of scattered light along different lines of sight (LOS) from the horizon to the zenith (Pinardi *et al.*, 2008). These elevation angles allow measurements over varying horizontal distances and provide sensitivity to different atmospheric layers. Lower elevation angles are particularly sensitive to the lower atmosphere, as the extended light path in the low troposphere amplifies light absorption by atmospheric constituents. This increased sensitivity enhances the detection of trace gases commonly found in the lower troposphere, such as NO_2, O_3, and CH_2O. Consequently, MAX-DOAS data are limited to measurements within the lower troposphere, extending up to approximately 5.5 km above ground level (Cede *et al.*, 2021).

3.2.2 Chemiluminescence Sensor

A chemiluminescence sensor is a gas analyser that uses the chemiluminescence method to measure nitrogen oxides in sample gases continuously. These sensors rely on NO_2-to-NO conversions followed by NO detection through light-emitting reactions. NO_2 is catalytically converted to NO on a heated molybdenum surface and then measured as NO by means of chemiluminescence in the reaction with ozone. This method not only converts NO_2 to NO but also partially converts other oxidised nitrogen compounds and can, therefore, cause overestimations of NO_2 between 17% and 30% (Steinbacher *et al.*, 2007). However, this technique is still widely applied, and measurements with these instruments currently provide the only available near-surface data for the regions under discussion.

3.2.3 TROPOMI Satellite

The Tropospheric Monitoring Instrument (TROPOMI) is a sensor aboard the European Space Agency's (ESA's) polar-orbiting Sentinel-5 Precursor (S5P) satellite (Azad and Ghandehari, 2022; van Geffen *et al.*, 2022). It was launched in 2017 to provide atmospheric trace gas, cloud and aerosol property measurements using shortwave infrared (SWIR), near-infrared (NIR), ultraviolet (UV) and visible (VIS) spectroscopy (van Geffen *et al.*, 2022) from an ascending Sun-

synchronous polar orbit, with the equator crossing about 13:30 local time (van Geffen *et al.*, 2022). The solar radiation is measured within the 405 – 465 nm wavelength range, and retrieval algorithms are used to derive the tropospheric NO_2 column density at 5.5 x 3.5 km^2 spatial resolution from August 2019 (Veefkind *et al.*, 2012). The first public release of TROPOMI data sets, including NO_2, was in July 2018 (van Geffen *et al.*, 2022; Eskes *et al.*, 2023). The offline (OFFL) level-2 (L2) tropospheric NO_2 column density data can currently be accessed via the Copernicus Data Space Ecosystem (CDSE; https://dataspace.copernicus.eu/, last accessed 21st June 2022). The S5P data processor has been upgraded since the start of the mission. With respect to NO_2 column amounts, the measurement process starts with the retrieval of slant column densities (SCDs). This is followed by separating the total SCDs into stratospheric and tropospheric components, depending on *a priori* vertical profile information using air-mass factors (AMFs), considering atmospheric cloud cover. The correct interpretation of TROPOMI data requires an understanding of the transfer of solar radiation in the atmosphere, and in particular of the specific absorption bands of the NO_2 pollutants.

3.3 Data

3.3.1 Pandora Data

The Pandora instrument used in this study (Pan159) is one of two official instruments on the African continent (https://blickm.ovh.pandonia-global-network.org/livemaps/pgn_stationsmap.png) and was deployed in Wakkerstroom in December 2019. The Pandora instrument at Wakkerstroom uses both DOAS techniques to measure the concentrations of NO_2, O_3, SO_2, and CH_2O. In this study, only MAX-DOAS mode products were used. The near-surface NO_2 concentrations (ppb) from the Wakkerstroom site are presented from 1st January to 31st December 2020. The tropospheric vertical column (TVC) concentrations (mol/m^2) presented in this study are from January 2020 to December 2021.

Although night-time measurements were taken using scattered light from the moon, these data were not available for analysis during the study period.

During the setup of Pandora instruments for MAX-DOAS measurements, one to three pointing azimuth (PAZI) directions are selected, typically including one direction towards a more polluted area and another in the opposite direction. For Pan159, the PAZI orientation is set at 270° (west), aligning with a view across the valley (wetland) towards the neck of the Volksrust road. Volksrust, a town approximately 27 km from Wakkerstroom, serves as a waypoint for travellers

between Johannesburg and Durban. This azimuth setting for Pan159 targets the expected pollution relative to its location. The maximum angle (MAX) of the instrument is set to 88°, reflecting the highest unobstructed viewing angle.

Sky scans are conducted in either detailed or quick modes, utilising an open hole or a U340 filter. Detailed sky scans involve zenith angles of [0, 40, 50, 60, 70, 75, 80, 82, 85, "MAX-2," "MAX-1," "MAX," "MAX-1," "MAX-2," 85, 82, 80, 75, 70, 60, 50, 40, 0], while quick sky scans use elevation angles of [0, 60, 75, "MAX-1," "MAX," "MAX-1," 75, 60, 0]. Each position is scanned twice for 15 seconds, totalling 30 seconds per position. Quick scans using the open hole filter are performed at 0, 60, 75, "MAX-1," "MAX," "MAX-1," 75, 60, and 0-degree zenith angles, also for 30 seconds per position. Depending on the routine schedule and sun searches for DS measurements, the measurement frequency is approximately 13 minutes.

Pan159 data are assigned Data Quality Flag (DQF) values to indicate their uncertainty and usability (see Table 3.1). Pandora Level 2 (L2) data quality flags are further detailed in Cede *et al.* (2021). This study used data with DQFs of 0/10 and 1/11 for the near-surface analyses and high-quality data with DQFs of 0 or 10 for the TVC analyses.

Table 3. 1: Pandora instrument data quality flags (DQFs) and their meanings

Data quality flag (DQF) value	Explanation
0	High-quality data (quality assurance applied)
1	Medium-quality data (quality assurance applied)
2	Low-quality data (quality assurance applied)
10	High-quality data (quality assurance not applied)
11	Medium-quality data (quality assurance not applied)
12	Low-quality data (quality assurance not applied)
20	Unusable data
21	Unusable data
22	Unusable data

The near-surface- and TVC-NO_2 data were obtained from https://data.ovh.pandonia-global-network.org/Wakkerstroom/Pandora159s1/L2/Pandora159s1_Wakkerstroom_L2_rnvh3p1-8.txt. For near-surface data analyses, the measurements were averaged weekly with standard deviations for the 12 months. This provided the best data recovery, given the missing data for several months due to the lack of electricity during those periods. For the TVC data analyses, annual and weekly means and medians were calculated for January 2020 to December 2021. The data were also grouped by season.

3.3.2 Eskom Data

This study used surface NO_2 concentrations spanning six years (2015 to 2020) from three Eskom air quality monitoring sites: Kendal, Majuba and Elandsfontein. These data were measured hourly. The original data were averaged weekly, and weekly means and standard deviations are reported in this study.

3.3.3 TROPOMI Data

This study utilised TVC-NO_2 data product version 2.4.0 (van Geffen *et al.*, 2022; Eskes and Eichmann, 2023; Eskes *et al.*, 2023) from January 2020 to December 2021. Each TROPOMI satellite ground pixel output is assigned a quality indicator, referred to as the "quality assurance

value" (qa_value), to denote the accuracy of the retrieved trace gas amount (van Geffen *et al.*, 2022). Only pixel outputs with qa_value ≥ 0.75, representing cloud-free and error-free conditions (Eskes *et al.*, 2023), were included in this study.

The original TROPOMI data were regridded to a 0.01° resolution, allowing for the selection of a region around Wakkerstroom that represents the area observed by the Pandora instrument using MAX-DOAS. A 0.1° x 0.05° area centred on Wakkerstroom was chosen, and the data from this region were averaged. Weekly means, medians, and standard deviations are reported in this study.

3.3.4 Evaluation Analyses

The evaluation approach (Judd *et al.*, 2020; Zhao *et al.*, 2020) utilised Pandora-2s TVC-NO_2 concentrations within two specific timeframes: 1) ±5 minutes of the TROPOMI overpass and 2) within the hour of the TROPOMI overpass. The two timeframes were chosen to ascertain that there are enough coincidence data for each TROPOMI overpass. For the analyses, only data from the TROPOMI pixel closest to the Wakkerstroom site were used.

All TROPOMI data included in the regression analyses had qa-values ≥ 0.75, while Pandora data had DQF values of 0 or 10. TROPOMI data with qa-values ≥ 0.75 exclude observations from cloudy scenes (cloud radiance fraction > 0.5), snow/ice-covered areas, or retrievals deemed unreliable. The ±5-minute coincidence measurements refer to Pandora observations taken within 5 minutes before or after the TROPOMI overpass, while the one-hour coincidence data encompass Pandora observations within the overpass hour, averaged for analysis.

Regression statistics, including the correlation coefficient (R), p-value, and regression line, were calculated using Theil-Sen regression in RStudio®. The normalised mean bias (NMB) was computed using Equation 1, with Equation 2 used for determining NMB percentage. Additionally, Relative Squared Errors (RSEs) were calculated for all regressions to assess the validity of the models used in this study.

Equation 1: Normalised Mean Bias = $$\frac{\sum_{1}^{n}(M - O)}{\sum_{1}^{n}(O)}$$

Equation 2: Normalised Mean Bias (%) = $\frac{\sum_{1}^{n}(M - O)}{\sum_{1}^{n}(O)}$ x100

*O = Pandora-2s measurements *M = TROPOMI measurements

3.3.5 Vertical Profiles Data

The Pandora-2s instrument in MAX-DOAS mode provides vertical profiles of NO_2. These data were obtained from the PGN official website (https://data.ovh.pandonia-global-network.org/Wakkerstroom/Pandora159s1/L2/Pandora159s1_Wakkerstroom_L2_rnvh3p1-8.txt).

3.3.6 *A priori* Profile Data

The NO_2 profiles (*a-priori* profile shapes) were obtained from the TM5-MP (Tracer Model, version 5), a chemistry-transport model used to generate highly resolved vertical profiles of NO_2 and other trace gases for satellite retrieval processes (Williams *et al.*, 2017). These profiles were extracted using a Python tool developed by the Koninklijk Nederlands Meteorologisch Instituut (KNMI). The Python tool to extract this auxiliary product is available in the Product User Manual (PUM TM5 AUX Product), accessible at Sentinel's official website (see https://sentiwiki.copernicus.eu/web/s5p-products).

3.3.7 Hybrid Single-Particle Lagrangian Integrated Trajectory (HYSPLIT) Frequency Cluster Data

The HYSPLIT model is a comprehensive system used for computing air parcel trajectories as well as performing complex simulations of transport, dispersion, chemical transformations, and deposition using meteorological data (Rolph, Stein and Stunder, 2017; Cui, Song and Zhong, 2021). Developed by the National Oceanic and Atmospheric Administration (NOAA) Air Resources Laboratory (ARL) (Stein *et al.*, 2015; Rolph, Stein and Stunder, 2017), this model is capable of tracking and forecasting the release of dust, ash, volcanic particles, and pollutants from both stationary and mobile emission sources (Rolph, Stein and Stunder, 2017). The simulations produce trajectories that are clustered and presented by their mean trajectory. Clustering is done using the similarity principle, where data points with higher similarity are grouped, and those with higher heterogeneity are separated into different groups (Cui, Song and Zhong, 2021). The trajectories are grouped until the total variance of the individual trajectories from

the cluster mean begins to increase significantly (Stunder, Heffter, and Draxler, 2007 loc sit Stein *et al.*, 2015).

Version 5.2.0 of the HYSPLIT model was utilised to determine the trajectories of air masses arriving at Wakkerstroom from 2020 to 2021, potentially carrying pollutants that could influence the NO_2 tropospheric levels. Backward trajectories were simulated at 700 hPa and 550 hPa based on the atmospheric partial profiles of the Pandora-derived TVC-NO_2 concentrations and a priori profile shapes from the TROPOMI retrieved TVC-NO_2 concentrations from January 2020 to December 2021. Ten- and five-day backward trajectories were used instead of one- or two-day backward trajectories, even given the short lifetime of atmospheric NO_2. Ten- and five-day backward trajectories were used because South Africa's atmosphere is predominantly stable under the influence of the continental high-pressure system that prevails for most days of the year. Using shorter timescale backward trajectories might not show the recirculation patterns or the source of the TVC-NO_2 concentrations.

To address objective one, ten-day backward trajectories were calculated for every day of 2020, starting at midday at the monitoring site. The trajectories were visually classified into five distinctive transport pathways, and the frequencies of each pathway were calculated as a percentage for a total of 366 days. Additionally, trajectory pathways were used to determine the likely atmospheric transport of the highest and lowest concentrations of NO_2 at Wakkerstroom.

Five-day backward trajectories were used to address objectives two and three. The HYSPLIT model simulated and merged the five-day backward trajectories to create trajectory clusters for 2020 and 2021, which were then grouped into four clusters based on spatial variance. These clusters were used to assess the nature and extent of primary air mass transport to Wakkerstroom, distinguishing between oceanic, clean continental, and polluted continental air masses. Transport pathways, in line with synoptic circulation patterns, assume that air masses mix as part of these patterns (Tyson, 1997).

3.3.8 Meteorological Data

The dispersion and transport of trace gases like nitrogen dioxide (NO_2) in the atmosphere are influenced by meteorological conditions, which play a crucial role in the stability of the atmosphere and, consequently, the chemical and physical processes that govern the accumulation of pollutants. Solar irradiance, which affects the ambient air temperature, is directly related to the dissociation of NO_2 in the atmosphere (Balashov *et al.*, 2014). Wind speed and direction also

contribute to the dispersion of pollutants by transporting them from and to emission sources (Balashov *et al.*, 2014). Additionally, the removal of pollutants from the atmosphere is influenced by rain and humidity, which lead to wet deposition (Seinfeld and Pandis, 2016).

Meteorological data from the Wakkerstroom monitoring site (Figure 1.1), measured using the HOBO® weather station and accessed through a CR300 logger, are utilised in this study. These measurements provide near-surface or ground-level data on temperature, rainfall, relative humidity, wind speed, and wind direction. All variables were recorded as hourly averages and were averaged weekly for this study. The wind direction data were averaged following a technical note by Grange (2014) using Rstudio®. The meteorological data used in the study covers the one-year analysis period for 2020 to address objective one.

Chapter 4

This Chapter contains the manuscript, Kai, R. F., Scholes, M.C., Piketh, S. J., and Scholes, R. J. Analysis of the first surface nitrogen dioxide concentration observations over the South African Highveld derived from the Pandora-2s instrument. *Clean Air Journal*. 2022, *32*(1), 1 – 11. https://dx.doi.org/10.17159/caj/2022/32/1.13242. The text in the Preface describes why this paper was written, and the text in the Postscript concludes with what was achieved and possible future directions of research.

4 Analysis of the first surface nitrogen dioxide concentration observations over the South African Highveld derived from the Pandora-2s instrument

4.1 Preface

Global studies provide evidence that NO_2 concentrations contribute significantly to pollution and negatively impact environmental and human health. There is a shortage of high-resolution data for ground-based NO_2 concentrations in the highly industrialised South African Highveld, but there is some published evidence that NO_2 concentrations are high. The sources of these NO_2 concentrations originate from coal-burning power stations, other industries, and biomass burning. The acquisition of the Pandora-2s instrument allowed for the monitoring and recording of near-surface NO_2 concentrations in Wakkerstroom, located downwind of a large number of pollution sources. This location allowed for the identification of the major source of the measured NO_2 concentrations. The instrument facilitated the measurements of near-surface NO_2 concentrations at well-resolved spatial and temporal resolution.

Research article

Analysis of the first surface nitrogen dioxide concentration observations over the South African Highveld derived from the Pandora-2s instrument

Refilwe F. Kai[*1], **Mary C. Scholes**[1], **Stuart J. Piketh**[2], **Robert J. Scholes**[3]

[1]University of the Witwatersrand, School of Animal, Plant and Environmental Sciences, Johannesburg, South Africa, [2]North-West University, Unit for Environmental Sciences and Management, Potchefstroom, South Africa

[3]University of the Witwatersrand, Global Change Institute, Johannesburg, South Africa

Received: 19 February 2022 - **Reviewed:** 25 March 2022 - **Accepted:** 5 May 2022

10.17159/caj/2022/32/1.13242

Abstract

Anthropogenic emissions from industry, biomass burning and traffic are significant contributors to the atmospheric loading of nitrogen dioxide on the South African Highveld. These sources are dispersed across the region and emit nitrogen oxides (NO and NO_2) into the atmosphere at different elevations above the earth's surface. Additionally, atmospheric stability in the form of surface and elevated inversions decreases the dispersion of air pollutants and stratifies pollutants into distinctive layers above the surface. This study explores the Highveld near-surface nitrogen dioxide concentrations obtained using the ground-based Pandora-2s monitoring system. The Pandora-2s instrument retrieves surface NO_2 levels from clear sky measurements using a fully parameterised algorithm. We present the first near-surface concentration measurements of atmospheric NO_2 at Wakkerstroom, a site between Volksrust and Amersfoort, downstream of major source conglomerates, the Majuba power station and other industries. These data are explored in the presence and context of potential background NO_2 concentrations in the area derived from other ground-based sensors. The quasicontinuous data show elevated surface NO_2 levels in week 37 (September) of 2020 (7.3 ± 5.7 ppb), while the lowest levels were observed in week 15 (April) of 2020 (0.2 ± 0.04 ppb). The elevated surface NO_2 levels are driven by dominant emission sources and transport trajectories, while the accuracy in the measurements is based on the high temporal resolution of the ground-based Pandora-2s instrument.

Keywords

Nitrogen dioxide, Pandora-2s, plumes, Eskom, Highveld

Introduction

The South African Highveld region, characterised by elevations of ~700 – 2000 m above sea level, comprises portions of the inland provinces, including Mpumalanga (Balashov et al., 2014; Freiman and Piketh, 2003). Mpumalanga is home to approximately ninety-six registered stationary facilities that emit pollutants into the atmosphere, including most of South Africa's coalfired power stations (https://saaelip.environment. gov.za/ accessed 23rd June 2021). These emissions and others from anthropogenic activities such as domestic biomass burning, vehicular emissions, and solid fuel combustion result in elevated levels of pollutants, particularly sulphur dioxide (SO_2), carbon dioxide (CO_2), particle matter (PM) and nitrogen oxides (NO_x) (NO + NO_2) (Alade, 2011; Belelie et al., 2019; Hickman et al., 2021; Naiker et al., 2012; Shikwambana et al., 2020). As a result, there is a persistent pool of pollutants in the Highveld atmosphere (Lourens et al., 2012). Coal-fired power stations produce electricity by converting thermal energy produced through coal combustion into electrical energy (Wang et al., 2020). During the coal combustion process, which accounts for ~65% of the global total NO_x emissions (Bauwens et al., 2020), nitrogen oxides are produced (Scorgie and Thomas, 2006), released into the atmosphere (Breeze, 2015), where they contribute to the atmospheric chemistry. Therefore, the plethora of emissions in the highly industrialised Highveld region contributes to the reported increased atmospheric levels of nitrogen oxides (NO_x) (NO + NO_2) (Celarier et al., 2008). As a result, the Mpumalanga Highveld is known as the major (> 80% of emissions in South Africa) emission region of nitrogen oxides (NO_x) (Collett et al., 2010). Atmospheric NO emissions are highly reactive and have

a distinctive diurnal cycle attributed to photolysis reactions (Celarier et al., 2008; Verhoelst et al., 2021). In the presence of solar radiation, they transform into NO_2. In the presence of volatile organic compounds (VOCs) and sunlight, the NO_2 forms ozone (O_3) (Hakkarainen et al., 2021; Wang and Hao, 2012), a secondary air pollutant. The rate at which O_3 is produced is determined by the NO_x emission time and location (Wedow et al., 2021). These emissions also play a role in forming secondary organic aerosols (SOAs), nitric acid and nitrates (Qi et al., 2020; Verhoelst et al., 2021). Therefore, these NO_x chemical transformations contribute to the formation of smog and acid rain (Qi et al., 2020; Verhoelst et al., 2021).

In addition to chemical processes, these emissions are subjected to various other processes linked with meteorological conditions, determining their dispersion and transport from the source region (Belelie et al., 2019). Ultimately, it has been deduced that principal pollutants such as NO_x play a critical role in indicating regional air quality (Behm and Haupt, 2020; Brancher, 2021; Wang and Hao, 2012; Zyrichidou et al., 2015).

Therefore, it is important to accurately quantify the distributions, trends and cycles of nitrogen dioxide levels in the atmosphere, particularly near the surface where most of the emissions originate. These have been measured from space using Low Earth Orbit (LEO) satellites since the 1970s (Verhoelst et al., 2021). However, the lack of continuous trace gas monitoring data is still a concern (de Lange et al., 2021; Omrani et al., 2020; Shabbir et al., 2016) in air quality research. The scarcity of data is also affected by the challenge in acquiring and extracting accurate atmospheric column trace gas measurements in cloudy conditions.

This study reports on the first near-ground (surface) nitrogen dioxide measurements from the Pandora-2s instrument in the Mpumalanga, South African Highveld. In contrast to the LEO satellites, the Pandora-2s is a ground-based instrument that derives measurements of atmospheric trace gases using one of three observation modes: direct sun, direct moon or MAXDOAS (multi-axis differential optical absorption spectroscopy) (Cede et al., 2021). In addition to that, it provides uninterrupted measurements instead of the once-a-day measurements from the current satellite instruments. This instrument was optimised to retrieve nitrogen dioxide column concentrations under cloudy conditions.

These first-time measurements will be used to assess the near- surface concentrations of NO_2 downwind the region of major Highveld emissions sources, in Wakkerstroom, Mpumalanga. We have used near-surface air quality data from three Eskom air quality monitoring sites (Kendal, Majuba and Elandsfontein) to compare the remotely derived NO_2 concentrations from the Pandora-2s instrument. Meteorological variables and kinematic backward trajectory analyses indicate near-ground nitrogen dioxide pollutant signatures.

Data and methodology

Four data sets have been used in this study: near-surface atmospheric column NO_2 concentrations from a Pandora-2s (Pan159) instrument; near-surface NO_2 gas concentrations from Eskom's Majuba, Kendal and Elandsfontein monitoring stations; surface meteorological data collected at Wakkerstroom; and backward kinematic trajectories calculated for Wakkerstroom. Details of the data and methods are provided below.

Instrumentation

The Pandora-2s instrument can obtain measurements in three observation modes; direct sun, direct moon or MAXDOAS (multi-axis differential optical absorption spectroscopy) (Cede et al., 2021). The MAXDOAS viewing geometry retrieves surface nitrogen dioxide concentrations (Herman et al., 2009) amongst other product outputs. The measurements are processed using the "L2 Air-Ratio Sky Algorithm (Cede et al., 2021). A fully parameterised algorithm (which does not require elaborative radiative transfer calculations) is then used to extract the real- time quasi-continuous surface concentration data (Cede, 2021; Tiefengraber et al., 2021).

Further details regarding the algorithm can be found in Cede (2021). Quasi-continuous data are discontinuous and are characterised by "events" (much higher than the average data) in the observations. These data are typical of atmospheric trace gas and meteorological variables measurements.

More characteristics of the dual spectrometer Pandora-2s instrument can be found in Herman et al. (2009) and Zhao et al. (2020, 2016). The extracted surface concentrations are from within the first 50 m above the ground. During winter and autumn, they are monitored between 06h00 and 17h00, and 05h00 to 18h00 in the summer and spring due to the instrument relying on sky radiance for measurements.

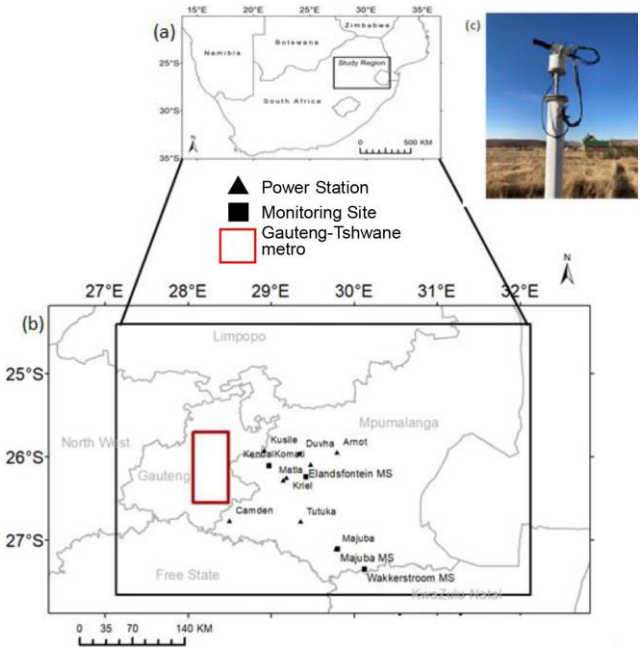

Figure 1: *a) A map of Southern Africa and surrounding countries. b) Map of the Gauteng and Mpumalanga provinces of South Africa, indicating the site locations where this study's surface nitrogen dioxide concentrations were monitored. c) Inset: The Pandora-2s (Pan159) instrument in situ at the Wakkerstroom monitoring site.*

Surface NO_2 data

The Pandora-2s instrument was primarily installed at Wakkerstroom to investigate the biogeochemical exchange of trace gases in ecosystem functions. Nitrogen biogeochemical flows, amongst others, contribute to the functioning of ecosystem services such as climate regulation (Watanabe and Ortega, 2011; Xu et al., 2021). The Wakkerstroom monitoring site is directly downwind of the Majuba Power station (PS) and the greater Highveld region and is ideally located to detect the high NO_x emissions and subsequent transport. The Pandora-2s instrument at Wakkerstroom, Mpumalanga, is part of the Pandora Global Network (PGN) ("NASA Pandora Project," last accessed: 18th September 2021) (Figure 1). The surface NO_2 data from the Wakkerstroom site are presented from 1st January to 31st December 2020. Although night-time measurements were taken using the moon as a reference, these data have not been included in this initial analysis. Weekly average surface concentrations have been calculated from the Pandora-2s data set. This provided the best data recovery, given missing data for several months.

Additionally, nitrogen dioxide data from three Eskom air quality monitoring sites (MS), namely Kendal, Majuba and Elandsfontein in Mpumalanga, are presented to provide comparative in situ surface measurements. The Elandsfontein MS is centrally located on the Highveld and represents an integrated plume from multiple significant NO sources. Kendal and Majuba monitoring sites are located downwind of the similarly named power stations to detect maximum surface concentrations (Thomas and Scorgie, 2006). The Kendal monitoring site is also ~30 km southwest of Emalahleni, with low-income townships where domestic coal is prevalent (Matimolane, 2019).

Data at the three Eskom monitoring sites above are continuous, with hourly averaging times collected between July 2015 and May 2020. In order to create comparable data sets, weekly average values were calculated from the continuous data sets.

NO_2 data description and acquisition

The Pandora-2s instrument data are processed to produce outputs; the total, tropospheric, and surface concentration. Data from the Pandonia global network (https://www.pandonia-globalnetwork.org/pgn-data/) were cleaned and analysed using Rstudio® and Excel® statistical software. Eskom provided the air quality monitoring data from Kendal, Majuba and Elandsfontein monitoring sites.

NO_2 data cleaning

The data from the Pandora instrument are filtered and flagged using data quality indicators, high, medium and low quality, which specify the confidence in the data. The quality of the data depend on the measurements' uncertainties during monitoring. Various factors contribute to the uncertainty in measurements; noise, permanent systematic effects, temporary systematic effect, calibration transfer uncertainty, transport uncertainty and drift correction uncertainty (Cede and Tiefengraber, 2013. The low-quality data should not be used for most purposes and are not presented in these observations. The first-time Pandora-2s instrument (Pan159) measurements at Wakkerstroom provided semi-continuous data that had gaps. The surface NO_2 concentrations are impacted by cloud cover as they depend on sky radiance for successful retrieval (Tiefengraber et al., 2021; Zhao et al., 2019).

Meteorological data

The dispersion and transport of trace gases such as nitrogen dioxide in the atmosphere depend on meteorological conditions (Goldberg et al., 2020). These conditions determine the atmosphere's stability and, therefore, the chemical and physical processes that affect the atmospheric accumulation of pollutants (Balashov et al., 2014). The ambient air temperature depends on solar irradiance, and they both affect the dissociation of NO_2 in the atmosphere (Balashov et al., 2014; Goldberg et al., 2020). The wind speed and direction contribute to the dispersion and transport of the pollutant around and to-and-from the source of emissions (Balashov et al., 2014). The removal rate of pollutants from the atmosphere is also dependent on rain and humidity through wet deposition (Seinfeld and Pandis, 2016).

Meteorological data from the Wakkerstroom monitoring site (Figure 1), measured using the HOBO® weather station and accessed through a CR300 logger, are used in this study. The measurements are near-surface/ground level values of temperature, rainfall, relative humidity, wind speed and wind direction. All variables were recorded as hourly averages. The wind direction data were averaged according to a technical note by Grange (2014) using Rstudio®. All variables data are available for the one year (2020) analysis period.

HYSPLIT backward trajectory analysis

The major atmospheric transport pathways to Wakkerstroom were computed using the HybridSingle-Particle Lagrangian Integrated Trajectory (HYSPLIT) model (https://www.ready.noaa.gov/HYSPLIT.php) at 850 hPa. The trajectory represents the temporal and spatial path of trace gases in masses of air in the atmosphere. Backward trajectories are used to identify the source region of atmospheric constituents (Bera et al., 2021).

Ten-day backward trajectories were used to determine the origin of the air masses to Wakkerstroom. The model uses a hybrid between the Lagrangian approach and the Eulerian methodology. The former uses a "moving frame of reference for the advection and diffusion calculations as the trajectories or air parcels move from their initial location", while the latter "uses a fixed three-dimensional grid as a frame of reference to compute pollutant air concentrations" (Stein et al., 2015).

Ten-day backward trajectories were calculated for every day of 2020, starting at the monitoring site at midday. The trajectories were visually classified into five distinctive transport pathways, and frequencies of each pathway were calculated as a percentage for the total of 366 days. Additionally, trajectory pathways were used to determine the likely atmospheric transport of the highest and lowest concentrations of NO_2 at Wakkerstroom.

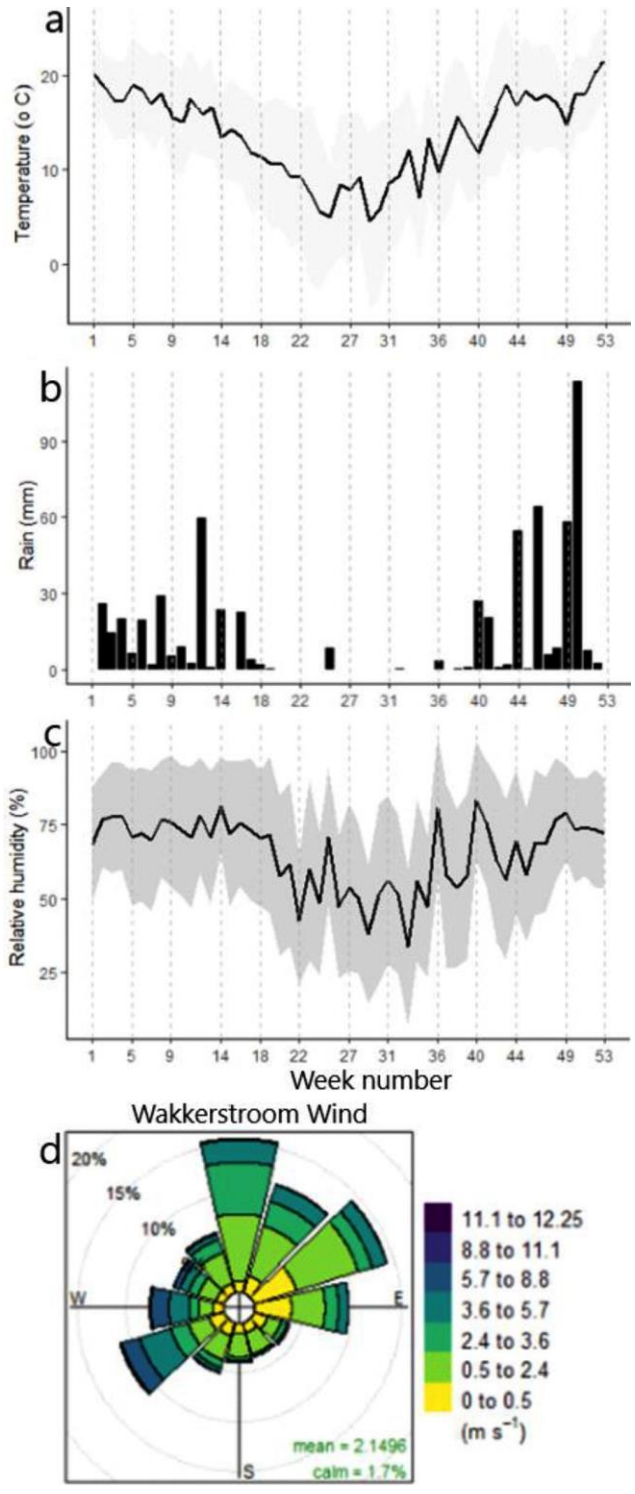

Figure 2: *Weekly averaged meteorological variables at Wakkerstroom, January to December 2020. a) temperature, b) rainfall, c) relative humidity, and d) wind direction and speed. The shaded areas (a and c) show the standard deviation, and the dashed vertical lines (a-c) the start of a new month.*

Results

Meteorology conditions at Wakkerstroom

The temperature data measured at Wakkerstroom are consistent with the seasonal variation in South Africa (Walt and Fitchett, 2020). Temperatures (Figure 2a) decrease in April, reaching an all-time low in July (week 29). The highest temperature was recorded in December 2020 (week 53).

The rainfall data (Figure 2b) shows less rainfall from May to early September 2020 with the wet season starting from October 2020. The highest rainfall was seen in week 50 (December 2020).

The relative humidity percentages (Figure 2c) were highest in weeks 36 (September 2020) and 40 (October 2020), while the lowest was seen in week 33 (August 2020).

The wind rose (Figure 2d) shows that the dominant wind directions for 2020 were from the northerly to easterly sectors (>40%) (Figure 2d). The wind also blew fairly frequently from the south-westerly and westerly sectors (~20%).

Atmospheric transport to Wakkerstroom

The transport pathways identified to Wakkerstroom are similar to the patterns obtained in previous studies for the Highveld (Freiman and Piketh, 2003) (Figure 3). Air transport is recirculated on the scale of approximately 500 km over the interior of South Africa for ~41% of days in 2020. Air originating from the south also represents an important pathway (30%). Approximately 5.2% (least) of the transport pathways originate from the southwest direction. Two other less dominant transport pathways were identified, namely, direct transport from the east coast of South Africa (~11) as well as recirculated air that passes over neighbouring countries to the North before reaching Wakkerstroom from the north-west (~13%). The trajectory

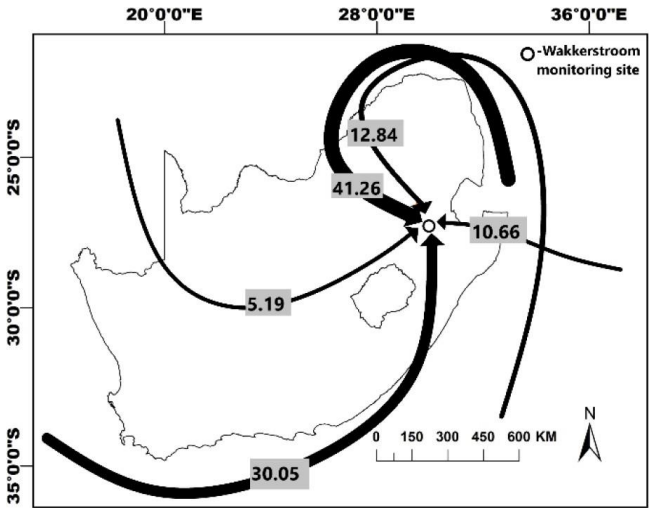

Figure 3: *Schematic diagram depicting a summary of HYSPLIT backward trajectory path frequencies at Wakkerstroom, Mpumalanga for the year 2020. The arrows are drawn relative to the pathway frequencies in the depicted direction. The numbers on the arrows show the percentage frequencies in the depicted direction.*

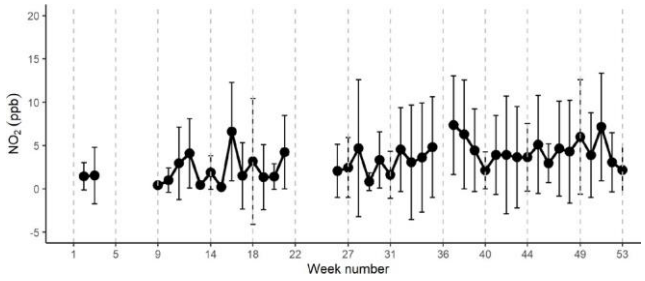

Figure 4: *Twelve months (53 weeks) of weekly Pandora-2s surface nitrogen dioxide concentration averages (diurnal averages) at the Wakkerstroom monitoring site in the Mpumalanga Highveld. The error bars show the standard deviation, and the dashed vertical lines show the beginning of a new month in 2020.*

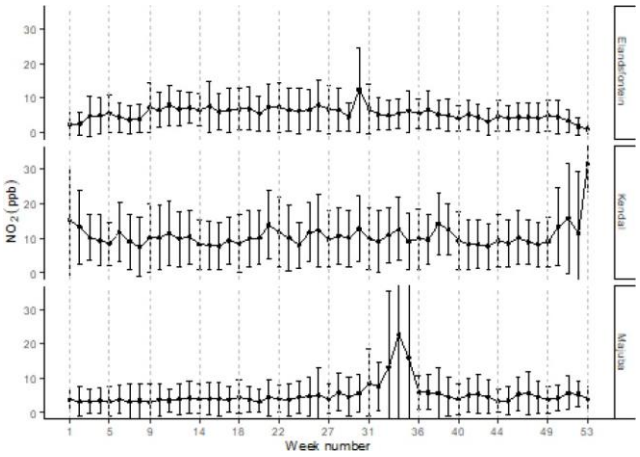

Figure 5: *Six years (2015 – 2020) of weekly averaged ambient air nitrogen dioxide concentrations from three Eskom monitoring sites (Elandsfontein, Kendal, and Majuba) in the Mpumalanga Highveld. The error bars show the standard deviation, and the dashed vertical lines show the beginning of a new month.*

analysis is consistent with the prominent wind pattern at Wakkerstroom shown in the wind rose (Figure 2d).

Surface nitrogen dioxide concentrations and meteorology over the Highveld

Surface level NO_2 concentrations measured by the Pandora-2s instrument are given in Figure 4. These average surface NO_2 concentrations fluctuate between 0.2 and 7.0 ppb (±0.04 and ±5.7) (Figure 4). These concentrations are lower than the South African National Air Quality Standards (NAAQS) of 40 ug/m^3 (21.3 ppb) per 1-year average. Maximum surface concentrations at Wakkerstroom only just exceeded 10 ppb. The highest concentrations were detected during weeks 37 (September 2020), 16 (April 2020) and 50 (December 2020), which fall in three different seasons. There is no distinct seasonal cycle visible in the Pandora-2s data at Wakkerstroom.

By comparison, the weekly variation of the surface nitrogen dioxide concentrations at the three Eskom monitoring sites did not show a great deal of variation throughout the year. Average weekly concentrations at Kendal, Majuba and Elandsfontein, were 10.4 (±9.1) ppb, 5.3 (±11.8) ppb and 5.8 (±5.6) ppb, respectively (Figure 5). The large standard deviation between the weekly averages is attributed to the high difference in the means ranging from 7.5 ppb to 31.47 ppb, 3.24 ppb to 27.62 ppb and 1.18 ppb to 12.53 ppb at Kendal, Majuba and Elandsfontein, respectively. Kendal MS showed the most weeks with higher NO_2 concentrations than the other monitoring stations. The Kendal MS is 2 km south south-east (almost directly below) of the Kendal PS and is aligned to capture the direct high concentration plumes from the Kendal PS. At the Kendal MS there is some indication of small increases during the initial summer months (November and December 2020). Concentrations at Elandsfontein and Majuba were lower overall. Majuba monitoring site showed the most significant evidence of a seasonal peak occurring from the end of July to the middle of September. At the Majuba MS, surface NO_2 concentrations exceeded 10 ppb during this season.

The comparison between the Pandora-2s data and the in-situ surface monitoring stations gives confidence that the algorithm for deriving surface concentrations from the column integrated data gives reasonable values at the Wakkerstroom site.

Atmospheric transport of highest and lowest NO_2 concentrations to Wakkerstroom

To better understand the drivers of the observations at Wakkerstroom, daily trajectories were calculated for the weeks with the highest (week 37, 51 and 16) and lowest (week 15 and 9) NO_2 concentrations.

The highest concentrations (7.5 ppb ±5.7) were detected from the 7th to the 13th September 2020 (week 37). Transport of air masses to the Wakkerstroom during this week was predominantly from the east and north-east. Four out of the seven days (Figure 6b-d and f) show trajectories that pass directly over eSwatini before arriving at the Wakkerstroom MS. The remaining three days have regional scale recirculation occurring (7th, 11th and 13th September 2020) (Figures 6a, 6e and 6g). The transport over eSwatini during this week is the most likely source of the elevated surface NO_2. Fire count data from the Moderate Resolution Imaging Spectro-radiometer (MODIS) confirms a high number of fire activity over the east coast of South Africa and in eSwatini during September 2020, particularly during week 37 (Figure 11).

The weeks with the second (7.1 ppb ±6.2) and third highest (6.6 ppb ±6.2) surface NO_2 weekly averaged concentrations (week 51 and week 16) from the Pandora-2s instrument show atmospheric transport dominated by regional scale recirculation, particularly week 16. The trajectories show transport over the eSwatini region, during week 51 (Figure 7 and 8). The regional scale recirculation transport patterns would certainly accumulate NO_2 concentrations over the source region of the Highveld as well as the greater Johannesburg (Gauteng-Tshwane metropolitan) region.

During the weeks with the lowest nitrogen dioxide concentrations (weeks 15 and 9), most of the air masses arriving

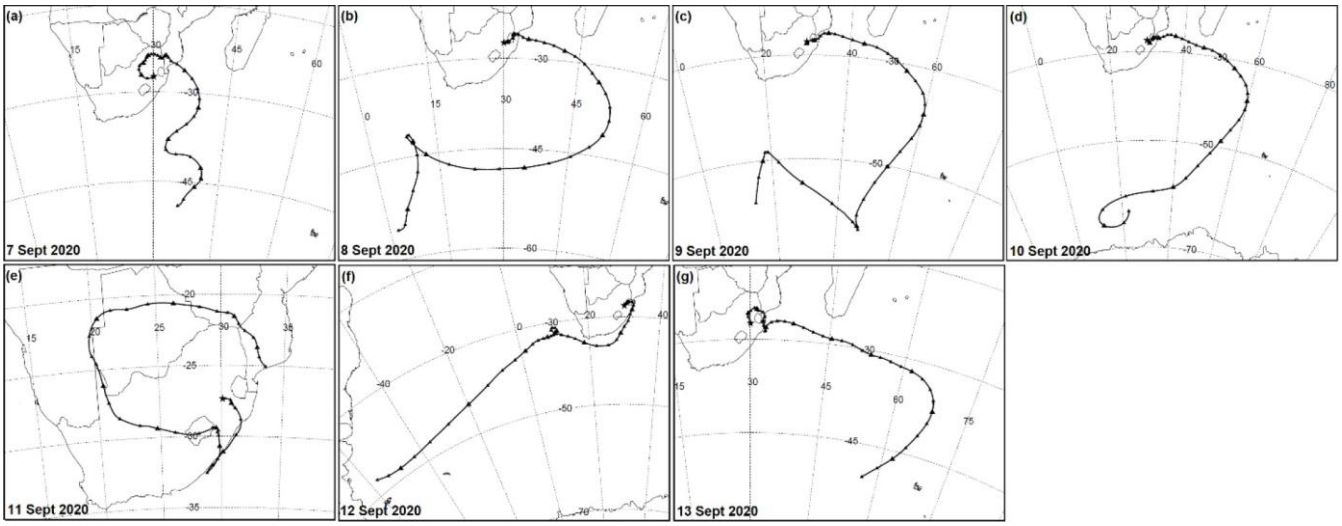

Figure 6: *The HYSPLIT backward trajectory paths to Wakkerstroom at 850 hPa during the week (week 37) (a-g) with the highest nitrogen dioxide concentration measurements from the Pandora-2s instrument at the Wakkerstroom monitoring site in 2020.*

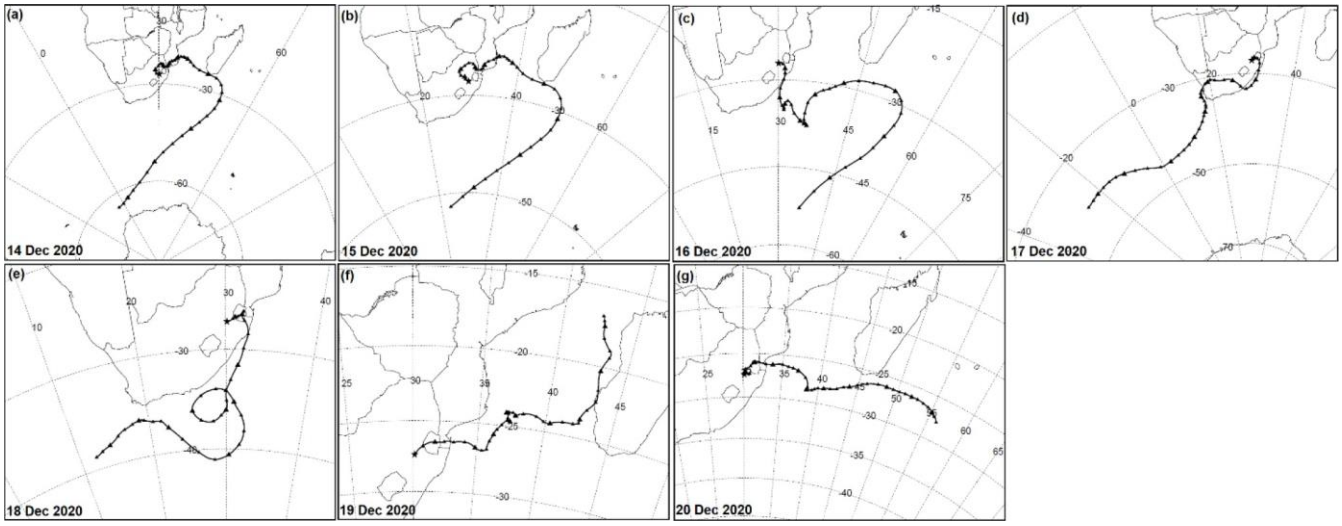

Figure 7: *The HYSPLIT backward trajectory paths at 850 hPa during the week (week 51) (a-g) with the second-highest nitrogen dioxide concentration measurements from the Pandora-2s instrument at the Wakkerstroom monitoring site in 2020.*

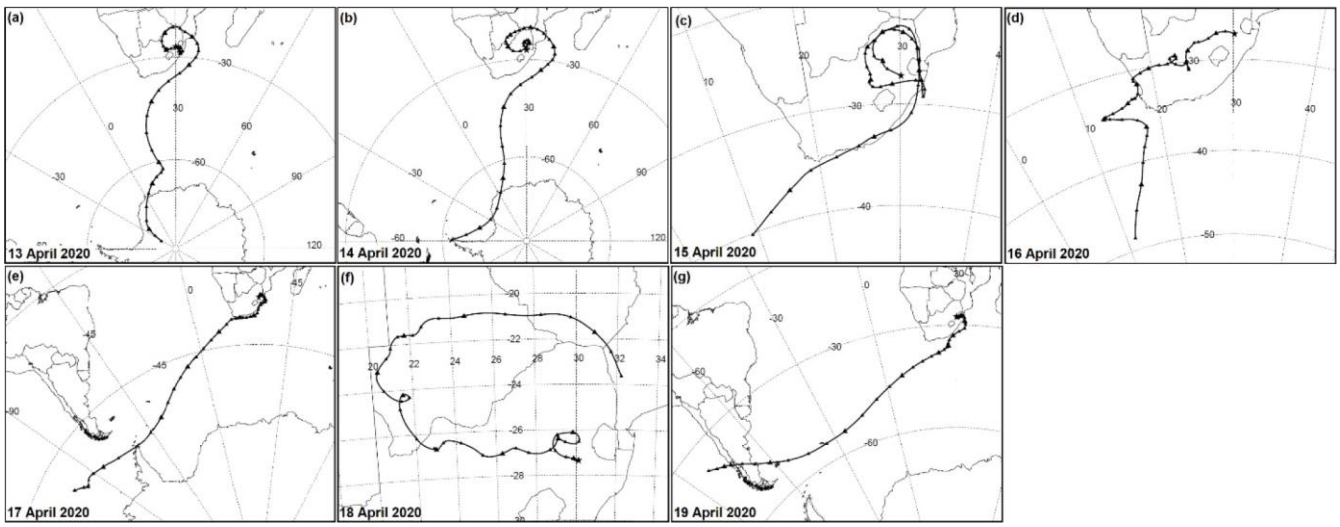

Figure 8: *The HYSPLIT backward trajectory paths at 850 hPa during the week (week 16) (a-g) with the third-highest nitrogen dioxide concentration measurements from the Pandora-2s instrument at the Wakkerstroom monitoring site in 2020.*

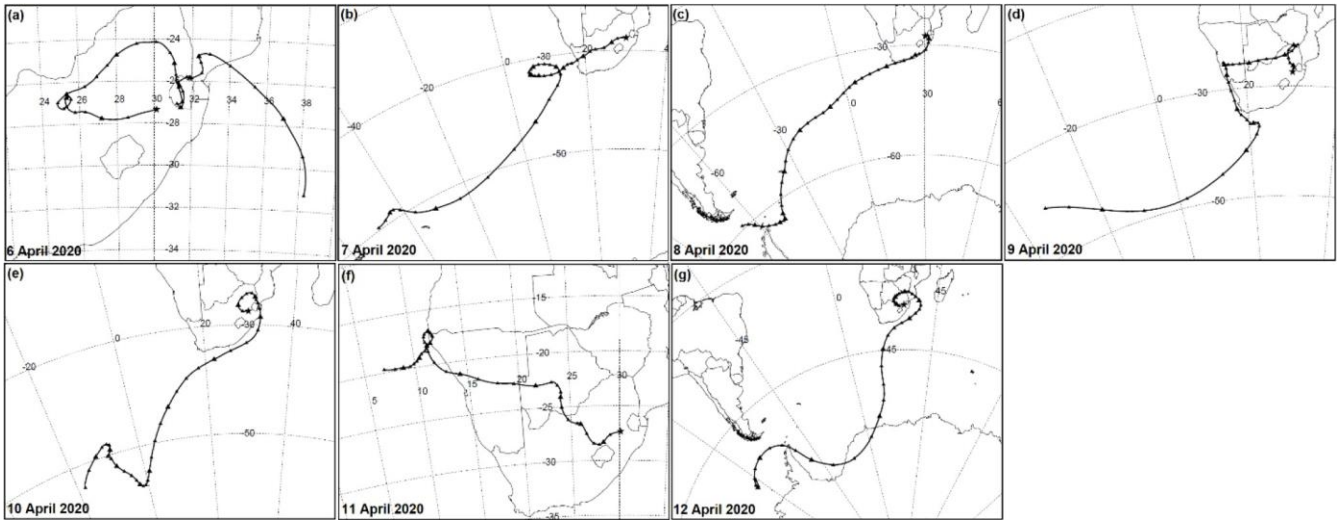

Figure 9: *The HYSPLIT backward trajectory paths at 850hPa during the week (week 15) (a-g) with the lowest nitrogen dioxide concentration measurements from the Pandora-2s instrument at the Wakkerstroom monitoring site in 2020.*

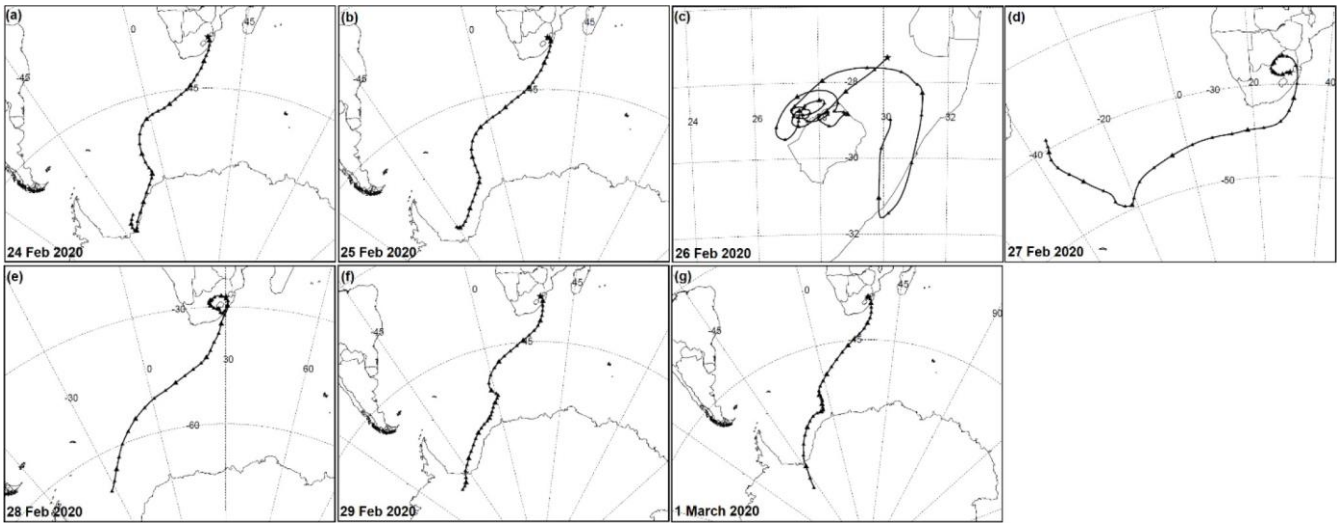

Figure 10: *The HYSPLIT backward trajectory paths at 850 hPa during the week (week 9) (a-g) with the lowest nitrogen dioxide concentration measurements from the Pandora-2s instrument at the Wakkerstroom monitoring site in 2020.*

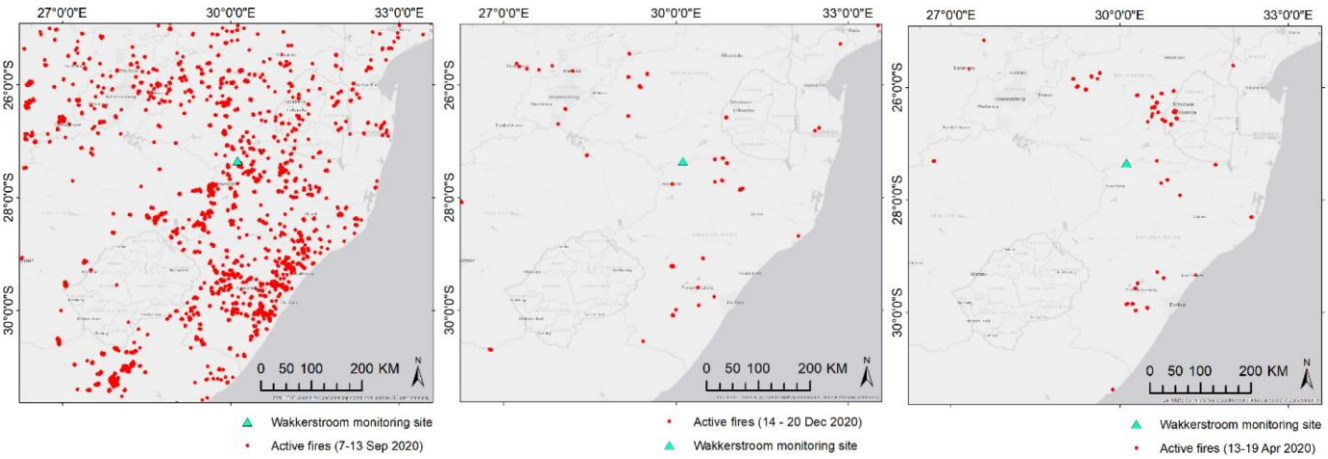

Figure 11: *The MODIS fire count (red dots) product for week 37 (left), 51 (centre) and 16 (right). The green triangle represents the site at Wakkerstroom.*

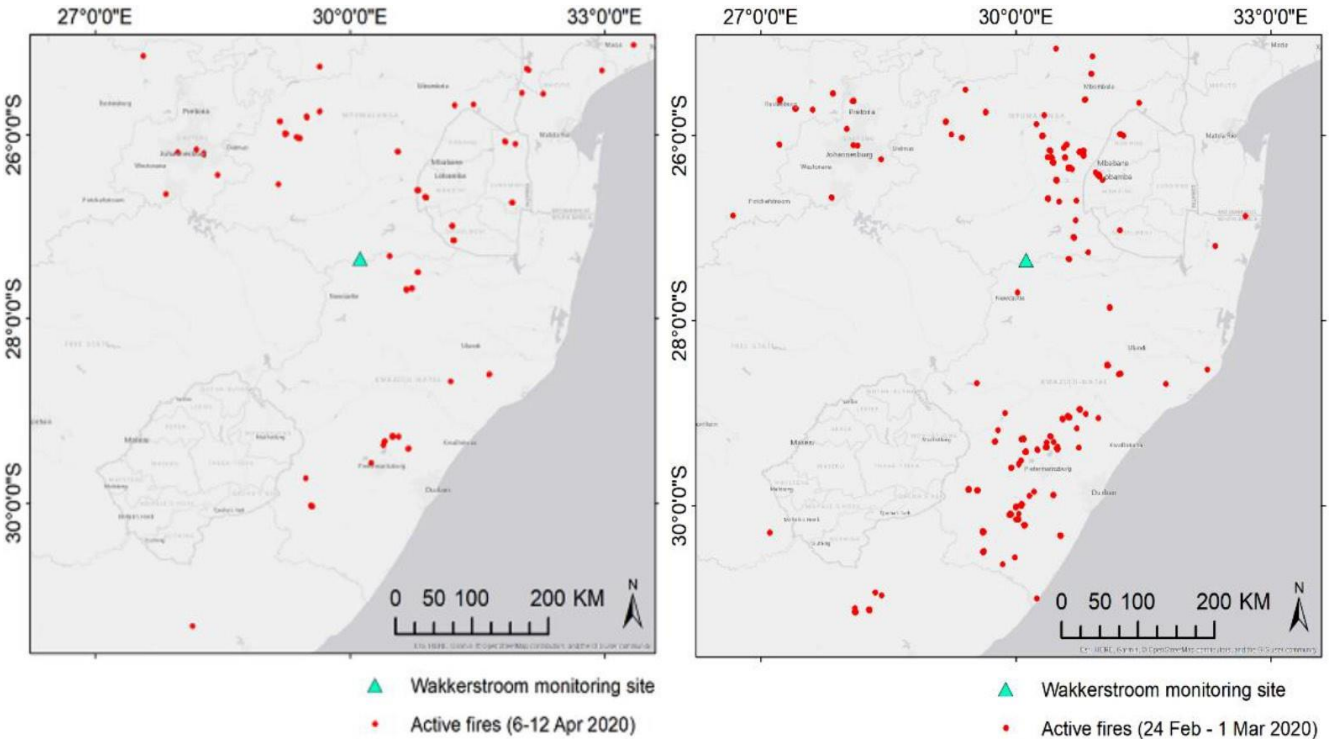

Figure 12: *The MODIS fire count (red dots) product for week 15 (left) and week 9 (right). The green triangle represents the site at Wakkerstroom.*

at the Wakkerstroom MS were directly from the south (Figures 9 and 10). This type of air mass trajectory is typically associated with cleaner air from the Southern Ocean. The trajectories spent very little time over the subcontinent before reaching the Wakkerstroom MS. Fire count data from MODIS shows that there was biomass burning activity during weeks 15 and 9 (Figure 12), however, since the airmass trajectories were dominantly from the Southern Ocean (Figures 9 and 10), these emissions had less effect on the levels of NO_2 concentrations to the Wakkerstroom MS during those weeks.

Discussion

Weekly NO_2 surface concentrations at the three conventional air quality monitoring stations and the Wakkerstroom MS with the Pandora-2s instrument are comparable, given their relative location to major sources. The sites closer to the power stations (Majuba and Kendal) have higher surface nitrogen dioxide levels than those further away, albeit downwind of the power stations (Figures 1, 4 and 5). Nitrogen dioxide has a short atmospheric lifetime and therefore does not get transported far from its source (Boersma et al., 2007). Interestingly, even though the Kendal and Majuba sites are both ca. 3 km south-southeast and south-east of direct emission sources, respectively, the Kendal site had higher weekly averaged surface nitrogen dioxide levels. This can be an indication of NO_2 loading; however, this study did not investigate the loading of NO_2 at the monitoring sites. No discernible seasonal cycle was observed at three of the four sites, including the Wakkerstroom site with the Pandora-2s instrument. However, the Majuba MS had slightly elevated concentrations in the spring. Distinctive atmospheric transport patterns associated with the highest and lowest concentrations of NO_2 have been identified. Although the regional scale recirculation was not surprising, high concentrations of NO_2 associated with biomass burning emissions transported from the east coast of South Africa and eSwatini were not expected and represented an important finding. The lowest concentrations were recorded during months when some biomass burning was observed; however, these concentrations were highly associated with air masses from the south coast of South Africa. It is encouraging that these data will indeed be instrumental in unpacking the biogeochemical cycling of trace gases over the study area. In the next phase of analysing Pandora-2s data from Wakkerstroom, the NO_2 concentrations in the middle and the upper troposphere will be extracted. These data will be invaluable at understanding the long-range transport of pollutants from the Highveld as well as providing important surface derived total column retrievals that can be compared to the many existing satellite retrievals. Until the installation of this instrument, there have been few attempts to validate the satellite retrieved concentration of NO_2 over the Highveld.

Conclusions

The first-time surface level NO_2 measurements retrieved from Wakkerstroom using the Pandora-2s instrument have introduced new confidence that the data products can be used in future to explore biogeochemical interactions in the Highveld area. This comes from the similarity in the Pandora-2s measurements to the already existing sensors in the Highveld and the instrument's capability to indicate elevated levels of surface NO_2 concentrations accurately. The Pandora-2s is a valuable instrument that promises to build and close the gap of high temporal resolution long-term data.

Acknowledgements

We would like to thank the principal investigator, network operators (Daniel Santana, Moritz Mueller) and local operator (Paul Grobler) for establishing and maintaining the Pandora instrument at the Wakkerstroom site. We thank Eskom for providing the data from the air quality monitoring sites, the Climatology Research Group (CRG) at the North-West University (NWU) and Hugo De Lemos for their assistance. Our gratitude also goes to the University of the Witwatersrand and the National Research Foundation (NRF) for funding. The PGN is a bilateral project supported with funding from NASA and ESA.

References

Alade OL (2011) Characteristics of Particulate Matter over the South African Industrialized Highveld. MSc thesis, University of Witwatersrand, Johannesburg.

Balashov NV, Thompson AM, Piketh SJ, Langerman KE (2014) Surface Ozone Variability and Trends Over the South African Highveld from 1990 to 2007. Journal of Geophysical Research: Atmospheres, 119: 4323–4342. https://doi. org/10.1002/2013JD020555

Bauwens M, Compernolle S, Stavrakou T, Müller JF, Gent J van, Eskes H, Levelt PF, A R van der, Veefkind JP, Vlietinck J, Yu H, Zehner C (2020) Impact of Coronavirus Outbreak on NO_2 Pollution Assessed Using TROPOMI and OMI Observations. Geophysical Research Letters, 47: 11. https://doi.org/10.1029/2020GL087978

Behm S, Haupt H (2020) Predictability of Hourly Nitrogen Dioxide Concentration. Ecological Modelling. 42. https://doi.org/10.1016/j.ecolmodel.2020.109076

Belelie MD, Burger RP, Mkhatshwa G, Piketh SJ (2019) Assessing the Impact of Eskom Power Plant Emissions on Ambient Air Quality over KwaZamokuhle. Clean Air Journal, 29: 29–37. https://doi.org/10.17159/2410-972x/2019/v29n1a2

Bera B, Bhattacharjee S, Sengupta N, Saha S (2021) Variation and Dispersal of PM_{10} and $PM_{2.5}$ During COVID-19 Lockdown over Kolkata Metropolitan City, India Investigated Through HYSPLIT Model. Geoscience Frontiers. https://doi.org/10.1016/j.gsf.2021.101291

Brancher M (2021) Increased Ozone Pollution Alongside Reduced Nitrogen Dioxide Concentrations During Vienna's First COVID-19 Lockdown: Significance for Air Quality Management. Environmental Pollution, 284. https://doi.org/10.1016/j. envpol.2021.117153

Breeze P (2015) Coal Combustion and the Environment, in: Breeze, P. (Ed), Coal-Fired Generation, Chapter 6, 53-72. Academic Press, Boston. https://doi.org/10.1016/B978-0-12-804006-5.00012-5

Cede A (2021) Manual for Blick Software Suite 1.8, Version 1-8-3. Manual, 183-185 pp https://www.pandonia-global-network.org/wpcontent/uploads/2021/05/BlickSoftwareSuite_Manual_v1-8-3.pdf. Accessed 17 September 2021.

Cede PA, Tiefengraber M (2013) CEOS Intercalibration of Ground-Based Spectrometers and Lidars. Minispectrometer Intercalibration and Satellite Validation. Report. https:// www.pandonia-global-network.org/wpcontent/uploads/2019/06/LuftBlick_CEOS_ICalMinispectrometers_ InterCalRecommendations_RP_2013002_v5.pdf

Celarier EA, Brinksma EJ, Gleason JF, Veefkind JP, Cede A, Herman JR et al. (2008) Validation of Ozone Monitoring Instrument Nitrogen Dioxide Columns. Journal of Geophysical Research: Atmospheres, 113. https://doi.org/10.1029/2007JD008908

Collett KS, Piketh SJ, Ross KE (2010) An Assessment of the Atmospheric Nitrogen Budget on the South African Highveld. South African Journal of Science, 106: 35–43. DOI: 10.4102/sajs.v106i5/6.220

De Lange A., Naidoo M, Garland RM, Dyson LL (2021) The Sensitivity of Simulated Surface-Level Pollution Concentrations to WRF-ARW-Model PBL Parameterisation Schemes Over the Highveld of South Africa. Atmospheric Research, 254. https://doi.org/10.1016/j.atmosres.2021.105517

Freiman MT, Piketh SJ (2003) Air Transport into and out of the industrial Highveld region of South Africa. Journal of Applied Meteorology, 42: 994–1002. 10.1175/1520-0450(2003)042<0994:ATIAOO>2.0.CO;2

Goldberg DL, Anenberg SC, Griffin D, McLinden CA, Lu Z, Streets DG (2020) Disentangling the Impact of the COVID-19 lockdowns on urban NO_2 from natural vvariability. Geophysical Research Letters, 47. https://doi.org/10.1029/2020GL089269

Grange S (2014) Technical note: Averaging wind speeds and directions. https://doi.org/10.13140/RG.2.1.3349.2006

Hakkarainen J, Szeląg ME, Ialongo I, Retscher C, Oda T, Crisp D (2021) Analysing nitrogen oxides to carbon dioxide emission ratios from space: A case study of Matimba Power Station in South Africa. Atmospheric Environment: X, 10. https://doi.org/10.1016/j.aeaoa.2021.100110

Herman J, Cede A, Spinei E, Mount G, Tzortziou M, Abuhassan N (2009) NO_2 column amounts from ground-based Pandora and MFDOAS spectrometers using the direct-sun DOAS technique: Intercomparisons and application to OMI validation. Journal of Geophysical Research: Atmospheres, 114. https://doi.org/10.1029/2009JD011848

Hickman JE, Andela N, Tsigaridis K, Galy-Lacaux C, Ossohou M, Bauer SE (2021) Reductions in NO_2 burden over north equatorial Africa from decline in biomass burning in spite of growing fossil

fuel use, 2005 to 2017. Proceedings of the National Academy of Sciences, 118:7. https://doi.org/10.1073/pnas.2002579118

Judd LM, Al-Saadi JA, Janz SJ, Kowalewski MG, Pierce RB, Szykman JJ et al. (2019) Evaluating the impact of spatial resolution on tropospheric NO_2 column comparisons within urban areas using highresolution airborne data. Atmospheric Measurement Techniques, 12: 6091–6111. https://doi.org/10.5194/amt-12-6091-2019

Lourens ASM, Butler TM, Beukes JP, Van Zyl PG, Beirle S, Wagner TK, et al. (2012) Re-evaluating the NO_2 hotspot over the South African Highveld. South African Journal of Science, 108. https://doi.org/10.4102/sajs.v108i11/12.1146

Matimolane M (2019) Air Quality Offsets Implementation Plan for Gert Sibande District Municipality: Tutuka, Majuba, Camden and Grootvlei Power Stations: March 2019 update (No. ENV19-R059). https://www. eskom. co.za/ AirQuality/Documents/ AQoffsetImplPlanGertSibandePubMeetingPres.pdf

Naiker Y, Diab RD, Zunckel M, Hayes ET (2012) Introduction of local air quality management in South Africa: overview and challenges. Environmental Science and Policy, 17: 62–71. https://doi.org/10.1016/j.envsci.2011.11.009

NASA Pandora Project. https://pandora.gsfc.nasa.gov/Research/ RNA/ Accessed 16 September.

NASA Pandora Project. https://pandora.gsfc.nasa.gov/PGN/ Accessed 18 September 2021.

Omrani H, Omrani B, Parmentier B, Helbich M (2020) Spatio- temporal data on the air pollutant nitrogen dioxide derived from Sentinel satellite for France. Data in Brief, 28. https://doi.org/10.1016/j.dib.2019.105089

Qi X, Zhu S, Zhu C, Hu J, Lou S, Xu L et al. (2020) Smog chamber study of the effects of NO_x and NH3 on the formation of secondary organic aerosols and optical properties from photo-oxidation of toluene. Science of Total Environment, 727:138632. https://doi.org/10.1016/j.scitotenv.2020.138632

Scorgie Y, Thomas R (2006) judd Mpumalanga Highveld cumulative scenario planning study: air pollution compliance assessment and health risk analysis of cumulative operations of current, RTS and proposed Eskom Power Station located within the Mpumalanga and Gauteng Provinces (No. APP/06/ESKOM-05 Rev 1.0). https://cer.org.za/wpcontent/uploads/2018/08/ Airshed_Infotox_MpumalangaCumulativeReport_Rev1.pdf

Seinfeld JH, Pandis SN (2016) Atmospheric Chemistry and Physics: From Air Pollution to Climate Change. John Wiley & Sons.

Shabbir Y, Khokhar MF, Shaiganfar R, Wagner (2016) Spatial variance and assessment of nitrogen dioxide pollution in major cities of Pakistan along N5-Highway. Journal of Environmental Science, 43: 4–14. https://doi.org/10.1016/j.jes.2015.04.038

Shikwambana L, Mhangara P, Mbatha N (2020) Trend analysis and first time observations of sulphur dioxide and nitrogen dioxide in South Africa using TROPOMI/Sentinel-5 P data. International Journal of Applied Earth Observation and Geoinformation, 91. https://doi.org/10.1016/j.jag.2020.102130

Stein AF, Draxler RR, Rolph GD, Stunder BJB, Cohen MD, Ngan F (2015) NOAA'S HYSPLIT Atmospheric Transport and dispersion modeling system. Bulletin of the American Meteorological Society, 96: 2059–2078. https://doi.org/10.1175/ BAMS-D-14-00110.1

Thomas R, Scorgie Y (2006) Air quality impact assessment for the proposed new coal-fired power station (Kendal north) in the Witbank area (No. APP/06/NMS-01 Rev 0.2). https://www.eskom.co.za/OurCompany/SustainableDevelopment/ EnvironmentalImpactAssessments/Documents/Air_quality_ part_1.pdf

Tiefengraber M, Cede A, Gebetsberger M, Müller M (2021) Fiducial Reference Measurements for Air Quality. New Algorithm and Product Development Plan (No. version 5.1). https://www. pandoniaglobal-network.org/wpcontent/uploads/2021/07/ Luft-Blick_FRM4AQ_NewAlgorithmPlan-ATBD_RP_2019005_ v5.1.pdf

Verhoelst T, Compernolle S, Pinardi G, Lambert JC, Eskes HJ, Eichmann KU et al. (2021) Ground-based validation of the Copernicus Sentinel-5P TROPOMI NO_2 measurements with the NDACC ZSL-DOAS, MAX-DOAS and Pandonia global networks. Atmospheric Measurement Techniques, 14: 481–510. https://doi.org/10.5194/amt-14-481-2021

Walt AJ van der, Fitchett JM (2020) Statistical classification of South African seasonal divisions on the basis of daily temperature data. South African Journal of Science, 116. https://doi.org/10.17159/sajs.2020/7614

Wang G, Deng J, Zhang Y, Zhang Q, Duan L, Hao J et al. (2020) Air pollutant emissions from coal-fired power plants in China over the past two decades. Science of the Total Environment, 741. https://doi.org/10.1016/j.scitotenv.2020.140326

Wang S, Hao J (2012) Air quality management in China: Issues, challenges, and options. Journal of Environmental Sciences, 24: 2–13. https://doi.org/10.1016/S1001-0742(11)60724-9

Watanabe MDB, Ortega E (2011) Ecosystem services and biogeochemical cycles on a global scale: valuation of water, carbon and nitrogen processes, Environmental Science & Policy,14 (6). https://doi.org/10.1016/j.envsci.2011.05.013

Wedow JM, Ainsworth EA, Li S (2021) Plant biochemistry influences tropospheric ozone formation, destruction,

deposition, and response. Trends in Biochemical Sciences, 1813. https://doi.org/10.1016/j.tibs.2021.06.007

Xu G, Xiao J, Oliver DM, Yang Z, Xiong K, Zhao Z, Zheng L, Fan H, Zhang F (2021) Spatio-temporal characteristics and determinants of anthropogenic nitrogen and phosphorus inputs in an ecologically fragile karst basin: Environmental responses and management strategies. Ecological Indicators, 133:108453. https://doi.org/10.1016/j.ecolind.2021.108453

Zhao X, Fioletov V, Cede A, Davies J, Strong K (2016) Accuracy, precision, and temperature dependence of Pandora total ozone measurements estimated from a comparison with the Brewer triad in Toronto. Atmospheric Measurement Techniques, 9: 5747–5761. https://doi.org/10.5194/amt-9-5747-2016

Zhao X, Griffin D, Fioletov V, McLinden C, Davies J, Ogyu A et al. (2019) Retrieval of total column and surface NO_2 from Pandora zenith-sky measurements. Atmospheric Chemistry and Physics, 19: 10619–10642. https://doi.org/10.5194/acp-19-10619-2019

Zhao X, Griffin D, Fioletov V, McLinden C, Cede A, Tiefengraber M et al. (2020) Assessment of the quality of TROPOMI high-spatial- resolution NO_2 data products in the Greater Toronto Area. Atmospheric Measurement Techniques, 13: 2131–2159. https:// doi.org/10.5194/amt-13-2131-2020

Zyrichidou I, Koukouli ME, Balis D, Markakis K, Poupkou A, Katragkou E et al. (2015) Identification of surface NO_x emission sources on a regional scale using OMI NO_2. Atmospheric Environment, 101: 82–93. https://doi.org/10.1016/j. atmosenv.2014.11.023

An earlier version of this paper was presented at the National Association of Clean Air (NACA) Conference in October 2021 and was published in its Proceedings.

4.2 Postscript

By deploying Pandora-2s in Wakkerstroom, this paper offers the first detailed, ground-based dataset for near-surface NO_2 concentrations in this region. Enhanced temporal and spatial data allowed for the understanding of the seasonal patterns of measured NO_2 concentrations and the identification of the dominant source. In the context of this thesis, this work is significant as it provides a foundational dataset for understanding NO_2 concentrations, particularly in relation to industrial emissions and atmospheric transport processes in the Highveld. This research is not only important to enhance regional air quality understanding but also serves as a comparative baseline for satellite NO_2 retrievals, especially in evaluating the accuracy of existing satellite measurements. The insights gained contribute to a broader understanding of pollution distribution in an area in the South African Highveld. Relying on satellite observations currently poses challenges in accurately capturing NO_2 concentrations near the ground due to their limitations in vertical sensitivity. However, satellites have a better spatial resolution but without the temporal resolution. It is challenging to accurately capture the heterogeneity of the NO_2 concentrations, particularly in a highly polluted area such as the industrialised Highveld of South Africa. The next Chapter of this thesis addresses the comparison of ground-based and satellite measurements.

Chapter 5

This Chapter contains the manuscript, Kai-Sikhakhane, R. F., Scholes, M. C., Piketh, S. J., van Geffen, J., Garland, R. M., Havenga, H., Scholes, R. J. Assessing Nitrogen Dioxide in the Highveld Troposphere: Pandora Insights and TROPOMI Sentinel-5P Evaluation. Atmosphere. 2024; 15(10):1187. https://doi.org/10.3390/atmos15101187. The text in the Preface describes why this paper was written, and the text in the Postscript concludes with what was achieved and possible future directions of research

5 Assessing Nitrogen Dioxide in the Highveld Troposphere: Pandora Ground-Based Insights and TROPOMI Sentinel-5P Validation

5.1 Preface

There is a lack of ground-based instruments in South Africa for the measurement of tropospheric vertical column NO_2 concentrations. Low Earth Orbiting Satellites provide spatially defined measurements but lack temporally resolved concentrations, which ground-based instruments could provide. Using data from both sources would significantly contribute to understanding the distribution of NO_2 concentrations in highly industrialised areas such as the South African Highveld. Studies evaluating tropospheric NO_2 satellite measurements using direct-sun ground-based measurements show that the horizontal spatial comparison is limited. This paper expands on previous work by assessing nitrogen dioxide (NO_2) concentrations in Wakkerstroom, focusing on how ground-based MAX-DOAS Pandora-2s observations complement satellite data from TROPOMI. By comparing data from these two instruments, the study aims to validate TROPOMI's utility for monitoring tropospheric NO_2 over the Highveld.

atmosphere

MDPI

Article

Assessing Nitrogen Dioxide in the Highveld Troposphere: Pandora Insights and TROPOMI Sentinel-5P Evaluation

Refilwe F. Kai-Sikhakhane [1,*], Mary C. Scholes [1], Stuart J. Piketh [2], Jos van Geffen [3], Rebecca M. Garland [4], Henno Havenga [2] and Robert J. Scholes [5,†]

1 School of Animal, Plant and Environmental Sciences, University of the Witwatersrand, Johannesburg 2001, South Africa; mary.scholes@wits.ac.za
2 Unit for Environmental Sciences and Management, North-West University, Potchefstroom 2531, South Africa; stuart.piketh@nwu.ac.za (S.J.P.); henno.havenga@nwu.ac.za (H.H.)
3 Royal Netherlands Meteorological Institute (KNMI), P.O. Box 201, 3730 AE De Bilt, The Netherlands; jos.van.geffen@knmi.nl
4 Department of Geography, Geoinformatics and Meteorology, University of Pretoria, Pretoria 0028, South Africa; rebecca.garland@up.ac.za
5 Global Change Institute, University of the Witwatersrand, Johannesburg 2001, South Africa
* Correspondence: 741786@students.wits.ac.za
† Deceased author.

check for updates

Citation: Kai-Sikhakhane, R.F.; Scholes, M.C.; Piketh, S.J.; van Geffen, J.; Garland, R.M.; Havenga, H.; Scholes, R.J. Assessing Nitrogen Dioxide in the Highveld Troposphere: Pandora Insights and TROPOMI Sentinel-5P Evaluation. *Atmosphere* **2024**, *15*, 1187. https://doi.org/10.3390/atmos15101187

Academic Editor: David F Plusquellic

Received: 5 August 2024
Revised: 23 September 2024
Accepted: 27 September 2024
Published: 3 October 2024

Abstract: Nitrogen oxides, particularly NO_2, are emitted through a variety of industrial and transport processes globally. The world's continuous economic development, including in developing countries, results in an increasing concentration of those gases in the atmosphere. Yet, there is scant information on the current state and recent evolution of these atmospheric pollutants over a range of spatial and temporal scales, especially in Africa. This, in turn, hinders the assessment of the emissions and the evaluation of potential risks or impacts on societies and their economies, as well as on the environment. This study attempts to fill the gap by leveraging data from a Pandora-2S ground-based, column-integrating instrument located in Wakkerstroom in the Mpumalanga Province of South Africa and space-based remote sensing data obtained from the TROPOMI instrument onboard the ESA Sentinel- 5P satellite. We compare these two spatially (horizontal) representative data sets using statistical tools to investigate the concentrations of emitted and transported NO_2 at this particular location, expecting that a significant positive correlation between the NO_2 tropospheric vertical column (TVC) data might justify using the TROPOMI data, available globally, as a proxy for tropospheric and boundary layer NO_2 concentrations over the Highveld of South Africa more generally. The data from the two instruments showed no significant difference between the interannual mean TVC-NO_2 in 2020 and 2021. The seasonal patterns for both instruments were different in 2020, but in 2021, both measured peak TVC-NO_2 concentrations in late winter (week 34). The instruments both detected higher TVC-NO_2 concentrations during transitions between seasons, particularly from winter to spring. The TVC-NO_2 concentrations measured in Wakkerstroom Mpumalanga are mostly contributed to by the emission sources in the low troposphere, such as biomass burning and emissions from local power stations.

Keywords: Pandora-2s; nitrogen dioxide; TROPOMI; Sentinel-5P; air quality; validation

Introduction

Developing countries contribute increasing amounts of pollution to the atmosphere [1,2], adding to the existing burden of air pollution from developed countries. In the United Kingdom (UK), nitrogen oxide (NO_x) emissions totalled 6433 tonnes in 2022 and 6.1 million tonnes in the United States of America (US) in 2023 [3]. The presence of NO_x in the atmosphere, particularly the lower troposphere, is detrimental to the environment (e.g., acidic deposition) and has negative health impacts, including cardiovascular and respiratory diseases [4–7]. The World Health Organization (WHO) reports that pollutants such as particulate matter (PM), carbon monoxide (CO), ozone (O_3), nitrogen dioxide (NO_2) and sulphur dioxide (SO_2) show the most evidence of having an impact on public health, in addition to any environmental impacts. The distribution patterns of these pollutants differ, with NO_2 showing a distinct urban-rural gradient of higher concentrations in more densely populated urban areas [8] and highly industrialised regions [9]. The only way to minimise these impacts is to regulate the emissions into the atmosphere [10].

Nitrogen dioxide (NO_2) is the most prevalent form of NO_x in the atmosphere. Anthropogenic activities such as biomass burning, incomplete combustion of coal (power generation) and transport lead to the generation of NO [10], which is then rapidly converted to NO_2 [11]. During the day, the formation of NO_2 is favoured, which then catalyses the formation of nitric acid (HNO_3). At night, ozone reacts with NO_2 to yield reactive nitrogen in the form of nitrate (NO_3^-) [12]. Reactive nitrogen is removed from the atmosphere through wet or dry deposition in the environment, contributing to the nitrogen status of terrestrial and aquatic ecosystems [13]. Studies show that South Africa's highly industrialised Highveld area has high tropospheric NO_2 concentrations, exceeding the national air quality standards [14]. These elevated concentrations are comparable to those of severely polluted regions of North America and Southeast Asia (between 1.30×10^{-4} and 3.72×10^{-4} mol/m^2) [4,15].

Consequently, cities near the industrialised Highveld, such as Johannesburg, experience higher annual NO_2 column concentrations than coastal cities away from the

Highveld [16]. NO_x emissions reported in the South African Mpumalanga (MP) Highveld are dominated by those emanating from coal-fired power stations and industrial activities [17,18] and contribute to the observed high levels of tropospheric NO_2 [4,7]. In addition to coal-burning power stations, other significant emission contributions to the Highveld tropospheric NO_2 column concentrations include biomass burning (particularly in the austral spring), the transport sector, and wood burning from informal household cooking and heating [16,19]. Power station emissions in the MP Highveld occur at ca. 250 m above the surface [20] and rise to altitudes of 500 m to 1000 m due to their heat content but are mixed downwards to the surface due to vertical mixing in the boundary layer under high solar radiation conditions [21]. These tropospheric pollutants are subjected to chemical and physical processes, which are highly dependent on meteorological conditions, resulting in their dispersion and transport [22].

The literature shows that NO_x concentrations in the Highveld of South Africa peak di- urnally at midday [14]. These peaks can be influenced by transboundary transported emissions [16], depending on the air mass' long- and short-range transport over the Mpumalanga Highveld. According to Freiman and Piketh [23], four major pollution transport pathways to the Highveld have been identified, depending on the source regions. Airflow to the region is driven by pathways from subtropical Africa, the Atlantic and the Indian Oceans, and flow over southern Africa. Emissions in the Highveld are recirculated or transported out of the region into the south Indian Ocean [23].

However, since temporally and spatially resolved instruments for trace gas monitoring are still sparse in Africa [24], we are faced with an incomplete understanding of the atmospheric chemistry in the tropospheric and total column. The available data in Africa, usually scanty in comparison to the northern hemisphere, is from campaigns testing novel technologies for a short period [25]. The transport of pollutants from neighbouring countries into South Africa can be documented using satellite remote sensing data combined with atmospheric circulation information generated by weather forecasting models [7,26,27].

There is a rich legacy of monitoring atmospheric NO_2 global distributions using remote sensing. From the late 1970s, limb-viewing and solar-occultation instruments were used [28,29]. However, these instruments have been replaced with satellites with higher spatial resolution, and improved retrieval methods have been implemented. The TROPO- spheric Monitoring Instrument (TROPOMI), on board the European Space Agency (ESA)

Sentinel-5 Precursor (S5P) payload, has a higher spatial resolution than its predecessor, the Ozone Monitoring Instrument (OMI). This feature, in turn, allows the documentation of NO_x emissions in individual cities and effectively identifies NO_2 hotspots [30]. Scientific investigations and accumulated expertise have shown that satellite data can be combined effectively with atmospheric circulation models and knowledge about chemical reactions to detect and monitor highly polluted areas against the prevailing background values.

TROPOMI uses the differential optical absorption spectroscopy (DOAS) technique to quantify the total trace gas amount along the effective light path from the sun through the atmosphere to the instrument [31]. TROPOMI produces high-resolution data (~5.5 × 3.5 km^2) [31] for the UV-Vis spectral range. This instrument is able to yield near-global measurements daily due to its 2600 km swath [31].

The proper interpretation of TROPOMI data requires a deep understanding of the transfer of solar radiation in the atmosphere, particularly the specific absorption bands of atmospheric NO_2 pollutants. Such a radiation model can be inverted against satellite data, and the latter can be used to document the spatial and temporal distribution of those NO_2 trace gases over the area of interest. This process, therefore, also requires prior knowledge of the underlying topography to determine the true extent of the slanted atmospheric columns in which radiation scattering and absorption are taking place for each grid cell of the satellite data [32,33].

The quantitative information retrieved from the satellite data can be compared subsequently with the independently acquired data from ground-based measurements, such as Pandora instruments [34], paying particular attention to the differences in spatial, temporal, and accuracy characteristics of those instruments. Due to TROPOMI's global coverage, it lacks temporal resolution. Therefore, data from ground-based instruments such as Pandora complement these high-quality, spatially resolved satellite data products.

Ground instruments can capture localised measurements, enabling researchers to study events at specific locations using high temporal resolution. The ability of ground-based instruments to vertically profile the measured trace gases in the atmosphere allows access to the integrated vertical profile concentrations from the satellite-derived measurements. Not only is it important to understand the horizontal distribution of NO_2 across the globe, but the vertical distribution is extremely important as it identifies the high-impact layers that impact atmospheric chemistry and environmental and health impacts.

Pandora instruments employ direct sun (DS) and multi-axis differential optical absorption spectroscopy (MAX-DOAS) techniques to measure atmospheric trace gas amounts [35]. The DS technique quantifies trace gas abundances in the atmospheric total column (TC) by using scattered light received from one viewing direction at a time: the sun. However, the MAX-DOAS technique uses scattered light from multiple viewing directions and angles. When using the standard Pandora routines for DS measurement, the instrument points directly at the sun for approximately 60 s at a time. For MAX-DOAS measurements, the instrument scans the sky at various elevation angles for a fixed pointing azimuth (PAZI) for 30 s per angle. The MAX-DOAS technique is more sensitive to atmospheric constituents abundant in the lower troposphere, such as NO_2. Literature shows that a detailed evaluation of satellite-derived NO_2 concentrations using ground-based instruments has been carried out using DS measurements since they are more vertically representative of the satellite-derived measurements. These evaluations show that TROPOMI underestimates NO_2 tropospheric vertical column (TVC) concentrations [1,29,36]. The global negative biases observed between TROPOMI and MAX-DOAS measurements are reported as high as 37% in clean to slightly polluted areas and can increase to 51% in highly polluted areas [29]. These biases differ by region and specific ground-based stations. The measurement biases observed are attributable to the different viewing geometries between these two instruments, biases in the satellite retrieval of cloud pressure, the surface albedo climatology, and the low resolution of the a priori profiles derived from global simulations of the TM5-MP chemistry model [29,37,38]. Duoros et al. [28] showed that replacing the global a priori information with local a priori information decreased the overall bias by 5% to

12%. Additionally, DS measurements are not horizontally representative of the TROPOMI footprint because measurements are taken at one point, and the field of view of the Pandora instrument is small, ~1.5°.
Dimitriopoulou et al. [39] show that using MAX-DOAS instruments to measure tropospheric NO_2 concentrations in different directions improves the spatial colocation of ground-derived measurements with satellite-derived measurements. In addition, the Pandora instrument's temporal resolution can capture the NO_2 diurnal variation that isn't captured by satellite measurements due to the polar-orbiting nature of the satellite instrument [4].
Since Pandora TVC measurements can be retrieved at very high temporal frequency, it is possible to select the values corresponding to the time of passage of TROPOMI over an area of interest and compare data sets acquired quasi simultaneously. A reasonable comparison between the TROPOMI- and Pandora-derived MAX-DOAS measurements can indicate the balancing association of these two datasets, indicating the need for ground instruments to supplement the temporally lacking, column-integrated TROPOMI measurements.
This study evaluates the heterogeneity of the TVC-NO_2 concentrations over Wakker- stroom in the Mpumalanga Highveld region of South Africa using Pandora, now known as Pan159, MAX-DOAS measurements. In addition, the TROPOMI-derived TVC measurements are presented and evaluated alongside the Pandora-derived measurements. The purpose of this comparison is to assess whether or not the TROPOMI data can be used as a reliable proxy for the tropospheric and boundary layer concentrations of NO_2 of the South African Highveld, a hotspot of emissions at a global scale.

Materials and Methods

1.1. Study Site Description

Wakkerstroom (27°21′17.7″ S, 30°08′37.8″ E) is located in the Mpumalanga Province of South Africa (Figure 1). The town covers an area of 87.68 km^2, with a population of ~7000 and a minimum elevation of approximately 1730 m a.s.l. The study site is relatively close to 12 coal-fired power stations (within ~48 km to 214 km). The power stations in the Highveld are direct emission sources of NO. Wakkerstroom is downwind of the majority of the power stations. The closest power stations to Wakkerstroom are Majuba and Camden. Camden is located northeast, while Majuba is located northwest of Wakkerstroom. The NO_x agricultural emissions from neighbouring townships and surrounding agricultural areas also increase the pollution load in the atmosphere [40]. As a result of this concentration of power stations, the Highveld has long been identified as a major source of NO_2 pollution, even on a subcontinental scale (Figure 2).

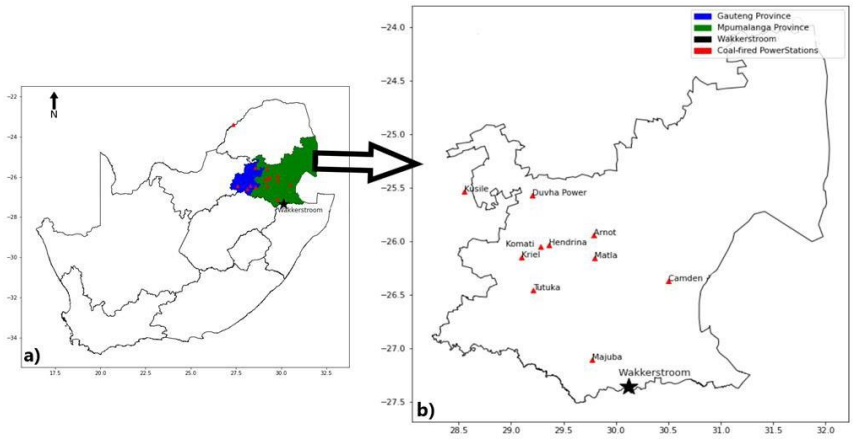

Figure 1. Map of South Africa depicting the (**a**) Mpumalanga (MP) and Gauteng (GP) Provinces with (**b**) the Mpumalanga Province of South Africa showing the coal-fired power stations in the MP

Highveld and Wakkerstroom where the Pandora instrument (Pan159) is situated. Source of shapefiles: https://www.igismap.com/south-africa-shapefile-download-boundary-line-polygon/ (accessed on 11 December 2022).

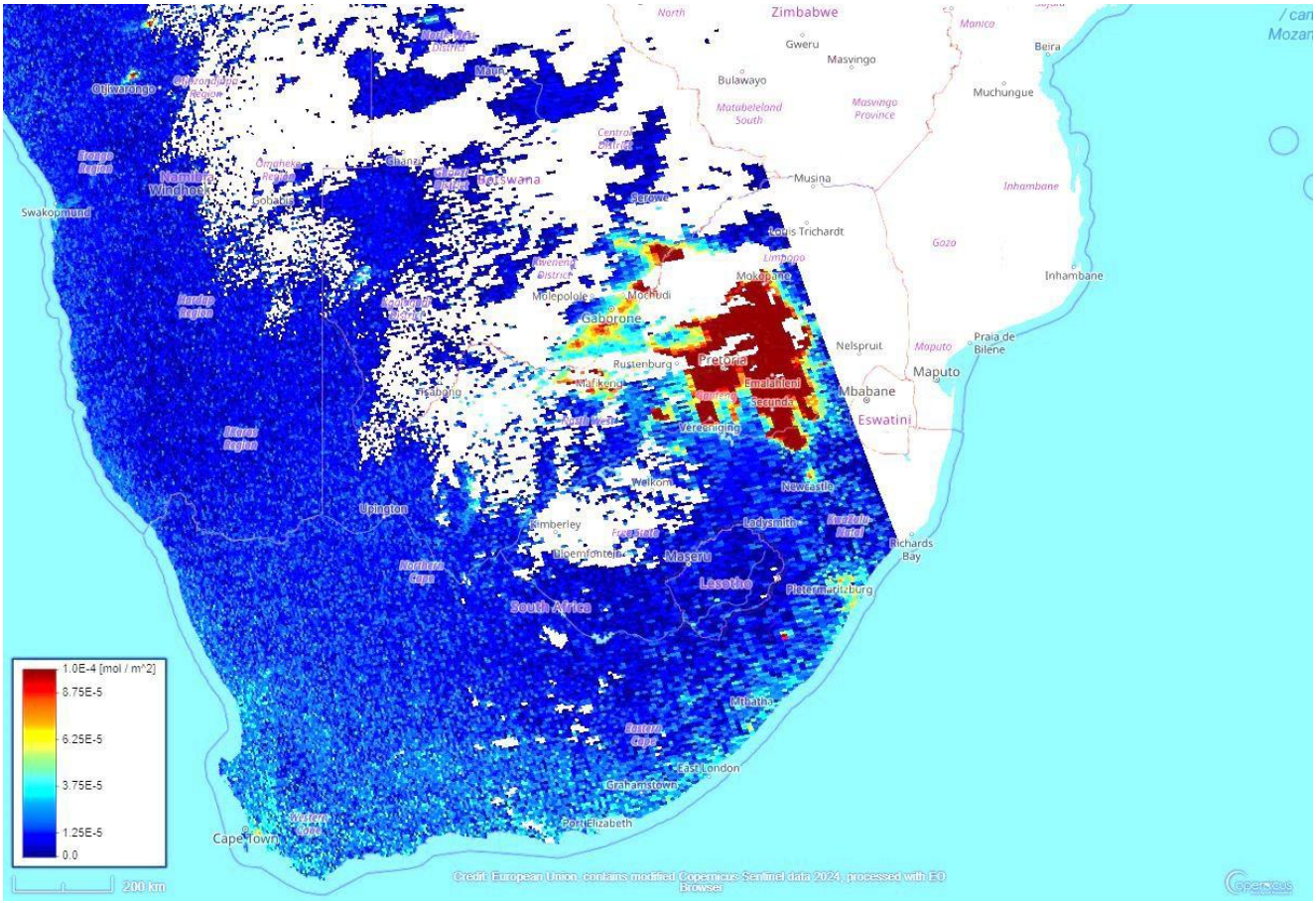

Figure 2. Map of the tropospheric column NO_2 concentrations (mol/m^2) over southern Africa, as derived from an analysis of TROPOMI data from the 7–20 June 2021. Source: https://browser.dataspace.copernicus.eu/ (accessed on 26 September 2024).

1.2. Research Techniques and Methods

1.2.1. Pandora-2s Instrument

The Pandora instrument installed in Wakkerstroom is part of the ground-based standardised Pandora sun photometer network (Pandora Global Network-PGN). The Pandora-2Spectrometer (2s) instrument is a dual ultraviolet (UV) and visible (VIS) spectrometer system that delivers integrated column direct sun/moon and sky-scanned observations of various trace gases, including O_3, NO_2, SO_2, and CH_2O [41]. It is also possible to derive an atmospheric profile of the selected trace gases. This device is a small, cost-effective instrument capable of providing high-precision observations from 280 nm to 530 nm. The Pandora instrument used in this study (Pan159) was deployed in Wakkerstroom in December 2019. It has a spectral range of 270 nm to 530 nm and 400 nm to 900 nm and a resolution of 0.6 nm/UV and 1.1 nm/VIS. The Pandora-2s is mounted on an azimuth and elevation tracker that is controlled by a microprocessor (https://sciglob.com/wp-content/uploads/2023/12/Pandora2S_datasheet-1.pdf (ac- cessed on 15 July 2021), making it possible to point the instrument in any direction.

Trace gases absorb solar radiation at specific wavelengths in the ultraviolet to visible spectrum range, resulting in spectral signatures [42]. Trace gas concentrations can, therefore, be determined by measuring their specific spectral signatures using the differential optical

absorption spectroscopy (DOAS) method. The DOAS method is used to determine atmospheric trace gas concentrations from direct sun DOAS (DS-DOAS) observations, multi-axis DOAS (MAX-DOAS), or both. It is possible to repeat the measurements every 80 s. The measured scattered sunlight spectra are analysed using "L2 direct" and "L2 Air-Ratio Sky" algorithms, respectively [43]. The latter algorithm compares observed and reference spectra to determine concentration profiles of atmospheric trace gases [43].
The DS-DOAS technique delivers total column trace gas amounts using direct sun (DS) geometry, which means that it points directly at the sun when measuring spectral signatures of the trace gases. The MAX-DOAS technique, an extension of the traditional DOAS method, scans the sky at various elevations and azimuth angles. This allows for the quasi-simultaneous observation of scattered light in different line-of-sight (LOS) directions from the horizon to the zenith, depending on the sun's position during observations [44]. The various elevation angles enable measurements at different horizontal distances and provide sensitivity to different atmospheric altitudes. Lower elevation angles are more sensitive to the lower atmosphere because the path length of light is longer in the low troposphere than at higher altitudes. The longer light path length enhances atmospheric constituents' light absorption, increasing sensitivity to trace gases primarily found in the lower troposphere, such as NO_2, O_3, and CH_2O. As a result, the MAX-DOAS data are only measured in the lower troposphere, up to approximately 5.5 km above ground level [45].

1.2.2. Pandora (Pan159) Data

The Pandora instrument at Wakkerstroom, Pan159, uses both DOAS techniques to measure the concentrations of NO_2, O_3, SO_2, and CH_2O. During the setup of the Pandora instruments for MAX-DOAS measurements, one to three pointing azimuth (PAZI) directions were selected: one direction over the more polluted area and another in the opposite direction. Pan159 was set at a 270° PAZI (west), which looks across the vlei (valley) to the neck of the Volksrust road. Volksrust is a town approximately 45 km from Wakkerstroom and serves as a stopover for travellers commuting between Johannesburg and Durban. Therefore, the set azimuth for Pan159 is in the direction of expected pollution relative to its location. The sky scans are detailed or quick and use an open-hole or a U340 filter. Measurements from detailed sky scan zenith angles [0, 40, 50, 60, 70, 75, 80,
82, 85, "MAX-2", "MAX-1", "MAX", "MAX-1", "MAX-2", 85, 82, 80, 75, 70, 60, 50, 40,
0] and quick sky scan elevation angles [0, 60, 75, "MAX-1", "MAX", "MAX-1", 75, 60, 0] using a U340 filter were taken for a total of 30 s at each position; each position is scanned twice for 15 s. Pan159 employs an open-hole filter for quick scans at 0, 60, 75, "MAX-1", "MAX", "MAX-1", 75, 60 and 0-degree zenith angles also for a total of 30 s. Therefore, the measurement frequency is approximately 13 min, depending on the routine schedule and sun searches for the DS measurements. The maximum angle (MAX) was set at 88° as this is the maximum angle of unobstructed view that the instrument can point and measure. The Pan159 angles determine the atmospheric vertical distance that the instrument can sample during measurements. The Pandora instrument in MAX-DOAS mode measures trace gases in the lower troposphere, where the majority of the significant trace gases are concentrated in the atmosphere. At higher altitudes, the signal-to-noise ratio of the trace gas measurements decreases because of the reduced air density and scattering effects. Therefore, Pandora MAX-DOAS measurements are optimised in the lower troposphere only. This study analyses the tropospheric vertical column (TVC) NO_2 concentrations (mol/m^2) from 2020 to 2021.
The quasi-continuous Pan159 data are assigned data quality flag (DQF) values to qualify their uncertainty and usability; see Table 1. Pandora level 2 (L2) data quality flags are discussed in [45]. This study uses high-quality data with DQFs of 0/10 only.

Table 1. Pandora instrument data quality flags (DQFs) and their meanings.

Data Quality Flag (DQF) Value	Explanation
0	High-quality data (quality assurance applied)
1	Medium-quality data (quality assurance applied)
2	Low-quality data (quality assurance applied)
10	High-quality data (quality assurance not applied)
11	Medium-quality data (quality assurance not applied)
12	Low-quality data (quality assurance not applied)
20	Unusable data
21	Unusable data
22	Unusable data

1.2.3. TROPOMI Instrument

The TROPOspheric Monitoring Instrument (TROPOMI) is a sensor aboard the European Space Agency's (ESA's) polar-orbiting Sentinel-5 Precursor (S5P) satellite [31,46]. It was launched in 2017 to provide atmospheric trace gas, cloud and aerosol property measurements using shortwave infrared (SWIR), near-infrared (NIR), ultraviolet (UV) and visible (VIS) spectroscopy [31] from an ascending sun-synchronous polar orbit, with the equator crossing about 13:30 local time at the location of overpass [31]. The solar radiation is measured within the 405 nm to 465 nm wavelength range, and retrieval algorithms are used to derive the tropospheric NO_2 column density at ~5.5 × 3.5 km^2 spatial resolution from August 2019 [47]. The first public release of TROPOMI data sets, including NO_2, was in July 2018 [31,48]. The offline (OFFL) level-2 (L2) tropospheric NO_2 column density data can currently be accessed via the Copernicus Data Space Ecosystem (CDSE; https://dataspace.copernicus.eu/, last accessed on 21 June 2022). The S5P data processor has been upgraded since the start of the mission. With respect to NO_2 column amounts, the measurement process starts with the retrieval of slant column densities (SCDs). This is followed by separating the total SCDs into stratospheric and tropospheric components, depending on a priori vertical profile information using air-mass factors (AMFs), considering atmospheric cloud cover. The correct interpretation of TROPOMI data requires an understanding of the transfer of solar radiation in the atmosphere, particularly the specific absorption bands of the NO_2 pollutants.

1.2.4. TROPOMI Data

This study used NO_2 data product version 2.4.0 [31,48,49] from January 2020 to December 2021. The TROPOMI satellite output for each ground pixel, including the TVC- NO_2 concentrations measured in the visible spectral range, was assigned a quality indicator, "quality assurance value", to indicate the quality of the retrieved trace gas amount [31]. Pixel output with qa-value ≥ 0.75 are expected to originate from cloud-free areas and are considered error-free [48] and are used in this study. The original TROPOMI data were re-gridded to 0.01°, allowing us to select an area around Wakkerstroom that is representative of the area measured by the Pandora instrument using MAX-DOAS. A 0.1° × 0.05° area around Wakkerstroom was selected and averaged. The non-normally distributed data were averaged weekly, and the means, medians and standard deviations (variations) are reported in this study.

1.2.5. Data Evaluation

The traditional evaluation method [1,50] applied in this study used Pandora-2s tropospheric NO_2 concentrations (1) ± 5 min of the TROPOMI overpass time and (2) an hour within the TROPOMI overpass time for analyses. For the purpose of this study, only data from the

TROPOMI pixel closest to the Wakkerstroom site were extracted. All TROPOMI data used to compute the regression statistics were of qa- values ≥ 0.75, and the Pandora data were of DQF 0 or 10. In general, the use of TROPOMI data with qa-values ≥ 0.75 excludes data observed over cloudy scenes (cloud radiance fraction > 0.5), scenes covered by snow/ice, and retrievals considered unreliable for any number of reasons. The ± 5 min Pandora coincidence measurements were 5 min before or after the TROPOMI overpass time. The 1 h coincidence measurements were Pandora measurements retrieved within the TROPOMI overpass hour. These measurements were averaged and used as the 1 h coincidence data.

Theil Sen regression analyses (Rstudio ®) were used to compute all the regression statistics (R; *p*-value and regression line), Equation (1) was applied to compute the normalised mean bias (NMB), and Equation (2) for the NMB percentage. The Relative Squared Errors (RSEs) for all the regressions were computed to validate the regression models in this study.

$$\text{Equation 1: Normalised Mean Bias} = \frac{\sum_{1}^{n}(M - O)}{\sum_{1}^{n}(O)}$$

$$\text{Equation 2: Normalised Mean Bias (\%)} = \frac{\sum_{1}^{n}(M - O)}{\sum_{1}^{n}(O)} \text{x100}$$

*O = Pandora-2s measurements *M = TROPOMI measurements

1.2.6. A Priori Profiles Data

The NO_2 profiles (a priori profile shapes) were extracted from the TM5-MP (Tracer Model, version 5), a chemistry-transport model employed to derive highly resolved vertical profiles of NO_2 and other trace gases used in satellite retrievals [51]. The profiles were extracted using the Python tool developed by the Koninklijk Nederlands Meteorolo- gisch Instituut (KNMI). The .py code for the auxiliary product can be accessed from the Product User Manual (see https://sentinel.esa.int/web/sentinel/user-guides/sentinel-5p- tropomi/software-tools (accessed on 10 November 2022)).

1.2.7. Hybrid Single-Particle Lagrangian Integrated Trajectory (HYSPLIT) Frequency Cluster Data

The HYSPLIT model is a complete system that computes simple air parcel trajectories and complex transport, dispersion, chemical transformation, and deposition simulations using meteorological data [52,53]. It was developed by the National Oceanic and Atmospheric Administration (NOAA) Air Resources Laboratory (ARL) [52,54]. This model can track and forecast the release of dust, ash, volcanic ash and pollutants from various stationary and mobile emission sources [52]. The simulations were produced as trajectories, which could be clustered and presented by their mean trajectory. Trajectories were clustered using the similarity principle: data objects with higher similarity were grouped, while those with higher heterogeneity were separated into different groups [53]. The trajectories were combined until the total variance of the individual trajectories about their cluster mean started to increase substantially [54].

Version 5.2.0 of the HYSPLIT model was used to determine the trajectories of the air

masses that arrived at Wakkerstroom during 2020 and 2021, possibly loaded with pollutants, affecting the NO_2 tropospheric levels. The backward trajectories were simulated at 700 hPa and 550 hPa. These levels were informed by the a priori profile shapes from the TROPOMI retrieved TVC-NO_2 concentrations and the atmospheric partial profiles of the Pandora-derived TVC-NO_2 concentrations from January 2020 to December 2021. The HYSPLIT model simulated and merged five-day backward trajectories to produce backward trajectory clusters for 2020 and 2021, respectively. The trajectories were merged into 4 clusters according to their spatial variance. The resultant clusters were used to determine the nature and extent of primary air mass transport to Wakkerstroom. They distinguish between oceanic, clean continental, and polluted continental air mass transport. Transport pathways concerning synoptic circulation patterns assume that air masses mix as part of these circulation patterns [55].

This study used five-day backward trajectories instead of one- or two-day backward trajectories, even in light of the short lifetime of atmospheric NO_2. Five-day backward trajectories were used because South Africa's atmosphere is predominantly stable under the influence of the continental high-pressure system that prevails for most days of the year. Short timescale backward trajectories might not show the recirculation patterns or the source of the TVC-NO_2 concentrations.

Results

1.3. Tropospheric Vertical Column NO_2 Concentrations

This section reports the integrated tropospheric vertical column nitrogen dioxide concentrations observed by the Pandora-2s and the TROPOMI satellite instruments at Wakkerstroom, Mpumalanga, from January 2020 to December 2021.

1.3.1. Annual Concentrations

The annual mean and median NO_2 concentrations in the lower tropospheric vertical column (LTVC) (1780 m to 6730 m a.s.l) retrieved using the MAX-DOAS Pandora technique are given in Table 2, together with the TROPOMI-derived TVC-NO_2 concentrations in Table 3.

Table 2. Interannual comparison of integrated MAX-DOAS tropospheric vertical column nitro- gen dioxide mean and median diurnal concentrations measured by the ground-based Pandora at Wakkerstroom in 2020 and 2021.

	Tropospheric Vertical Column NO_2 (mol/m^2)	
Year	**Annual Mean (±Stdev)**	**Annual Median**
2020	$5.06 \times 10^{-5} \pm 8.97 \times 10^{-5}$	2.10×10^{-5}
2021	$5.03 \times 10^{-5} \pm 9.40 \times 10^{-5}$	1.44×10^{-5}
p-value	>0.05	<0.05

Table 3. The diurnal mean and median tropospheric vertical column nitrogen dioxide concentrations in 2020 and 2021 measured in Wakkerstroom using the TROPOMI satellite.

	Tropospheric Vertical Column NO_2 (mol/m^2)	
Year	**Annual Mean (±Stdev)**	**Annual Median**
2020	$6.17 \times 10^{-5} \pm 1.06 \times 10^{-4}$	2.86×10^{-5}
2021	$7.06 \times 10^{-5} \pm 1.04 \times 10^{-4}$	2.94×10^{-5}
p-value	>0.05	>0.05

The Pandora-derived concentrations at Wakkerstroom for 2020 ($5.06 \times 10^{-5} \pm 8.97 \times 10^{-5}$ mol/m^2) were statistically similar (p-value > 0.05) to those in 2021 ($5.03 \times 10^{-5} \pm$

9.40×10^{-5} mol/m^2) (Table 2). These values also align with the Ozone Monitoring Instrument (OMI)-derived results reported by Matandirotya and Burger [16] for 2019 and 2020 over Johannesburg. Johannesburg is adjacent to the Highveld area and the two air sheds are known to influence one another [56]. It also indicates that the values are, on average, representative of this hotspot of NO_2 emissions in South Africa.

Compared with other commercial and industrial regions around the world, the annual mean concentrations at Wakkerstroom in 2020 are similar to mean concentrations at sites in mid-western Brazil in the same year measured using the OMI satellite instrument and not a ground-based instrument [57].

Due to the gamma distribution pattern of atmospheric NO_2 concentrations and other atmospheric variables, the median is a more reliable measure of central tendency. However, the median values measured at Wakkerstroom for the two years are not the same. The median concentrations in 2020 (2.10×10^{-5} mol/m^2) are significantly higher (p-value < 0.05) than in 2021 (1.44×10^{-5} mol/m^2) (Table 2).

The mean and median TROPOMI-derived annual TVC-NO_2 concentrations were $6.17 \times 10^{-5} \pm 1.06 \times 10^{-4}$ mol/m^2 and 2.86×10^{-5} mol/m^2, respectively, in 2020 (Table 3). They were not significantly different (p-value > 0.05) from the values measured during 2021 ($7.06 \times 10^{-5} \pm 1.04 \times 10^{-4}$ mol/m^2 and 2.94×10^{-5} mol/m^2).

The annual mean and median TVC-NO_2 concentrations derived from TROPOMI are higher than the Pandora-derived TVC-NO_2 concentrations. This is expected since the Pandora instrument only accounts for approximately 1/3 of the tropospheric column compared to the total tropospheric column derived from the TROPOMI instrument. The similar interannual mean concentrations found in this study from both instruments sug- gest the dominance of regionally significant factors influencing tropospheric NO_2 levels, particularly in the low troposphere, over the Highveld.

The ground-based Pandora data at Wakkerstroom indicate that the emissions in the LTVC were significantly higher in 2020 than in 2021, but in the total tropospheric column data from the TROPOMI instrument, there were no significant changes.

The TVC-NO_2 concentrations at Wakkerstroom are highly variable, as shown by the large standard deviation around the mean concentrations of the highly temporally resolved data (Tables 2 and 3). The variation can be attributed to anthropogenic and natural factors such as changes in local emissions, atmospheric circulation and stability, air mass transport, and weather patterns [23,58].

To explore this variability, we analysed the seasonality of the data. In South Africa, the seasons are delineated as follows: summer (December to February, DJF), autumn (March to May, MAM), winter (June to August, JJA), and spring (September to November, SON). Spring is characterised by the onset of rainfall over the region, while summer is the wet season. Autumn and winter are dry over the Highveld [59,60].

An overall season pattern emerges out of the weekly average MAX-DOAS data over Wakkerstroom. The early summer and early spring (late winter) seasons recorded the highest mean concentrations of LTVC-NO_2 over Wakkerstroom for both years. The highest Pandora-derived LTVC-NO_2 concentrations in 2020 were observed in the summer during week 50 (mean: $1.68 \times 10^{-4} \pm 1.88 \times 10^{-4}$ mol/m^2; median: 9.33×10^{-5} mol/m^2) (Figure 3).

While Figure 3 (2020 data) shows peak LTVC-NO_2 concentrations in austral summer, Figure 4 for 2021 data shows contrasting patterns of peak seasonal LTVC-NO_2 concentrations (mean: $1.63 \times 10^{-4} \pm 8.67 \times 10^{-5}$ mol/m^2; median: 1.36×10^{-4} mol/m^2) in late winter (week 34). The lowest mean ($5.51 \times 10^{-6} \pm 3.18 \times 10^{-6}$ mol/m^2) and median (4.83×10^{-6} mol/m^2) LTVC-NO_2 concentrations were measured during the autumn and the early winter months, with the exception of one episode in week 23 (Table A1).

The TROPOMI data show a distinctly different seasonal pattern of highest and lowest concentrations of tropospheric NO_2. The observations from the satellite-based instrument show an early winter and early spring peak in both years. The lowest concentrations between 2020 and 2021 do not coincide. In 2020, the lowest concentrations are observed in late summer and early autumn (this is more or less the same as the ground-based data).

In 2021, minimum concentrations are observed in the late summer period. The weekly aggregated TROPOMI-derived data show peak weekly mean TVC concentrations ($1.75 \times 10^{-4} \pm 3.71 \times 10^{-4}$ mol/m^2) in the winter (in week 27) (Figure 5).

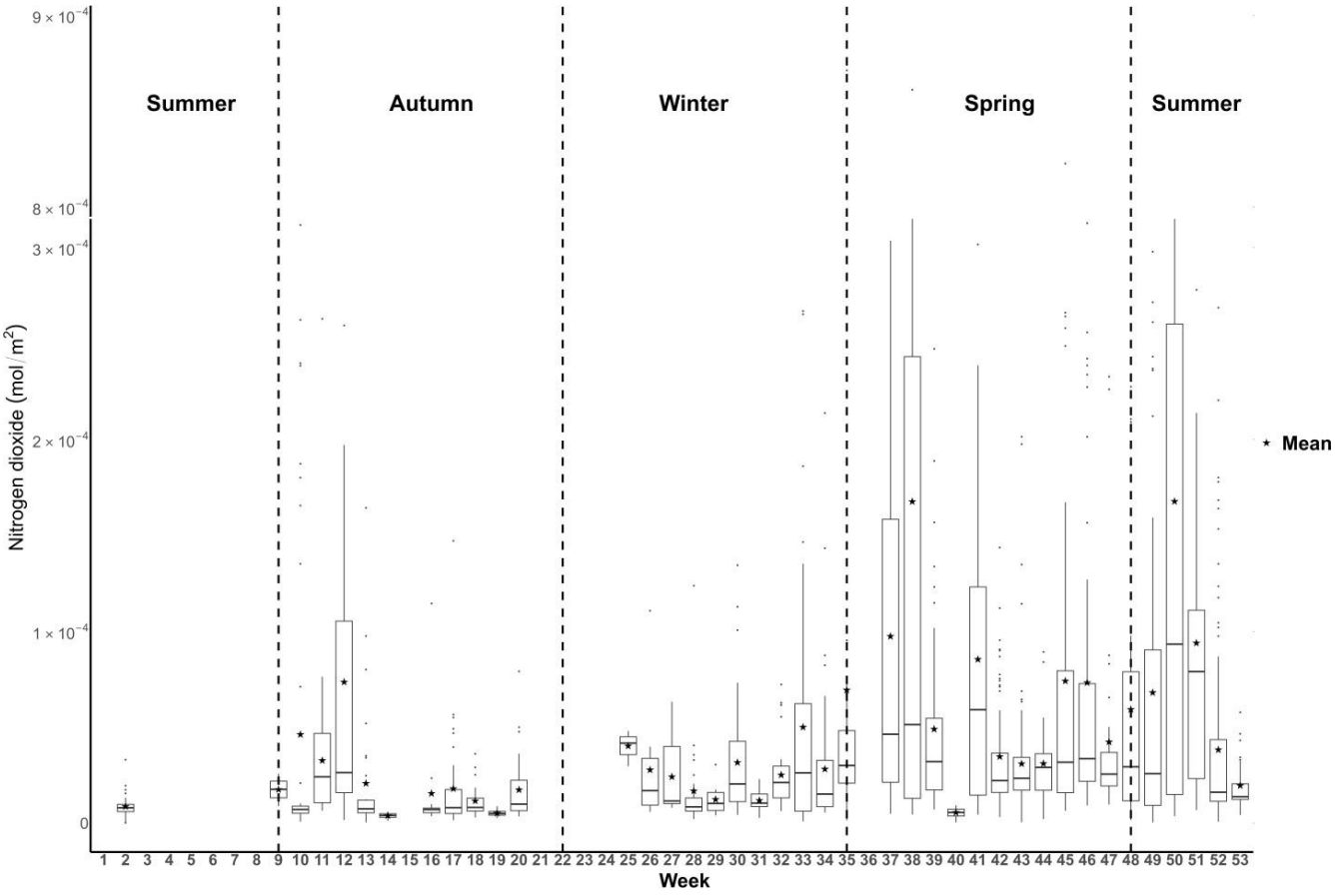

Figure 3. Boxplot of weekly averaged MAX-DOAS Pandora-derived low-tropospheric nitrogen dioxide concentrations (mol/m^2) in Wakkerstroom, Mpumalanga, for January to December 2020. A star denotes the weekly mean and the black dots represent all mean values higher than the upper quartile. The vertical dashed lines indicate the start of the four seasons: autumn, winter, spring and summer. The y-axis scale was cut between 3×10^{-4} and 8×10^{-4} mol/m^2 to make the figure more legible at low ($<3 \times 10^{-4}$ mol/m^2) NO_2 concentrations where the majority of the NO_2 concentrations measured. The data are expressed in full in Appendix B.

Further inspection of the TROPOMI-derived weekly data shows that during week 27, six out of the seven weekly measured concentrations were in the magnitude of $\times 10^{-5}$ except one, which was $\times 10^{-3}$. However, during week 39, only two of the six available daily concentrations were in the $\times 10^{-5}$ magnitude, and the rest were in the $\times 10^{-4}$. This indicates that a one-day event drove the high mean TVC-NO_2 concentration seen in week 27 (winter), while the elevated concentrations in spring were probably driven by the biomass-burning episodes during that week, as reported by [61].

The minimum mean ($3.33 \times 10^{-6} \pm 4.47 \times 10^{-6}$ mol/m^2) and median (2.47×10^{-6} mol/m^2) concentrations in 2020 were measured in week 13, autumn (Figure 5). This is due to the advection of clean air from the Southern Ocean observed at lower tropospheric levels during this time [61].

The 2021 TROPOMI-derived TVC-NO_2 data (Figure 6) show weekly mean ($3.16 \times 10^{-4} \pm 2.44 \times 10^{-4}$ mol/m^2) and median (2.68×10^{-4} mol/m^2) peaks in the late winter (week 34). The full data set can be seen in Appendix B. The similarity of this finding to that of the Pan159 LTVC-NO_2 concentrations (Figure 4) in the same year indicates that

the low tropospheric sources contributed more to the integrated column concentrations.

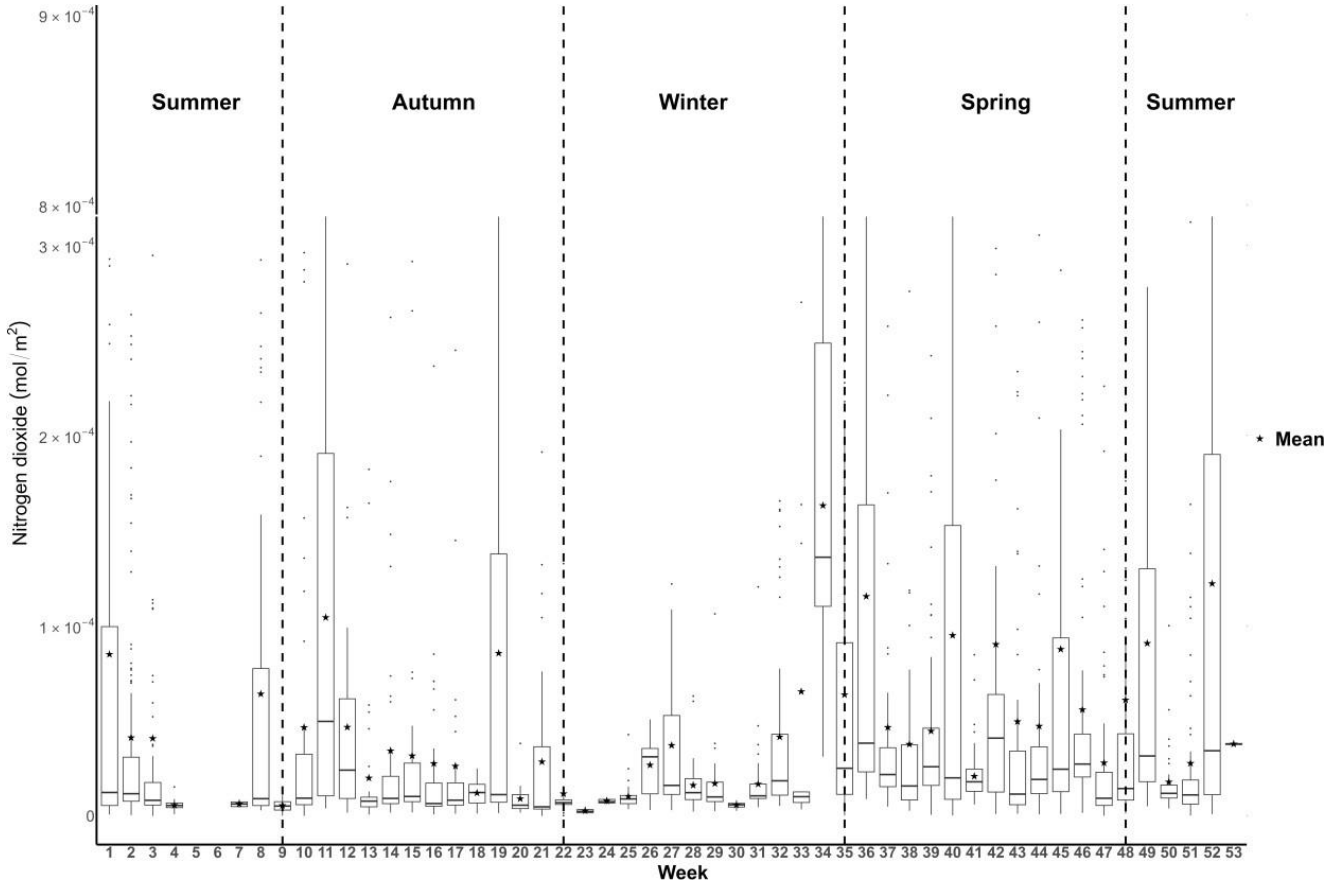

Figure 4. Weekly averaged boxplots of MAX-DOAS Pandora-derived low tropospheric nitrogen dioxide concentrations (mol/m^2) in Wakkerstroom, Mpumalanga, for 2021. A star denotes weekly means. The vertical dashed lines indicate the start of the four seasons: autumn, winter, spring and summer. The y-axis scale was cut between 3×10^{-4} and 8×10^{-4} mol/m^2 to make the figure more legible at low (<3×10^{-4} mol/m^2) NO_2 concentrations where the majority of the NO_2 concentrations measured. The data are expressed in full in Appendix B.

The elevated concentrations observed from the ground-based instrument were not the expected results. Although the concentrations in early summer 2021 are lower than in 2020, the concentrations remain higher than in winter. Previous studies have found elevated concentrations during the winter [56,62]. The difference is that the previous studies used ground-based in situ measurements that have no way of looking at the integrated tropospheric column. The elevated summer concentrations are surprising because this is the wet and warm season, associated with unstable meteorological conditions, increasing the vertical motion and dispersion of trace gases in the atmosphere [63,64]. In addition, the increased precipitation during the wet seasons increases the removal of pollutants from the atmosphere through wet deposition [17,56]. A key difference between the two seasons is the atmospheric stability, which determines the mixing of NO_2 from major sources through the column. It was expected that NO_2 measured in the tropospheric column would be integrated, thus not really showing a big difference between the seasons, especially summer and winter. It seems that the vertical mixing is impacting the detected concentrations. This is coupled with the transport pathways of NO_2 from the main source region, the industrialised Highveld, to the site. During summer, the transport pathway is controlled by the easterly wave perturbations [65].

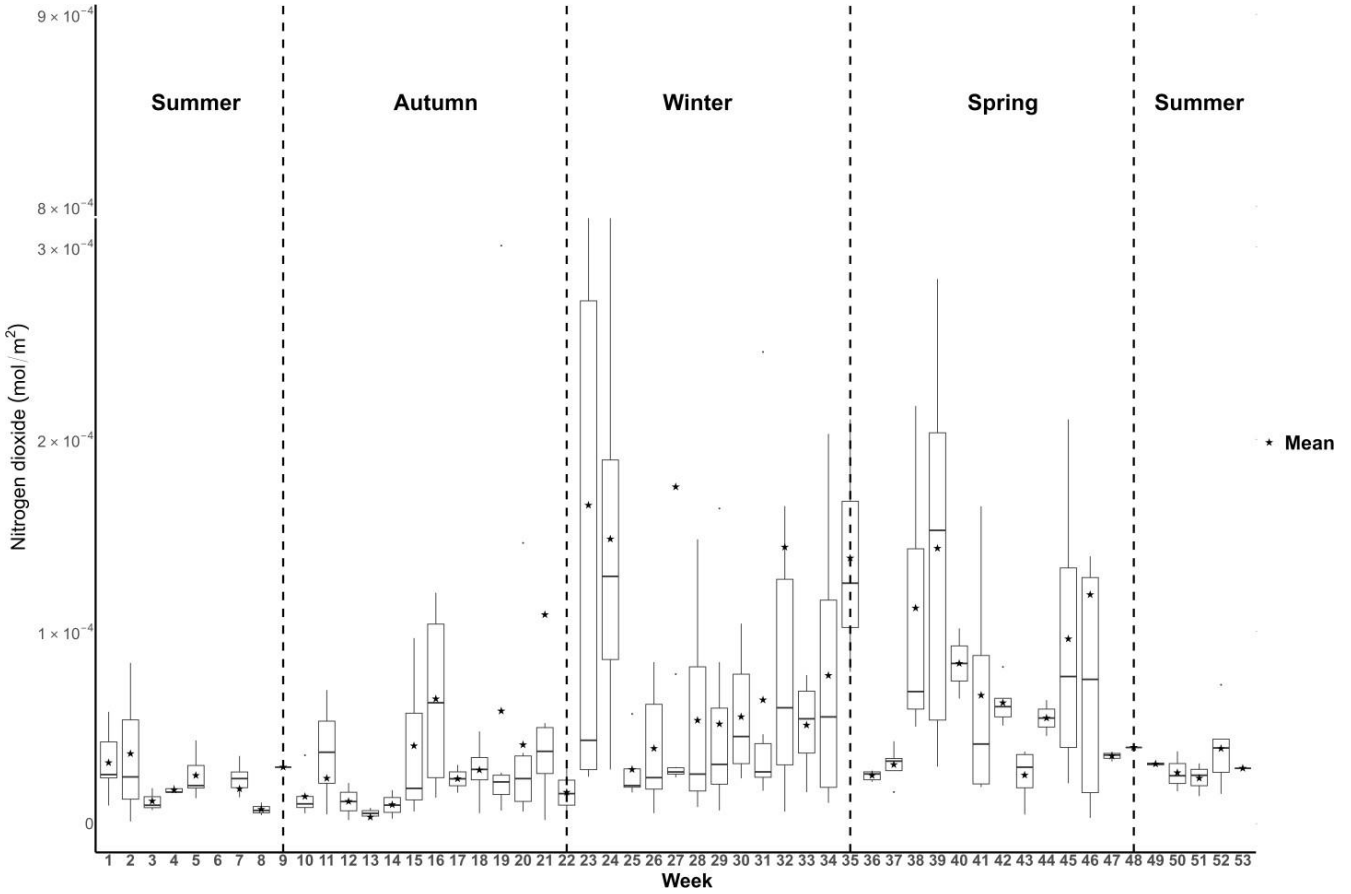

Figure 5. TROPOMI-derived tropospheric nitrogen dioxide concentrations over Wakkerstroom, Mpumalanga, averaged weekly for 2020. The means are represented by a star. The vertical dashed lines indicate the start of the four seasons: autumn, winter, spring and summer. The y- axis scale was cut between 3×10^{-4} and 8×10^{-4} mol/m^2 to make the figure more legible at low ($<3 \times 10^{-4}$ mol/m^2) NO_2 concentrations where the majority of the NO_2 concentrations were mea- sured. The data are expressed in full in Appendix B.

In contrast, winters are characterised by the formation of surface inversion layers inhibiting vertical atmospheric mixing and effectively trapping the primary pollutants [17]. The winters in the Highveld are dry and cold, resulting in additional combustion of coal and wood for domestic heating [17]. Furthermore, the transition from winter to spring and the spring are also characterised by occurrences of biomass burning [56].

These conflicting findings challenge the established understanding of TVC-NO_2 con- centration patterns during the winter season.

Due to the lack of pollutant measurements in South Africa and the spatial and temporal variability, it would be extremely useful if the TROPOMI data could be utilised as a proxy of gaseous pollutant concentrations over the most polluted regions of South Africa. From the data presented in Figures 3–6, this seems not to be an ideal practice. On average (not considering the extreme values), however, if we compare the Pandora and TROPOMI tropospheric column data (Figure 7), we see that it is possible to use a longer-term average value (weekly) as a proxy of the state of gaseous pollutants over the Highveld. There are some differences, as one would expect, but overall, the TROPOMI data give a fair estimate of the NO_2 concentrations over Wakkerstroom, as they capture the majority of the integrated concentrations from the lower troposphere. The highest concentrations occur in the late winter and early spring, with early summer and winter also showing elevated levels of NO_2. The

question that remains is whether Wakkerstroom is a representative site of the industrialised Highveld. Wakkerstroom is in close proximity to some of the largest power plant emissions in South Africa. The site is also downwind of the industrial and urban complex of the Highveld. As with most sites over the Highveld, the site is also influenced by a series of other sources, namely local burning as well as the seasonal peak of biomass burning. We would argue that this analysis shows that TROPOMI can be used to generate proxies of indexes of air quality weekly or longer when longer-term average data are utilised.

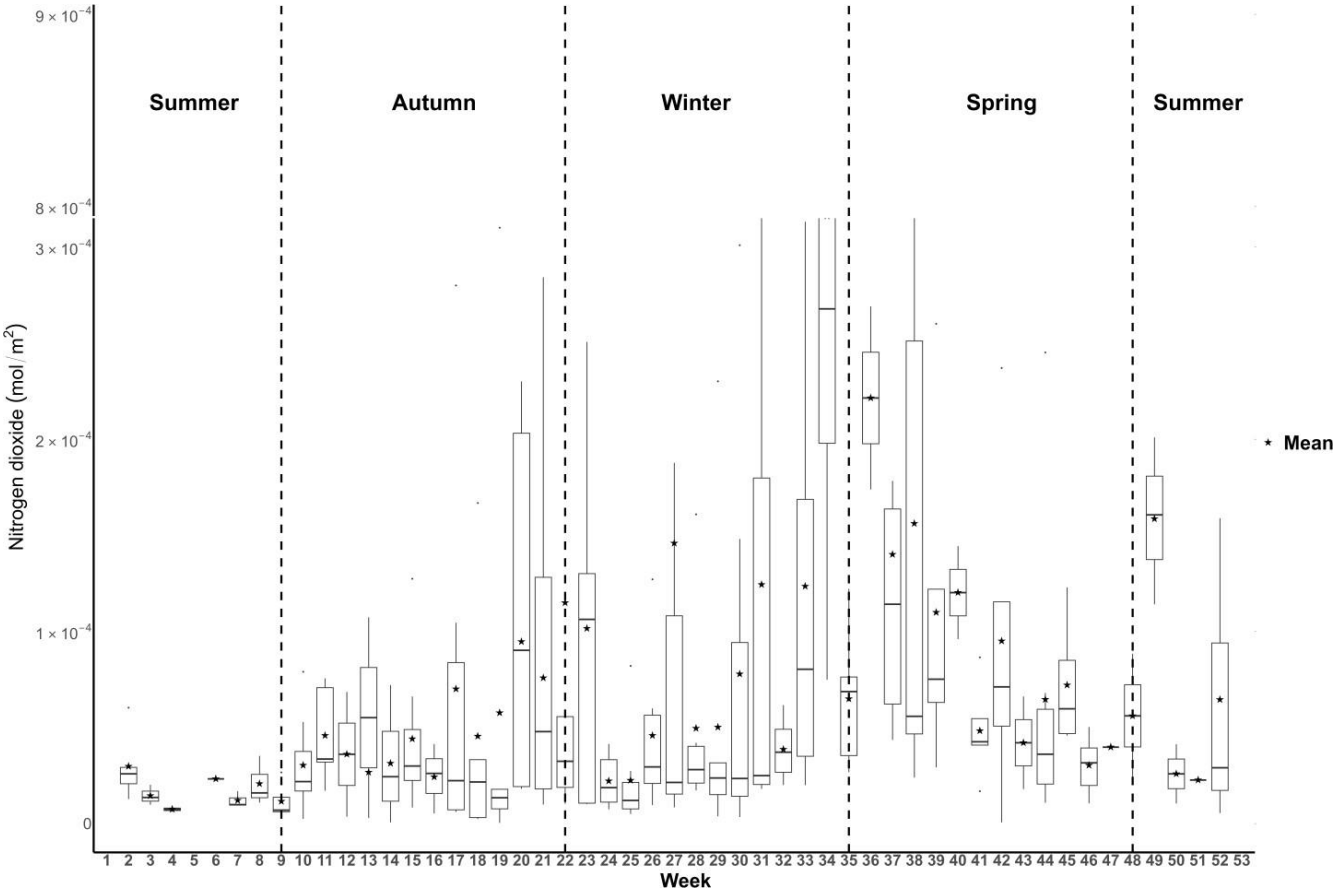

Figure 6. TROPOMI-derived tropospheric nitrogen dioxide concentrations over Wakkerstroom, Mpumalanga, averaged weekly for 2021. The means are represented by a star. The vertical line indicates the start of a new season. The vertical dashed lines indicate the start of the four seasons: autumn, winter, spring and summer. The y-axis scale was cut between 3×10^{-4} and 8×10^{-4} mol/m^2 to make the figure more legible at low ($<3 \times 10^{-4}$ mol/m^2) NO_2 concentrations where the majority of the NO_2 concentrations were measured. The data are expressed in full in Appendix B.

For both instrument measurements, the mean TVC-NO_2 concentrations for 2020 and 2021 (Figure 7) at Wakkerstroom increased consistently during seasonal transitions, specifically from winter to spring. A more variable increase is seen in the transition between autumn and winter. Another consistency between the TROPOMI and Pandora TVC-NO_2 concentrations is the increase in concentrations in 2021 during the austral summer season (Figure 7). The high Pandora measurements reflect the local variability diurnally and temporally in the lower tropospheric column NO_2 concentrations. The TROPOMI data, in contrast, do not show that because of its daily overpass, unlike the Pan159 instrument that measures more frequently.

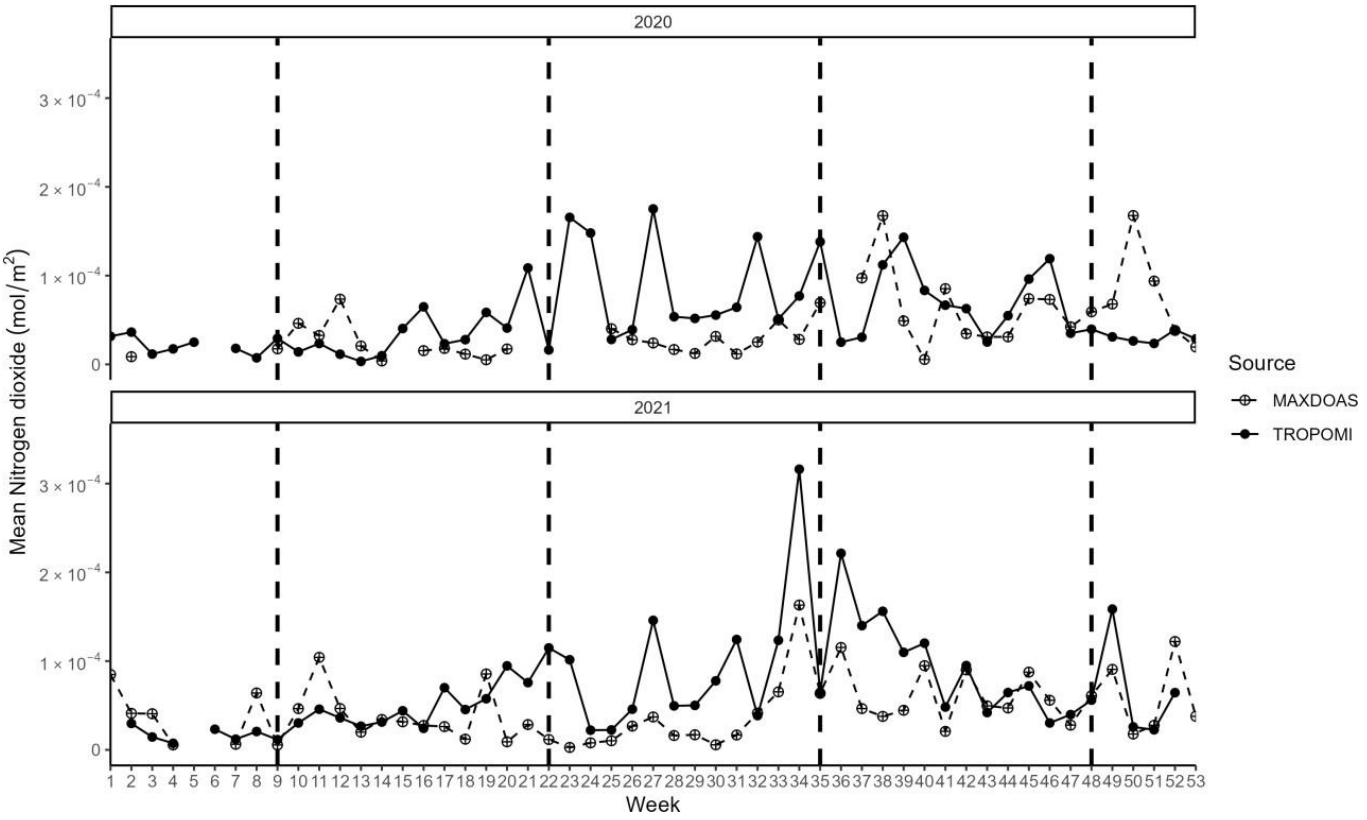

Figure 7. Comparison of weekly averaged TVC-NO_2 concentrations over Wakkerstroom, Mpumalanga, in 2020 (top panel) and 2021 (bottom panel), measured using TROPOMI (solid lines with solid circle) and Pandora instruments (MAX-DOAS) (dash lines with open circle).

1.3.2. TROPOMI and Pandora-Derived Tropospheric NO_2 Concentrations

The TROPOMI-derived annual mean and median TVC-NO_2 concentrations in 2020 and 2021 were higher than the Pandora-derived concentrations for the same years (Tables 2 and 3). This is expected since the two instruments are sensitive at different tropospheric levels and retrieved TVC-NO_2 concentrations from two different integrated TVC volumes. The data sets were evaluated to further elucidate the complementary relationship between the two instruments' TVC-NO_2 data products.

The Theil Sen Regression analyses were performed using ±5 min (±5 min) (Figure 8 left panel) and ±1 h (±1 h) (Figure 8 right panel) Pandora-derived coincidence data to the TROPOMI sensing time to compare the TROPOMI and Pandora-derived TVC-NO_2 concentrations over Wakkerstroom. The two coincidence data sets (Figure 8) show a positive correlation between the TROPOMI and Pandora-derived data sets (p-value < 0.05). The ±5 min (n = 48) coincidence data show a strong determination coefficient (R^2) of 0.64 with a slope of 1.1. The correlation between the TROPOMI and Pandora ±1 h coincidence data (n = 149) (Figure 8 right panel) is strong (R^2 = 0.57) but less than that of the ±5 min data. There is a stronger correlation between the TROPOMI and the Pandora data sets when TVC-NO_2 concentrations are lower (Figure 8). This is probably because the majority of the concentrations measured are from the low troposphere where both instruments are measuring.

The RSE values were used to validate the regression models, and all models are valid with RSE values approaching zero.

Further analyses of the ±1 h coincidence data show that concentrations in summer are better correlated than during other seasons (Figure 9).

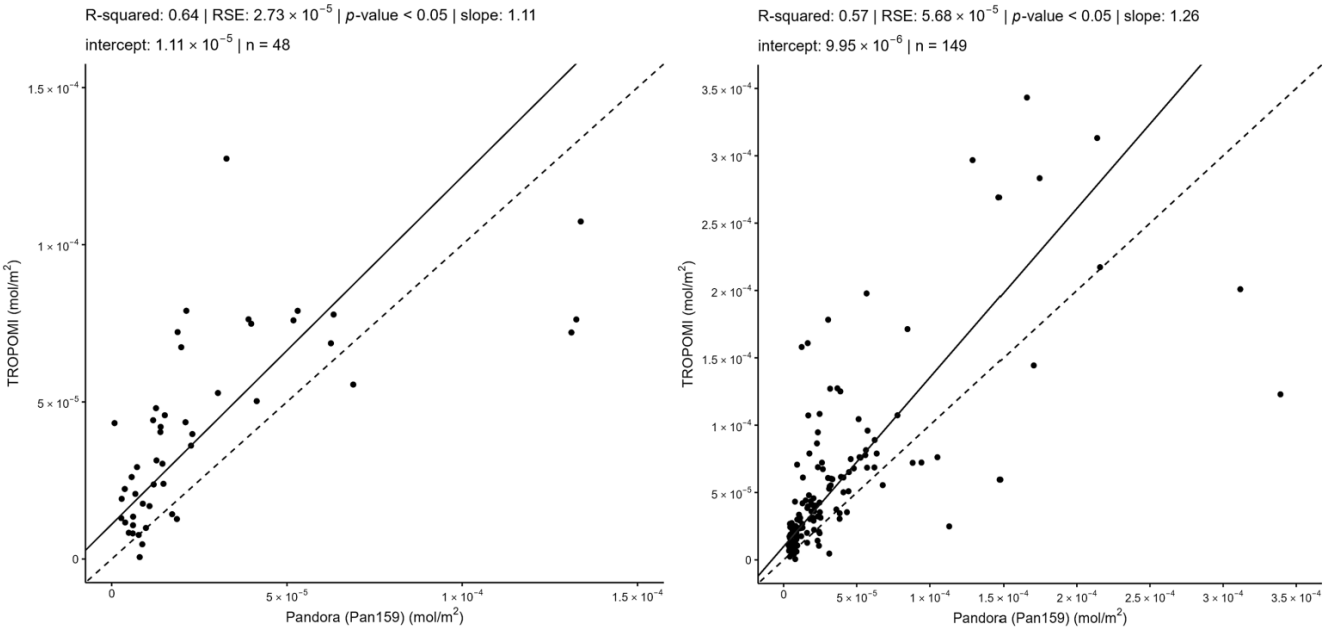

Figure 8. Theil Sen regression analysis of ±5 min (left panel) and ±1 h (right panel) coincidence TROPOMI and Pandora data over Wakkerstroom in 2020 and 2021. The black dashed line is the 1:1 line, and the black solid line is the regression line (±5 min NMB%~54%; ±1 h NMB%~64%).

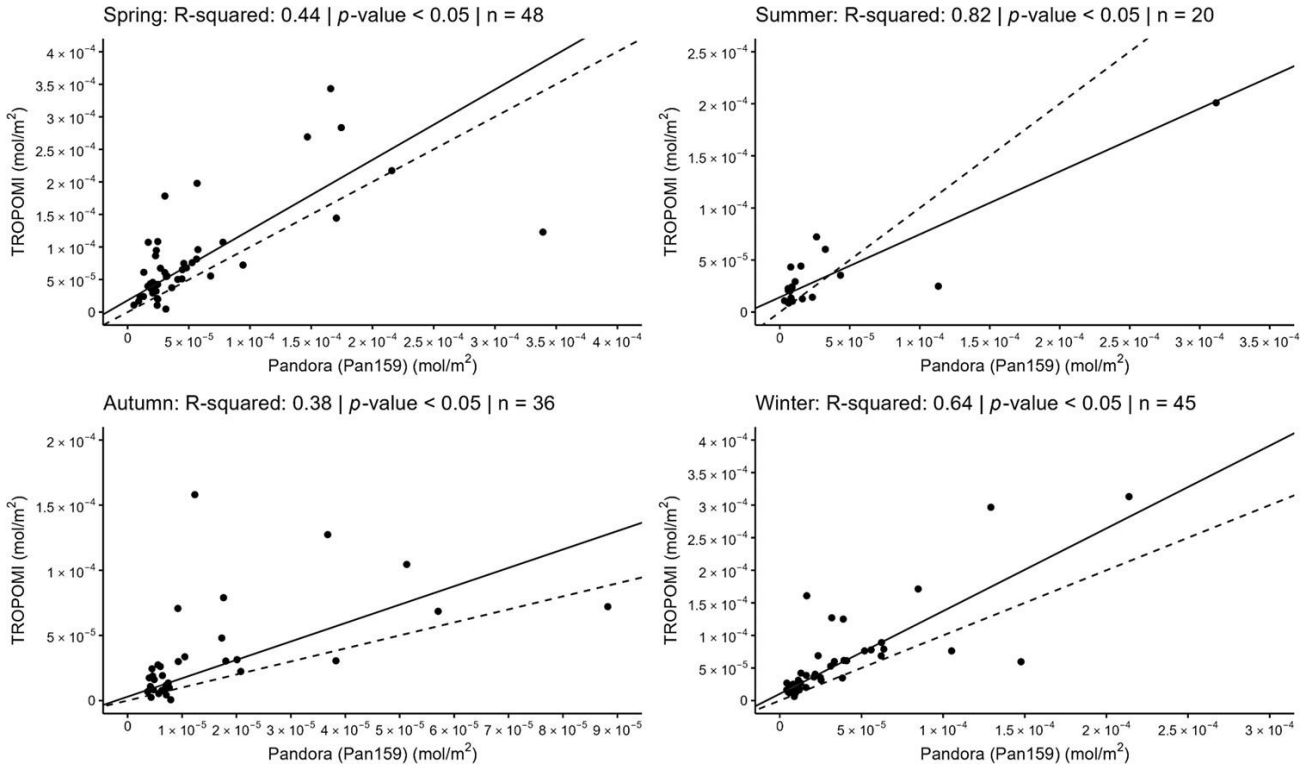

Figure 9. The seasonal correlation between the TROPOMI sensing time and the ±1 h Pandora coincidence data over Wakkerstroom using the Theil Sen regression analysis. The black dashed line is the 1:1 line, and the black solid line is the regression line.

Diverse factors play a role in this disagreement between TROPOMI and Pan159 data sets, including averaging differences [2], different viewing geometries of the instruments, and

NO_2 concentrations that are not uniformly mixed throughout the troposphere due to emissions and vertical atmosphere mixing [66]. The Pandora-derived MAX-DOAS concentrations are predominantly in the lower troposphere, whereas the TROPOMI-derived concentrations are aggregated for the entire tropospheric column. The last of the factors explaining the disagreement in the TVC-NO_2 concentrations of the two instruments is especially important in the southern African context, where three dynamics exacerbate the problem of vertical stratification. Firstly, the interior of the South Africa Highveld is on an elevated plateau that is approximately 1700 m or more above sea level. Those elevations mean the major local emissions can be trapped closer to the ground due to temperature inversion [67,68]. In addition, the dispersion of pollutants on the Highveld may not be as efficient at lower elevations due to the low air density at higher elevations. Secondly, southern Africa has been shown to have a highly stratified vertical atmospheric structure that prevails for many months of the year. The atmospheric stratification is driven by subsidence, creating distinct and substantial thermodynamic barriers at approximately 3000 m and 5000 m a.s.l [69]. Finally, two major sources of NO_2 over the subcontinent include biomass burning, with ground emissions that can be carried up to the middle troposphere by turbulence, and power station emissions that have stacks designed to release emissions at a height above the stable layer to avoid downward mixing of the emissions in the presence of surface layer conversions. These factors create conditions, especially over the Highveld, of distinctly elevated plumes of concentrated pollution that can persist in the atmosphere for many days [70].
The inconsistency in the seasonal trends of atmospheric trace gas concentrations in the Highveld, particularly for short-lived pollutants such as NO_2, from satellite and ground- based instruments, indicates that the persistent stable layers in the Highveld atmosphere contribute to the complexity and disparity of the measurements.

1.4. Tropospheric Vertical Column Nitrogen Dioxide Profiles

Figure 10 shows the Pandora MAX-DOAS LTVC-NO_2 concentrations as a function of altitude in 2020 and 2021. It confirms that the Pan159 instrument measures LTVC-NO_2 concentrations aggregated from ~50 m to 4.5 km above the ground. Between the maximum vertical distance of 2.5 km and 3.5 km a.g.l is where the Pandora instrument measured the highest concentrations of NO_2 in the low troposphere. At altitudes above 4 km a.g.l and below ~1.5 km a.g.l, the concentrations were low (Figure 10). Some of the highest Pandora MAX-DOAS LTVC-NO_2 concentrations were measured at ~3 km a.g.l.
There are several stable layers in the Highveld atmosphere that could act as a vertical barrier [69], interfering with the mixing of the emitted NO_2 concentrations in the atmosphere. The boundary layer is at approximately 1300 m a.g.l (700 hPa), followed by the 500 hPa stable layer, which is at approximately 3800 m a.g.l. The 500 hPa stable layer coincides with the decrease in concentrations higher than 4 km a.g.l. If emissions are released above the boundary, there is less possibility of those emissions mixing down since the layer traps pollutants separating the emissions above and below the layer [69]. This is possibly why high concentrations are seen between the 700 hPa and 500 hPa stable layers.
The Tracer Model version 5, massively parallel version (TM5-MP) chemistry transport model a priori profile shape data of the TROPOMI-derived TVC-NO_2 retrievals over Wakkerstroom, Mpumalanga, in South Africa, are presented in Figure 11. These data show the a priori profile shapes for the stratospheric and the tropospheric vertical columns in 2020 and 2021. The highest concentrations were recorded in the lower atmosphere, between 800 and 600 hPa.

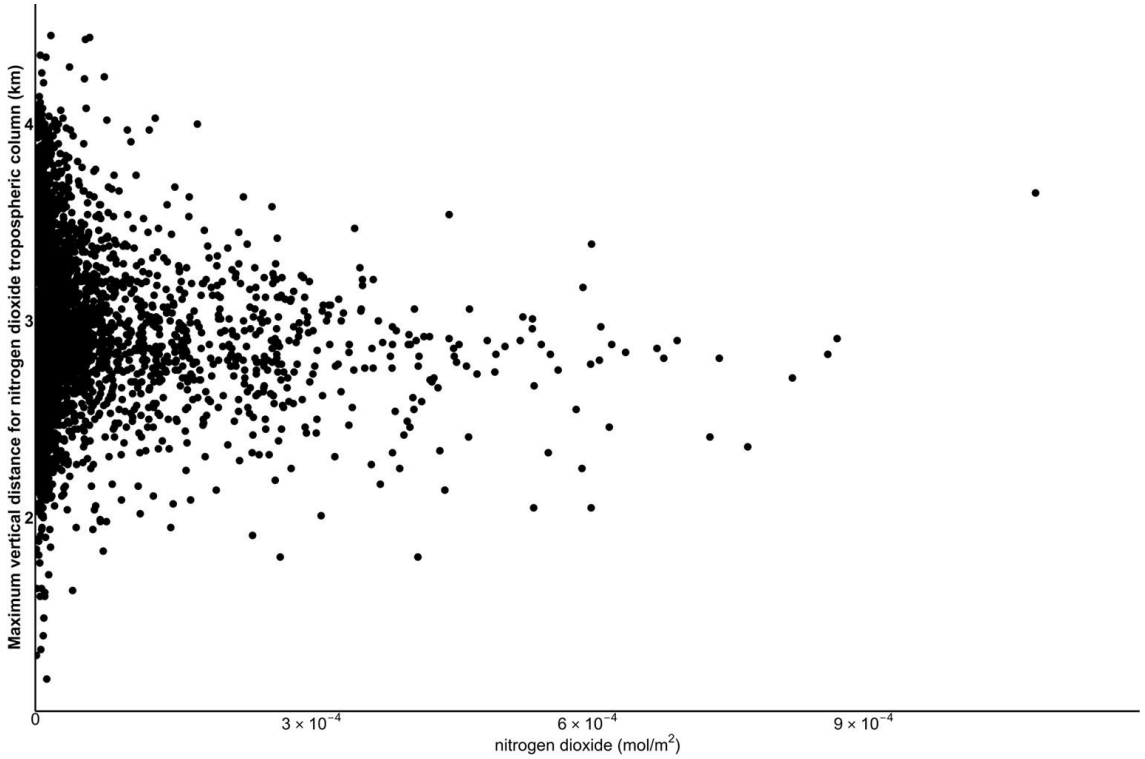

Figure 10. The maximum height Pandora MAX-DOAS tropospheric vertical column nitrogen dioxide profiles at Wakkerstroom, Mpumalanga Province. The vertical distance measured by Pan159 is above ground level (a.g.l). The altitude corresponds to atmospheric hPa (2 km a.g.l = ~650 hPa; 3 km a.g.l = ~550 hPa; 4 km a.g.l = ~500 hPa).

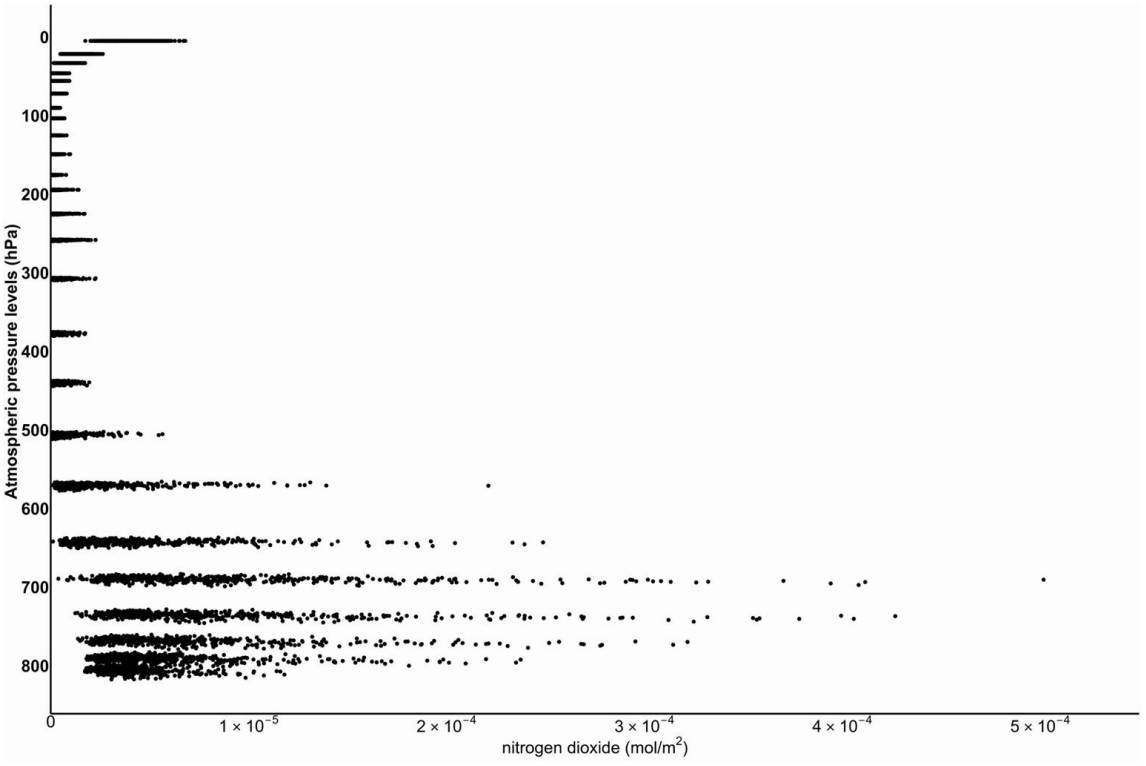

Figure 11. TROPOMI a priori profiles over the Wakkerstroom Highveld in 2020 and 2021.

1.5. Backward Trajectories (HYSPLIT)

In this research, three periods of elevated concentrations of NO_2 have been identified over Wakkerstroom. It is important to establish the atmospheric transport pathways associated with these increases in pollution to understand the potential contributing sources. Five-day backward trajectories have been used for this purpose.

In 2021, the late winter and early spring LTVC-NO_2 concentration peaks (week 34) were characterised by 50% air masses transported from the north of Wakkerstroom passing through the secondary hotspot over the Gauteng-Tshwane metro and coal-fired power station emissions at 550 hPa (Figure 12b). The air mass circulation was also dominated by continental recirculation patterns. The early summer LTVC-NO_2 concentration peaks in 2020 were associated with recirculation of air masses at the lower troposphere from Mozambique over Limpopo Province and the Johannesburg and Ekurhuleni urban Metros before reaching Wakkerstroom at an altitude of 3 km a.g.l. (Figure 12a). Additionally, 32% of the westerly air masses also pass over the Johannesburg-Tshwane metro and the clustered power stations over the MP Highveld before reaching Wakkerstroom at 550 hPa during early summer. These main trajectories (3 and 2) were approximately at or below the 550 hPa level.

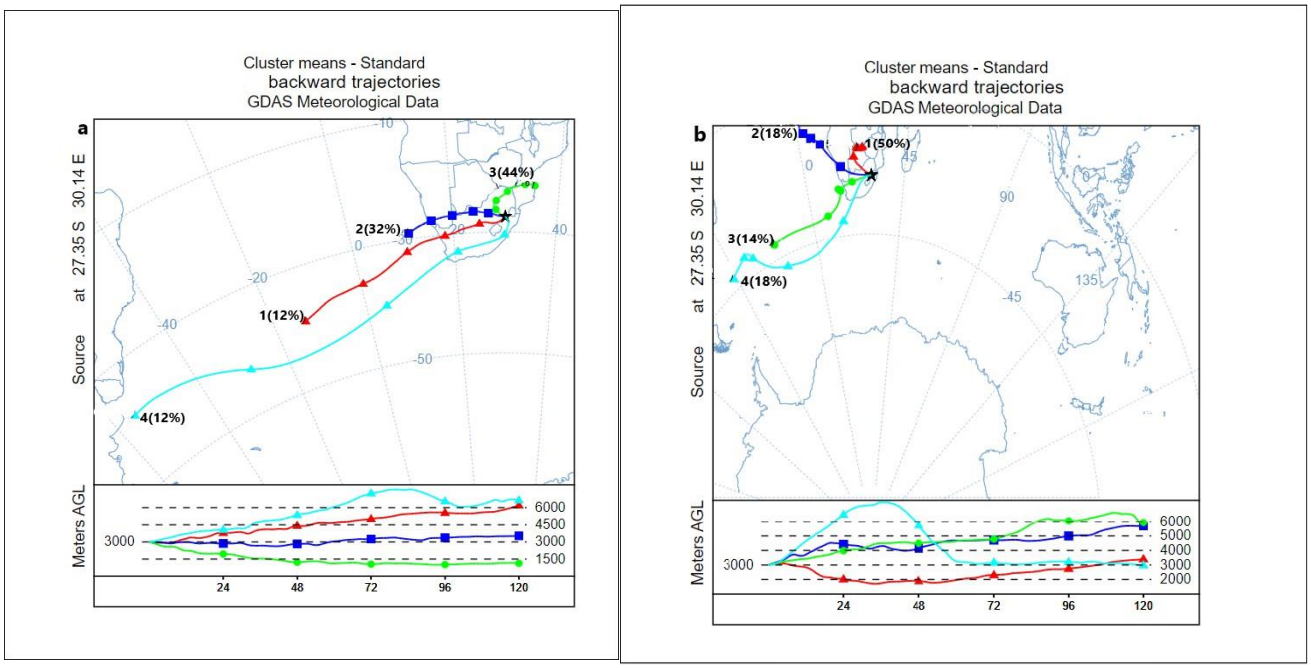

Figure 12. Five-day backward trajectories to Wakkerstroom, Mpumalanga, at 550 hPa for (**a**) week 50 in 2020 and (**b**) week 34 in 2021 for the observed peak LTVC-NO_2 concentrations measured by the Pan159 instrument.

These backward trajectories indicate sources of low-level emitters, such as biomass burning from southern Mozambique and local emissions from the Highveld. In addition, there are coal-fired power stations along that (from the west) transport pathway, causing additional loading of NO_2 concentrations as the air parcels are transported to Wakker- stroom. Fluctuations in local emissions are affected by shifts in commuting patterns of travellers passing through Volksrust from Johannesburg to KwaZulu-Natal or vice versa, the frequency of fossil fuel combustion and biomass burning. The literature has shown that fossil fuel combustion and biomass burning follow seasonal patterns, with increased fossil fuel combustion during the colder months (winter) and biomass burning from June to September in southern Africa [71,72].

The highest concentration of TVC-NO_2 identified from the TROPOMI satellite instru- ment

was at ~700 hPa (Figure 11), which is more representative of the lower tropospheric column. Therefore, backward trajectories at 700 hPa were investigated to find out what the major air mass trajectories were at that atmospheric level. In 2020, the transport patterns to Wakkerstroom were dominated by westerly and southwesterly winds (Figure 13a) from above 2500 m a.g.l. This was not surprising as westerly airflow increases significantly to the Highveld during the early winter season [23]. This type of transport is associated with air masses free of industrial emissions [23]. However, the trajectories in week 27 linger over land as they pass over the Gauteng-Tshwane metro and the clustered power stations before they reach Wakkerstroom, allowing for the accumulation of emissions. In 2021, the main transport (63%) was recirculated African flow (Figure 13b, cluster 1). This type of transport is prevalent at the 700 hPa level to the Highveld [23] in the early winter season. It promotes the accumulation of pollutants from neighbouring countries and areas around Wakkerstroom. This is an indication that most of the TROPOMI-derived TVC-NO_2 concentrations detected at Wakkerstroom in 2021 are due to emissions from elevated plumes caused by power stations, biomass burning, and other industries. These plumes easily reach the base of the 700 hPa stable layer.

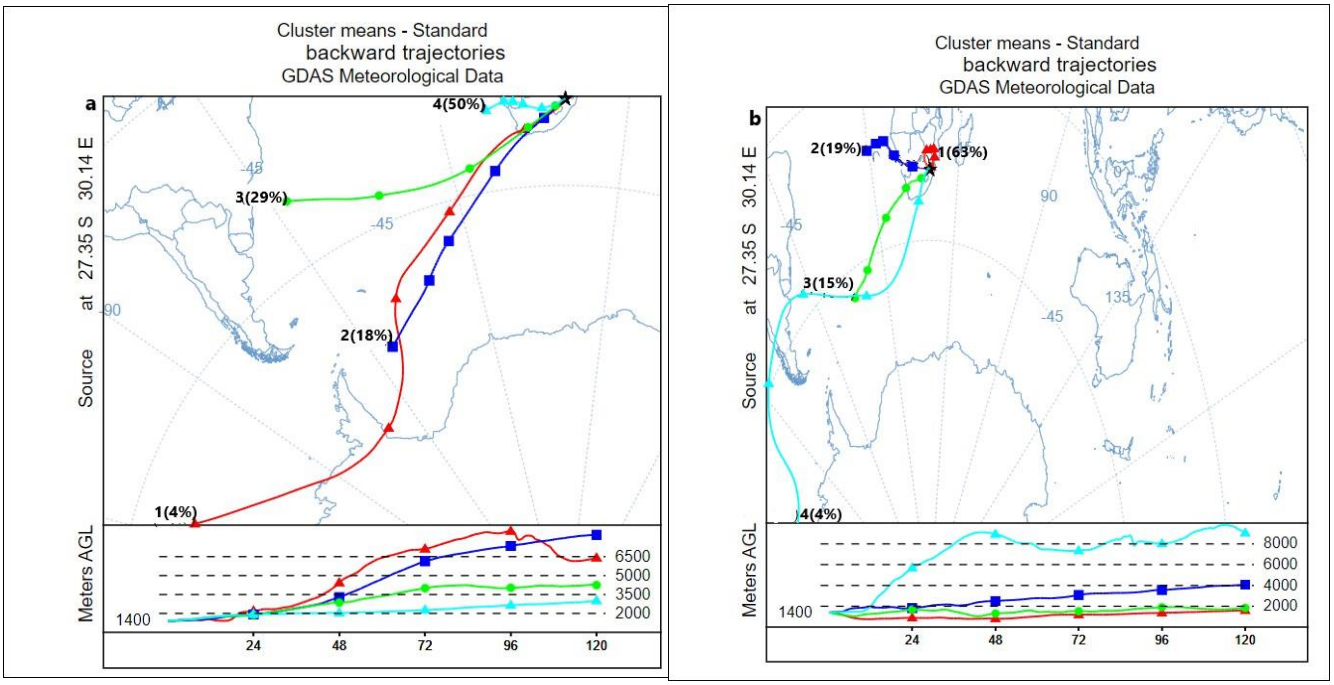

Figure 13. Five-day backward trajectories to Wakkerstroom, Mpumalanga, at 700 hPa for (**a**) week 27 in 2020 and (**b**) week 34 in 2021.

Discussion

The operation of the Pandora-2s instrument in the Mpumalanga Highveld of South Africa as part of the Pandonia Global Network (PGN) is significant as it is one of the only two Pandora instruments installed on continental Africa (https://blickm.pandonia-global- network.org/livemaps/pgn_stationsmap.png (accessed on 10 August 2024)), and it is located in an area subject to significant industrial pollution [56]. This is especially relevant because poor and deteriorating air quality is a major public health threat in this country. Furthermore, the high frequency of measurements available from the Pandora instrument effectively complement the wide spatial coverage but low frequency of data acquisitions from low earth orbiting (LEO) satellites, such as the TROPOMI satellite. Pandora-derived concentrations in this study are measured to an approximate maximum vertical atmospheric distance of 5 km above the ground (a.g.l). The highest concentration identifies the altitude of the highest concentrations of NO_2, as it was identified by the MAX-DOAS observations. In contrast, the entire tropospheric column extends from the planetary surface (sea level or

continental altitude) to 12 or 15 km.

The highest concentrations of tropospheric NO_2 are observed in the spring (late winter). Concentrations during this season are highly variable (Figures 3 and 4). The variability is likely associated with a source that is not fixed in space and variable in time. Biomass burning is the most likely source, as it is known to be transported over the Highveld during the spring season. From a previous analysis of lower tropospheric data derived from the Pandora instrument, it was shown that the emissions are transported towards the site from neighbouring South African countries—Mozambique and eSwatini—which contribute to the atmospheric NO_2 loading in the Highveld [61].

The reported elevated TVC-NO_2 concentrations can be attributed to the well-defined inversion layers that are present during winter, which trap pollutants, the slow wind speeds and recirculation patterns that limit dispersion as well as the absence of rainfall to scavenge the pollutants from the atmosphere [58,73,74]. In contrast, the 2020 median (1.52×10^{-4} mol/m^2) peaked in spring (week 39). The spike in the TVC-NO_2 concentration median indicates an event that elevated the measured concentrations. This is similar to the elevated surface NO_2 concentrations reported in 2020 over Wakkerstroom, which resulted from biomass burning in eSwatini [61].

Biomass-burning emissions have been identified to represent a large perturbation to global atmospheric chemistry [75]. NO_2 concentrations peaking in September can be attributed to biomass-burning emissions from the east of Wakkerstroom and other sources from the surrounding low-cost townships. In addition, considering the location of the Pandora instrument–downstream from major NO_2 pollutant sources, but not located next to or within those sources–the changes in emissions from the surrounding power stations are also possible contributors to the observed NO_2 concentrations.

The use of Pandora MAX-DOAS measurements to compare the TROPOMI-derived TVC-NO_2 concentrations has shown that the Pandora MAX-DOAS technique increases the spatial and temporal compatibility of the two data sets. Implementing two or more azimuthal directions for sky-scan measurements will further close the gap of scarce, highly spatially and temporally resolved air quality data and complement the relatively high spatial resolution global data from the TROPOMI satellite.

The Pandora-derived MAX-DOAS concentration seasonal patterns changed from a seasonal high in the summer of 2020 to the winter of 2021, while the TROPOMI seasonal pattern showed high NO_2 concentrations in the winter of both years. The similarity in the 2021 peak winter TVC-NO_2 concentrations for both instruments (even though the TROPOMI instrument measured higher TVC-NO_2 concentrations) indicates the aligned spatial resolution between the two data sets attributed to the sky scan measurements at various elevation angles and the contribution of the regional low troposphere sources to the measured total TVC-NO_2 concentrations. The similar seasonal variations between the Pandora-derived LTVC-NO_2 concentrations and the TROPOMI-derived concentrations indicate that the sources in the lower troposphere contribute a larger portion to the tropo- spheric column than sources higher in the troposphere, such as transported NO_2-laden air masses. This is evident when interrogating the weekly averaged data instead of the annual data. Both instruments identified peak concentrations in the lower troposphere, showing that the TROPOMI instrument is a good proxy of NO_2 distribution over Wakkerstroom.

Recirculation, transport from southern Mozambique, and northern and westerly air- flow to Wakkerstroom were identified as the air mass transport pathways contributing significantly to the measured elevated LTVC- and TVC-NO_2 concentrations in Wakker- stroom.

The temporal heterogeneity of NO_2 over the Mpumalanga Highveld can be seen using the Pandora-2s and the TROPOMI satellite instruments. This study showed that MAX-DOAS measurements from Pandora correlate positively ($R > 0$) with the TROPOMI satellite data when using 5 min and 1 h contemporaneous data, respectively. Ascertaining the bias between TROPOMI and ground-based instrument measurements is more complex for individual measurement stations. The overestimated TROPOMI measurements of the Pandora coincidence data are expected due to the sensitivity of the two instruments at different atmospheric levels during measurements. However, this shows that MAX-DOAS- derived

TVC-NO_2 concentrations can represent the area of satellite-derived TVC-NO_2 concentrations even when measuring in one azimuthal direction; hence, similar mean seasonal patterns but different median-informed seasonal patterns.
This can be attributed to the spatiotemporal heterogeneity of NO_2 and the sensitivity of the instruments at different atmospheric levels and that of the satellite in highly polluted areas—reflection, absorption, refraction and scattering are increased throughout the column during high pollution events. The presence of aerosols and other pollutants in the atmosphere, particularly in the stable layers, causes the satellite instrument to be more sensitive to NO_2 at the high atmospheric layers where the MAX-DOAS-derived concentrations are not measured. This is caused by the path length of the light to the instrument in the presence of other pollutants, resulting in more light absorption by the NO_2 trace gas.

Conclusions

The Pandora-2s instrument data complement TROPOMI satellite data due to its high temporal resolution data. These complementary data sets have shown similar seasonal TVC NO_2 concentration peaks despite indicating a significant local lower troposphere source in the Wakkerstroom area. Power stations and other local sources, such as biomass burning, contribute to the observed NO_2 levels in the Highveld. Seasonal TVC-/LTVC-NO_2 spikes, particularly in winter, are linked to inversion layers, low wind speeds, recirculation, and a lack of rainfall, which trap pollutants. The elevated LTVC-NO_2 concentrations in the early spring are attributed to biomass burning in neighbouring regions like Mozambique and eSwatini. This source is transported to the Highveld and contributes to the atmospheric NO_2 load. The spatiotemporal heterogeneity of NO_2 and the sensitivity differences between MAX-DOAS (ground-based) and satellite instruments make it challenging to compare measurements directly. However, both can provide important data on NO_2 distribution in Wakkerstroom.

Author Contributions: Conceptualisation, R.F.K.-S., M.C.S., R.J.S., S.J.P. and R.M.G.; Methodology, R.F.K.-S., M.C.S., S.J.P., R.M.G. and R.J.S.; Formal Analysis, R.F.K.-S.; Investigation, R.F.K.-S.; Resources, R.F.K.-S.; Data Curation, R.F.K.-S., J.v.G. and H.H.; Writing—Original Draft Preparation, R.F.K.-S.; Writing—Review and Editing, R.F.K.-S., M.C.S., S.J.P., R.M.G., H.H. and J.v.G.; Visualization, R.F.K.-S.; Supervision, M.C.S., S.J.P. and R.M.G.; Project Administration, R.F.K.-S., M.C.S. and S.J.P.; Funding Acquisition, M.C.S., R.J.S. and S.J.P. All authors have read and agreed to the published version of the manuscript.

Funding: This research was funded by Prof. Mary C. Scholes, grant number MCH021, and Prof. Stuart J. Piketh through the Climatology Research Group (CRG) in the Unit for Environmental Science and Management at the North-West University.

Institutional Review Board Statement: Not applicable.

Informed Consent Statement: Not applicable.

Data Availability Statement: Publicly available datasets were analysed in this study. This data can be found here: https://dataspace.copernicus.eu/ (accessed on 13 September 2023) for the TROPOMI data and http://data.pandonia-global-network.org/Wakkerstroom/Pandora159s1/L2/Pandora159s1_Wakkerstroom_L2_rnvs3p1-8.txt (accessed on 8 January 2023) for the Pandora-2s data.

Acknowledgments: We thank PI(s) and staff (local operator: Paul Grobler) for their effort in establishing and maintaining the Wakkerstroom Pandora (Pan159) instrument. The PGN is a bilateral project supported by funding from NASA and ESA. The authors would like to extend their sincere appreciation to Deborah Stein Zweers, Ankie Piters, Gaia Pinardi and Stephen Broccardo. A special thank you to Michel Verstraete and Stephen Broccardo for the discussion sessions. We also thank the Climate Research Group (CRG) from the North-West University in South Africa.

Conflicts of Interest: The authors declare no conflict of interest. The funders had no role in the design of the study; in the collection, analyses, or interpretation of data; in the writing of the manuscript; or in the decision to publish the results.

Appendix A

Table A1. Pandora MAX-DOAS retrieved weekly frequency (n) data capture in 2020 and 2021 over Wakkerstroom, South Africa.

Week	n_2020	n_2021
1	0	6
2	2	7
3	0	7
4	0	5
5	0	0
6	0	0
7	0	1
8	0	7
9	1	5
10	7	6
11	3	6
12	3	5
13	3	4
14	2	7
15	0	6
16	3	7
17	4	6
18	5	3
19	5	6
20	4	5
21	0	7
22	0	5
23	0	1
24	0	3
25	1	6
26	3	5
27	4	4
28	5	6
29	4	6
30	6	3
31	6	5
32	5	7
33	7	2

Table A1. *Cont.*

Week	n_2020	n_2021
34	7	4
35	4	7
36	0	4
37	3	6
38	6	6
39	7	6
40	1	7
41	5	7
42	7	7
43	6	6
44	4	7
45	5	6
46	5	7
47	3	7
48	2	7
49	5	7
50	6	5
51	3	7
52	7	6
53	2	1
Total	171	279

Appendix B

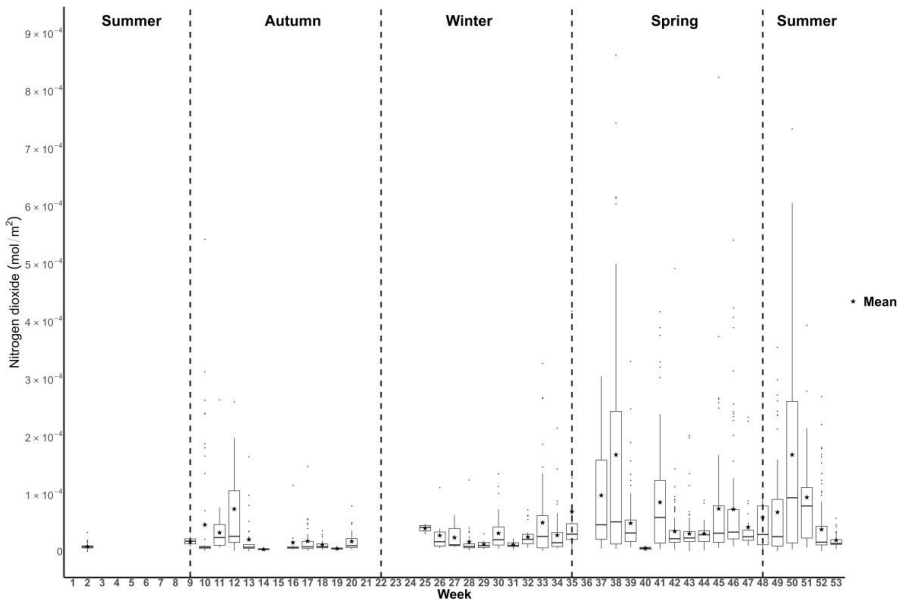

Figure A1. Boxplot of weekly averaged MAX-DOAS Pandora-derived low-tropospheric nitrogen dioxide concentrations (mol/m^2) in Wakkerstroom, Mpumalanga, for January to December 2020. A star denotes weekly means and the black dots represent all mean values higher than the upper

quartile. The vertical dashed lines indicate the start of the four seasons: autumn, winter, spring and summer. The y-axis scale was cut between 3×10^{-4} and 8×10^{-4} mol/m^2 to make the figure more legible at low (<3×10^{-4} mol/m^2) NO_2 concentrations where the majority of the NO_2 concentrations measured.

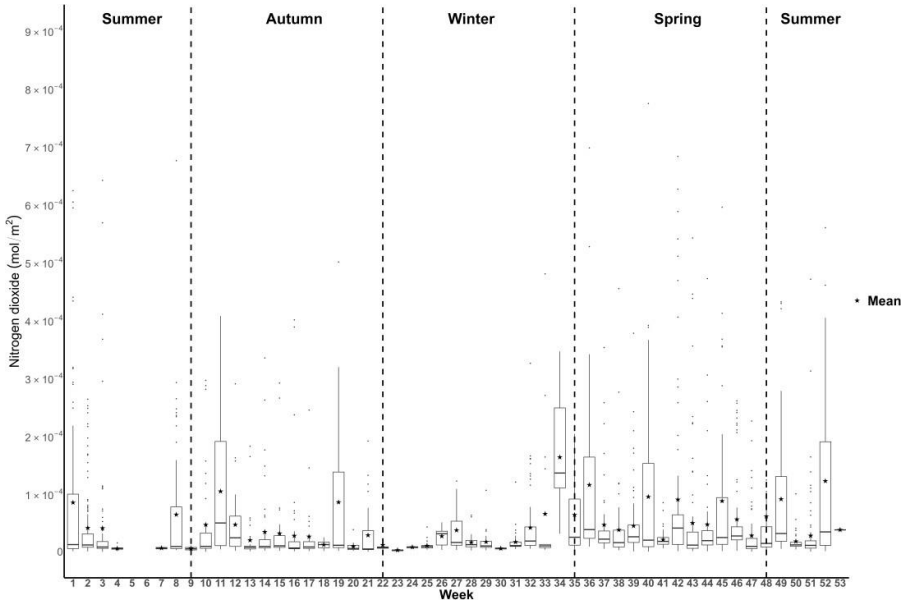

Figure A2. Weekly averaged boxplots of MAX-DOAS Pandora-derived low-tropospheric nitrogen dioxide concentrations (mol/m^2) in Wakkerstroom, Mpumalanga, for 2021. A star denotes weekly means. The vertical dashed lines indicate the start of the four seasons: autumn, winter, spring and summer. The y-axis scale was cut between 3×10^{-4} and 8×10^{-4} mol/m^2 to make the figure more legible at low (<3×10^{-4} mol/m^2) NO_2 concentrations where the majority of the NO_2 concentrations measured.

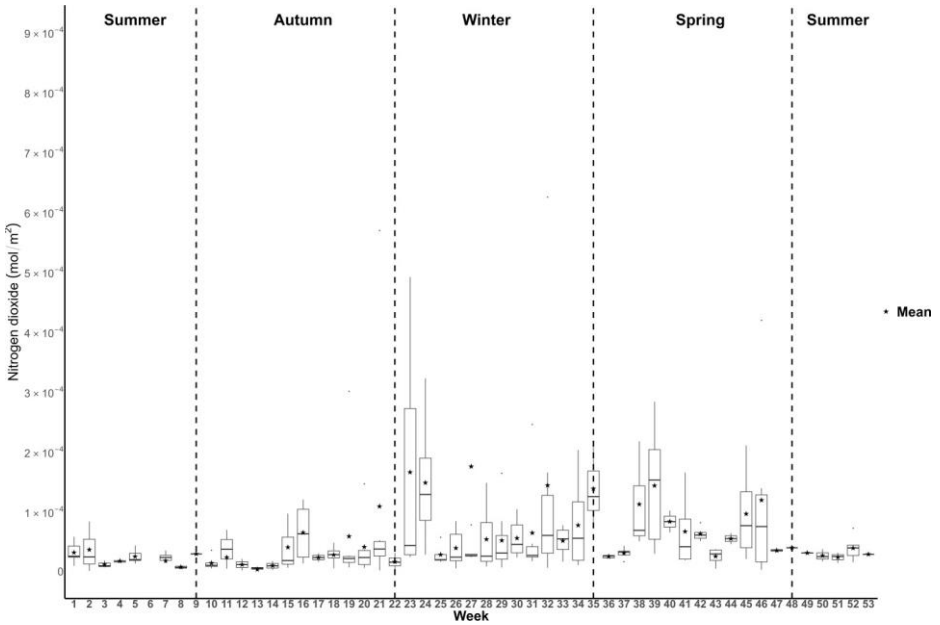

Figure A3. TROPOMI-derived tropospheric nitrogen dioxide concentrations over Wakkerstroom, Mpumalanga, averaged weekly for 2020. The means are represented by a star. The vertical dashed lines indicate the start of the four seasons: autumn, winter, spring and summer.

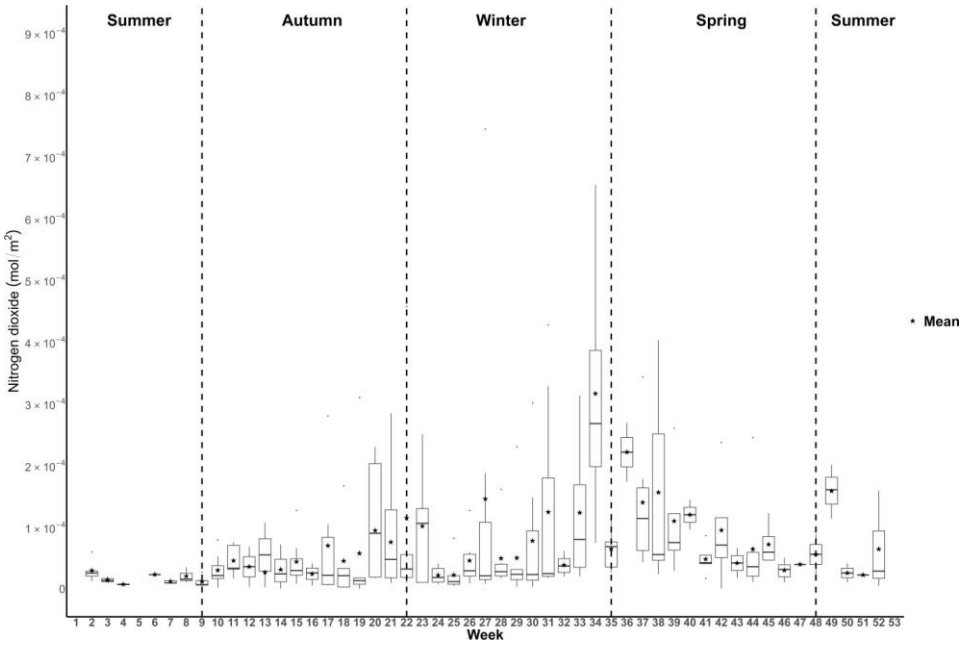

Figure A4. TROPOMI-derived tropospheric nitrogen dioxide concentrations over Wakkerstroom, Mpumalanga, averaged weekly for 2021. The means are represented by a star. The vertical line indicates the start of a new season. The vertical dashed lines indicate the start of the four seasons: autumn, winter, spring and summer.

References

1. Judd, L.M.; Al-Saadi, J.A.; Szykman, J.J.; Valin, L.C.; Janz, S.J.; Kowalewski, M.G.; Eskes, H.J.; Veefkind, J.P.; Cede, A.; Mueller, M.; et al. Evaluating Sentinel-5P TROPOMI tropospheric NO_2 column densities with airborne and Pandora spectrometers near New York City and Long Island Sound. *Atmos. Meas. Tech.* **2020**, *13*, 6113–6140. [CrossRef] [PubMed]
2. Benzerrouk, Z.; Abid, M.; Sekrafi, H. Pollution haven or halo effect? A comparative analysis of developing and developed countries. *Energy Rep.* **2021**, *7*, 4862–4871. [CrossRef]
3. Tiseo, I. Nitrogen Oxide Emissions in the European Union 1990–2021, by Sector [WWW Document]. 2023. Available online: https://www.statista.com/markets/408/energy-environment/ (accessed on 13 April 2024).
4. Lourens, A.S.; Butler, T.M.; Beukes, J.P.; Van Zyl, P.G.; Beirle, S.; Wagner, T.K.; Heue, K.-P.; Pienaar, J.J.; Fourie, G.D.; Lawrence, M.G. Re-evaluating the NO_2 hotspot over the South African Highveld. *S. Afr. J. Sci.* **2012**, *108*, 6. [CrossRef]
5. Vallero, D. Air Pollutant Hazards. In *Fundamentals of Air Pollution*, 5th ed.; Vallero, D., Ed.; Academic Press: Boston, MA, USA, 2014; Chapter 7; pp. 197–214. [CrossRef]
6. Shikwambana, L.; Sivakumar, V. Investigation of various aerosols over different locations in South Africa using satellite, model simulations and LIDAR. *Meteorol. Appl.* **2019**, *26*, 275–287. [CrossRef]
7. Shikwambana, L.; Mhangara, P.; Mbatha, N. Trend analysis and first time observations of sulphur dioxide and nitrogen dioxide in South Africa using TROPOMI/Sentinel-5 P data. *Int. J. Appl. Earth Obs. Geoinf.* **2020**, *91*, 102130. [CrossRef]
8. Goldberg, D.L.; Lu, Z.; Streets, D.G.; De Foy, B.; Griffin, D.; Mclinden, C.A.; Lamsal, L.N.; Krotkov, N.A.; Eskes, H. Enhanced Capabilities of TROPOMI NO_2: Estimating NO_X from North American Cities and Power Plants. *Environ. Sci. Technol.* **2019**, *53*, 12594–12601. [CrossRef]
9. Saxena, P.; Sonwani, S. *Criteria Air Pollutants and Their Impact on Environmental Health*;

Springer Nature: Singapore, 2019. [CrossRef]
10. Ashmore, M. Air Pollution. In *Encyclopedia of Biodiversity*, 2nd ed.; Levin, S.A., Ed.; Academic Press: Amsterdam, The Netherlands, 2013; pp. 136–147. [CrossRef]
11. Fino, A. Air Quality Legislation. In *Encyclopedia of Environmental Health*, 2nd ed.; Nriagu, J., Ed.; Elsevier: Oxford, UK, 2019; pp. 61–70. [CrossRef]
12. Gauss, M.; Ellingsen, K.; Isaksen, I.S.A.; Dentener, F.J.; Stevenson, D.S.; Amann, M.; Cofala, J. Changes in nitrogen dioxide and ozone over Southeast and East Asia between year 2000 and 2030 with fixed meteorology. *Terr. Atmos. Ocean. Sci.* **2007**, *18*, 475–492. [CrossRef]
13. Adesina, J.A.; Piketh, S.J.; Qhekwana, M.; Burger, R.; Language, B.; Mkhatshwa, G. Contrasting indoor and ambient particulate matter concentrations and thermal comfort in coal and non-coal burning households at South Africa Highveld. *Sci. Total Environ.* **2020**, *699*, 134403. [CrossRef] [PubMed]
14. Belelie, M.D.; Burger, R.P.; Mkhatshwa, G.; Piketh, S.J. Assessing the impact of Eskom power plant emissions on ambient air quality over KwaZamokuhle. *Clean Air J.* **2019**, *29*, 29–37. [CrossRef]
15. Beirle, S.; Platt, U.; Wenig, M.; Wagner, T. Highly resolved global distribution of tropospheric NO_2 using GOME narrow swath mode data. *Atmos. Chem. Phys.* **2004**, *4*, 1913–1924. [CrossRef]
16. Matandirotya, N.R.; Burger, R. An assessment of NO_2 atmospheric air pollution over three cities in South Africa during 2020 COVID-19 pandemic. *Air Qual. Atmos. Health* **2022**, *16*, 263–276. [CrossRef] [PubMed]
17. Laakso, L.; Vakkari, V.; Virkkula, A.; Laakso, H.; Backman, J.; Kulmala, M.; Beukes, J.P.; van Zyl, P.G.; Tiitta, P.; Josipovic, M.; et al. South African EUCAARI measurements: Seasonal variation of trace gases and aerosol optical properties. *Atmos. Chem. Phys.* **2012**, *12*, 1847–1864. [CrossRef]
18. Department of Forestry, Fisheries and the Environment. *National GHG Inventory Report South Africa: 2000–2020*; Department of Forestry, Fisheries and the Environment: Pretoria, South Africa, 2022.
19. Swap, R.J.; Annegarn, H.J.; Suttles, J.T.; King, M.D.; Platnick, S.; Privette, J.L.; Scholes, R.J. Africa burning: A thematic analysis of the Southern African Regional Science Initiative (SAFARI 2000). *J. Geophys. Res. Atmos.* **2003**, *108*, 8465. [CrossRef]
20. Medupi Power Station—Final Scoping Report [WWW Document]. 2005. Available online: https://www.eskom.co.za/ OurCompany/SustainableDevelopment/EnvironmentalImpactAssessments/Pages/Medupi_Final_Scoping_Report.aspx (accessed on 12 April 2024).
21. Sillman, S. Tropospheric Ozone and Photochemical Smog. In *Treatise on Geochemistry*; Holland, H.D., Turekian, K.K., Eds.; Pergamon: Oxford, UK, 2003; pp. 407–431. [CrossRef]
22. Speight, J.G. Chemicals and the Environment. In *Environmental Organic Chemistry for Engineers*; Speight, J.G., Ed.; Butterworth- Heinemann: Oxford, UK, 2017; Chapter 1; pp. 1–41. [CrossRef]
23. Freiman, M.T.; Piketh, S.J. Air Transport into and out of the Industrial Highveld Region of South Africa. *J. Appl. Meteorol. Climatol.* **2003**, *42*, 994–1002. [CrossRef]
24. Rahal, F. Low-cost sensors, an interesting alternative for air quality monitoring in Africa. *Clean Air J.* **2020**, *30*, 1–2. [CrossRef]
25. Mbandi, A. Air Pollution in Africa in the time of COVID-19: The air we breathe indoors and outdoors. *Clean Air J.* **2020**, *30*, 1–3. [CrossRef]
26. Vandaele, A.C.; Hermans, C.; Simon, P.C.; Carleer, M.; Colin, R.; Fally, S.; Mérienne, M.F.; Jenouvrier, A.; Coquart, B. Measurements of the NO_2 absorption cross-section from 42,000 cm^{-1} to 10,000 cm^{-1} (238–1000 nm) at 220 K and 294 K. *J. Quant. Spectrosc. Radiat. Transf.* **1998**, *59*, 171–184. [CrossRef]
27. Finch, D.P.; Palmer, P.I.; Zhang, T. Automated detection of atmospheric NO_2 plumes from satellite data: A tool to help infer anthropogenic combustion emissions. *Atmos. Meas. Tech.* **2022**, *15*, 721–733. [CrossRef]
28. Douros, J.; Eskes, H.; van Geffen, J.; Boersma, K.F.; Compernolle, S.; Pinardi, G.; Blechschmidt, A.-M.; Peuch, V.-H.; Colette, A.; Veefkind, P. Comparing Sentinel-5P TROPOMI NO_2 column observations with the CAMS regional air quality

ensemble. *Geosci. Model Dev.* **2023**, *16*, 509–534. [CrossRef]
29. Verhoelst, T.; Compernolle, S.; Pinardi, G.; Lambert, J.-C.; Eskes, H.J.; Eichmann, K.-U.; Fjæraa, A.M.; Granville, J.; Niemeijer, S.; Cede, A.; et al. Ground-based validation of the Copernicus Sentinel-5P TROPOMI NO_2 measurements with the NDACC ZSL-DOAS, MAX-DOAS and Pandonia global networks. *Atmos. Meas. Tech.* **2021**, *14*, 481–510. [CrossRef]
30. Xue, R.; Wang, S.; Zhang, S.; He, S.; Liu, J.; Tanvir, A.; Zhou, B. Estimating city NO_X emissions from TROPOMI high spatial resolution observations—A case study on Yangtze River Delta, China. *Urban Clim.* **2022**, *43*, 101150. [CrossRef]
31. van Geffen, J.; Eskes, H.; Compernolle, S.; Pinardi, G.; Verhoelst, T.; Lambert, J.-C.; Sneep, M.; ter Linden, M.; Ludewig, A.; Boersma, K.F.; et al. Sentinel-5P TROPOMI NO_2 retrieval: Impact of version v2.2 improvements and comparisons with OMI and ground-based data. *Atmos. Meas. Tech.* **2022**, *15*, 2037–2060. [CrossRef]
32. Lorente, A.; Boersma, K.F.; Yu, H.; Dörner, S.; Hilboll, A.; Richter, A.; Liu, M.; Lamsal, L.N.; Barkley, M.; De Smedt, I.; et al. Structural uncertainty in air mass factor calculation for NO_2 and HCHO satellite retrievals. *Atmos. Meas. Tech.* **2017**, *10*, 759–782. [CrossRef]
33. Cooper, M.; Martin, R.; Henze, D.; Jones, D. Effects of a priori profile shape assumptions on comparisons between satellite NO_2 columns and model simulations. *Atmos. Chem. Phys.* **2020**, *20*, 7231–7241. [CrossRef]
34. Ialongo, I.; Virta, H.; Eskes, H.; Hovila, J.; Douros, J. Comparison of TROPOMI/Sentinel-5 Precursor NO_2 observations with ground-based measurements in Helsinki. *Atmos. Meas. Tech.* **2020**, *13*, 205–218. [CrossRef]
35. Hönninger, G.; von Friedeburg, C.; Platt, U. Multi axis differential optical absorption spectroscopy (MAX-DOAS). *Atmos. Chem. Phys.* **2004**, *4*, 231–254. [CrossRef]
36. Choi, S.; Lamsal, L.N.; Follette-Cook, M.; Joiner, J.; Krotkov, N.A.; Swartz, W.H.; Pickering, K.E.; Loughner, C.P.; Appel, W.; Pfister, G.; et al. Assessment of NO_2 observations during DISCOVER-AQ and KORUS-AQ field campaigns. *Atmos. Meas. Tech.* **2020**, *13*, 2523–2546. [CrossRef]
37. Prunet, P.; Lezeaux, O.; Camy-Peyret, C.; Thevenon, H. Analysis of the NO_2 tropospheric product from S5P TROPOMI for monitoring pollution at city scale. *City Environ. Interact.* **2020**, *8*, 100051. [CrossRef]
38. Cede, A.; Tiefengraber, M.; Gebetsberger, M.; Spinei Lind, E. Pandonia Global Network Data Products ReadmeDocument, V1.8-3, Tech. rep. 2021. Available online: https://www.pandonia-global-network.org/wp-content/uploads/2021/01/PGN_ DataProducts_Readme_v1-8-3.pdf. (accessed on 10 October 2022).
39. Dimitropoulou, E.; Hendrick, F.; Pinardi, G.; Friedrich, M.M.; Merlaud, A.; Tack, F.; De Longueville, H.; Fayt, C.; Hermans, C.; Laffineur, Q.; et al. Validation of TROPOMI tropospheric NO_2 columns using dual-scan multi-axis differential optical absorption spectroscopy (MAX-DOAS) measurements in Uccle, Brussels. *Atmos. Meas. Tech.* **2020**, *13*, 5165–5191. [CrossRef]
40. Lynch, J.; Cain, M.; Frame, D.; Pierrehumbert, R. Agriculture's Contribution to Climate Change and Role in Mitigation Is Distinct from Predominantly Fossil CO_2-Emitting Sectors. *Front. Sustain. Food Syst.* **2021**, *4*, 518039. [CrossRef]
41. Herman, J.; Cede, A.; Spinei, E.; Mount, G.; Tzortziou, M.; Abuhassan, N. NO_2 column amounts from ground-based Pandora and MFDOAS spectrometers using the direct-sun DOAS technique: Intercomparisons and application to OMI validation. *J. Geophys. Res. Atmos.* **2009**, *114*. [CrossRef]
42. Abad, G.G.; Souri, A.H.; Bak, J.; Chance, K.; Flynn, L.E.; Krotkov, N.A.; Lamsal, L.; Li, C.; Liu, X.; Miller, C.C.; et al. Five decades observing Earth's atmospheric trace gases using ultraviolet and visible backscatter solar radiation from space. *J. Quant. Spectrosc. Radiat. Transf.* **2019**, *238*, 106478. [CrossRef]
43. Cede, A.; Tiefengraber, M.; Gebetsberger, M.; Spinei Lind, E. Pandonia Global Network Data Products ReadmeDocument, V1.8-5, Tech. rep. 2022. Available online: https://www.pandonia-global-network.org/wp-content/uploads/2022/12/PGN_ DataProducts_Readme_v1-8-6.pdf (accessed on 25 June 2023).

44. Pinardi, G.; Hendrick, F.; Clemer, K.; Lambert, J.-C.; Bai, J.; Roozendael, M.V. On the use of the maxdoas technique for the validation of tropospheric NO_2 column measurements from satellite. In Proceedings of the 2008 EUMETSAT Meteorological Satellite Conference, Darmstadt, Germany, 8–12 September 2008.
45. Cede, A.; Tiefengraber, M.; Gebetsberger, M.; Spinei Lind, E. Pandonia Global Network Data Products ReadmeDocument, V1.8-5, Tech. rep. 2021. Available online: https://www.pandonia-global-network.org/wp-content/uploads/2022/01/PGN_ DataProducts_Readme_v1-8-5.pdf (accessed on 18 May 2023).
46. Azad, S.; Ghandehari, M. Emissions of nitrogen dioxide in the northeast U.S. during the 2020 COVID-19 lockdown. *J. Environ. Manag.* **2022**, *312*, 114902. [CrossRef]
47. Veefkind, J.P.; Aben, I.; McMullan, K.; Förster, H.; de Vries, J.; Otter, G.; Claas, J.; Eskes, H.J.; de Haan, J.F.; Kleipool, Q.; et al. TROPOMI on the ESA Sentinel-5 Precursor: A GMES mission for global observations of the atmospheric composition for climate, air quality and ozone layer applications. *Remote Sens. Environ.* **2012**, *120*, 70–83. [CrossRef]
48. Eskes, H.J.; van Geffen, J.H.G.M.; Boersma, K.F.; Eichmann, K.-U.; Pedergnana, M.; Sneep, M.; Veefkind, J.P.; Loyola, D. *S5P/TROPOMI Level-2 Product User Manual Nitrogen Dioxide*; ESA: Paris, France, 2020.
49. Eskes, H.J.; Eichmann, K.-U. S5P MPC Product Readme Nitrogen Dioxide, Report S5P-MPC-KNMI-PRF-NO_2, V2.0, ESA. 2021. Available online: https://sentinels.copernicus.eu/documents/247904/3541451/Sentinel-5P-NitrogenDioxide-Level-2-Product- Readme-File (accessed on 23 September 2024).
50. Zhao, X.; Griffin, D.; Fioletov, V.; McLinden, C.; Cede, A.; Tiefengraber, M.; Müller, M.; Bognar, K.; Strong, K.; Boersma, F.; et al. Assessment of the quality of TROPOMI high-spatial-resolution NO_2 data products in the Greater Toronto Area. *Atmos. Meas. Tech.* **2020**, *13*, 2131–2159. [CrossRef]
51. Williams, J.E.; Boersma, K.F.; Le Sager, P.; Verstraeten, W.W. The high-resolution version of TM5-MP for optimized satellite retrievals: Description and validation. *Geosci. Model Dev.* **2017**, *10*, 721–750. [CrossRef]
52. Rolph, G.; Stein, A.; Stunder, B. Real-time Environmental Applications and Display sYstem: READY. *Environ. Model. Softw.* **2017**, *95*, 210–228. [CrossRef]
53. Cui, L.; Song, X.; Zhong, G. Comparative Analysis of Three Methods for HYSPLIT Atmospheric Trajectories Clustering. *Atmosphere* **2021**, *12*, 698. [CrossRef]
54. Stein, A.F.; Draxler, R.R.; Rolph, G.D.; Stunder, B.J.B.; Cohen, M.D.; Ngan, F. Noaa's Hysplit Atmospheric Transport and Dispersion Modeling System. *Bull. Am. Meteorol. Soc.* **2015**, *96*, 2059–2078. [CrossRef]
55. Tyson, P.D. Atmospheric transport of aerosols and trace gases over southern Africa. *Prog. Phys. Geogr. Earth Environ.* **1997**, *21*, 79–101. [CrossRef]
56. Lourens, A.S.; Beukes, J.P.; Van Zyl, P.G.; Fourie, G.D.; Burger, J.W.; Pienaar, J.J.; Read, C.E.; Jordaan, J.H. Spatial and temporal assessment of gaseous pollutants in the highveld of South Africa. *S. Afr. J. Sci.* **2011**, *107*, 8. [CrossRef]
57. De Souza, A.; Aristone, F.; Abreu, M.C.; De Oliveira-Júnior, J.F.; Fernandes, W.A.; Pobocikova, I. Spatio-temporal variations of tropospheric nitrogen dioxide in South Mato Grosso based on remote sensing by satellite. *Meteorol. Atmos. Phys.* **2022**, *134*, 19. [CrossRef]
58. Tyson, P.D.; Garstang, M.; Swap, R. Large-Scale Recirculation of Air over Southern Africa. *J. Appl. Meteorol.* **1996**, *35*, 2218–2236. [CrossRef]
59. Thoithi, W.; Blamey, R.C.; Reason, C.J.C. Dry Spells, Wet Days, and Their Trends across Southern Africa during the Summer Rainy Season. *Geophys. Res. Lett.* **2021**, *48*, e2020GL091041. [CrossRef]
60. Mpungose, N.; Thoithi, W.; Blamey, R.C.; Reason, C.J.C. Extreme rainfall events in southeastern Africa during the summer. *Theorerical Appl. Climatol.* **2022**, *150*, 185–201. [CrossRef]

61. Kai, R.F.; Scholes, M.; Piketh, S.J.; Scholes, R.J. Analysis of the first surface nitrogen dioxide concentration observations over the South African Highveld derived from the Pandora-2s instrument. *Clean Air J.* **2022**, *32*, 1–11. [CrossRef]
62. Venter, A.; Lourens, A.S.M. Ambient air quality data reported at Sasol Secunda monitoring stations during COVID-19 lockdown— Mpumalanga, South Africa. *Clean Air J.* **2021**, *31*, 1–7. [CrossRef]
63. Tyson, P.D.; Garstang, M.; Swap, R.; Kâllberg, P.; Edwards, M. An Air Transport Climatology for Subtropical Southern Africa. *Int. J. Climatol.* **1996**, *16*, 265–291. [CrossRef]
64. Ibebuchi, C.C. Circulation pattern controls of wet days and dry days in Free State, South Africa. *Meteorol. Atmos. Phys.* **2021**, *133*, 1469–1480. [CrossRef]
65. Tyson, P.D.; Preston-Whyte, R.A. *The Weather and Climate of Southern Africa*; Oxford University Press: Oxford, UK, 2000.
66. Zhao, X.; Griffin, D.; Fioletov, V.; McLinden, C.; Davies, J.; Ogyu, A.; Lee, S.C.; Lupu, A.; Moran, M.D.; Cede, A.; et al. Retrieval of total column and surface NO_2 from Pandora zenith-sky measurements. *Atmos. Chem. Phys.* **2019**, *19*, 10619–10642. [CrossRef]
67. de Lange, A.; Naidoo, M.; Garland, R.M.; Dyson, L.L. The sensitivity of simulated surface-level pollution concentrations to WRF-ARW-model PBL parameterisation schemes over the Highveld of South Africa. *Atmos. Res.* **2021**, *254*, 105517. [CrossRef]
68. Rorich, R.P.; Galpin, J.S. Air quality in the Mpumalanga Highveld region, South Africa. *S. Afr. J. Sci.* **1998**, *94*, 109–114.
69. Cosijn, C. Stable discontinuities in the atmosphere over South Africa. *S. Afr. J. Sci.* **1996**, *92*, 381–386.
70. Hobbs, P.V. Clean air slots amid dense atmospheric pollution in southern Africa. *J. Geophys. Res. Atmos.* **2003**, *108*, 8490. [CrossRef]
71. Scholes, R.J.; Kendall, J.; Justice, C.O. The quantity of biomass burned in southern Africa. *J. Geophys. Res. Atmos.* **1996**, *101*, 23667–23676. [CrossRef]
72. Nkosi, C.; Piketh, S.; Burger, R.; Annegarn, H. Variability of domestic burning habits in the South African Highveld: A case study in the KwaDela Township (April 2017). In Proceedings of the 2017 International Conference on the Domestic Use of Energy (DUE), Cape Town, South Africa, 4–5 April 2017; pp. 23–29. [CrossRef]
73. Garstang, M.; Tyson, P.D.; Swap, R.; Edwards, M.; Kållberg, P.; Lindesay, J.A. Horizontal and vertical transport of air over southern Africa. *J. Geophys. Res. Atmos.* **1996**, *101*, 23721–23736. [CrossRef]
74. Tyson, P.D.; D'Abreton, P.C. Transport and recirculation of aerosols off Southern Africa—Macroscale plume structure. *Atmos. Environ.* **1998**, *32*, 1511–1524. [CrossRef]
75. Andreae, M.O.; Merlet, P. Emission of trace gases and aerosols from biomass burning. *Glob. Biogeochem. Cycles* **2001**, *15*, 955–966. [CrossRef]

5.2 Postscript

The findings of this paper have shown the importance of incorporating ground-based measurements to validate and contextualise satellite-derived NO_2 data. The Pandora-TROPOMI comparison reveals seasonal patterns in NO_2 concentrations that satellites alone may not fully capture, especially during the transition of seasons marked by biomass burning or seasonal shifts in meteorology. Additionally, this paper points to the benefits of using MAX-DOAS Pandora-2s data at weekly resolution to elucidate seasonal patterns, whereas the monthly averages were more closely aligned with TROPOMI data. In the context of this thesis, this paper offers key insights into the limitations and complementary nature of satellite and ground-based measurements for atmospheric NO_2 monitoring. These findings are crucial for understanding the spatial and temporal variability of NO_2 in the Highveld and for exploring the potential of satellite data to provide reliable proxies for near-surface and tropospheric NO_2 concentrations.

Further refinement of data integration techniques, e.g. cloud-slicing approaches of Pandora-2s and TROPOMI data, will also enhance the interpretation and applicability of satellite-derived NO_2 measurements in regional studies. This paper's integration of high-temporal-resolution MAX-DOAS Pandora-2s data with TROPOMI observations allows for a more comprehensive analysis of NO_2 patterns across the region, contributing to the thesis's broader objectives of understanding the distribution of NO_2 in the Highveld atmosphere.

Chapter 6

This Chapter provides a detailed discussion of the major findings of this study in the context of the objectives outlined in Chapter 1 and the published literature. It also highlights the contribution of this study to science.

6 General Discussion and Conclusion

The South African Highveld, an elevated region ~ 1800 m a.s.l, is a significant source of industrial emissions, particularly from coal-fired power stations, petrochemical plants, and smelting industries. This area has been identified as a global hotspot for pollutants such as NO_x and SO_2 through satellite data. Over the past three decades, extensive research has focused on understanding the atmospheric conditions that lead to pollutant accumulation and transport in this region, which has prevailing atmospheric conditions characterised by winter and summer synoptic-scale circulation patterns, including easterly lows and anticyclonic high-pressure systems. The pollutants in the Highveld are transported in anticyclonic recirculation patterns and east coast plumes, with substantial quantities moving off the eastern seaboard of South and Southern Africa. In addition, the Highveld atmosphere's vertical structure is highly stratified, with multiple inversion layers trapping pollution below the layers and limiting pollutant vertical mixing.

Advancements in satellite remote sensing techniques over the past two decades have improved the visualisation of pollution plumes across the Highveld. However, despite enhanced spatial resolution, establishing accurate proxies for air pollution indices over South Africa remains challenging due to weak correlations between satellite- and ground-based instrument-retrieved data. Remote sensing data retrieval algorithms can be affected by many factors, including the elevation of a region, particularly in areas such as the Highveld. Therefore, understanding the relationship between the data retrieved from satellite and ground-based instruments while considering the complexities introduced by factors which influence the retrieval methods is crucial for quantifying pollution sources and the effects of the emissions on the environment and the population.

This study focused on understanding major sources of NO_2 concentrations in the Highveld by analysing near-surface and tropospheric vertical column NO_2 concentrations in Wakkerstroom, a town in the Mpumalanga Highveld. Located downwind of major NO_x emission sources and

near agricultural emissions, Wakkerstroom provides insights into the interaction between the various NO_2 sources in the region. This study used ground-based and satellite instruments to measure NO_2 concentrations with high temporal and spatial resolution. This dual approach addresses the lack of comprehensive NO_2 data in the region and improves the understanding of atmospheric dynamics and pollution patterns specific to Wakkerstroom. The findings from this study can be applied more broadly to the Mpumalanga Highveld, contributing to a better understanding of NO_2 emissions, their sources, concentrations, and transport in this region.

6.1 Near-surface NO_2 Concentrations in Wakkerstroom

Near-surface NO_2 concentrations were measured using ground-based instruments: a Pandora-2s instrument in Wakkerstroom and three Eskom-owned conventional air quality monitors located downwind of the Kendal and Majuba power stations and at Elandsfontien. The Pandora-derived data spanned from 1 January to 31 December 2020, while data from the conventional air quality monitoring sensors covered 1 July 2015 to 31 May 2020. This study marks the first extended use of a ground-based remote sensing instrument to quantify near-surface NO_2 concentrations in the Highveld.

The Pandora instrument in Wakkerstroom recorded measurements approximately every 13 minutes, while the data from the Eskom-owned air quality monitors measured concentrations hourly. These concentrations were averaged to produce weekly concentrations. The Pandora-derived concentrations ranged between 0.2 ppb ± 0.04 ppb and 7.5 ppb ± 5.7 ppb, with the highest concentrations observed in week 37 (September). The Eskom-owned air quality monitors measured weekly averaged NO_2 concentrations ranging from 1.2 ppb to 31.5 ppb. The study found that the monitors near the power stations (Majuba and Kendal) recorded peak weekly average concentrations in winter (27.6 ppb) and summer (31.5 ppb), respectively. In contrast, the Pandora instrument and the Elandsfontein monitor, located further from the power stations, showed peak concentrations in September and July. These findings, particularly the elevated concentrations during spring and summer measured by the Pandora instrument in 2020 and the Kendal monitor (average of 6 years), contradict previous literature that reported peak surface NO_2 and NO_x concentrations in winter (Collett, Piketh and Ross, 2010; Lourens *et al.*, 2011; Laakso *et al.*, 2012).

The spatial and temporal variability in NO_2 concentrations across the four Highveld sites challenges the expected winter peak due to slow winds, reduced radiation, and temperature inversions (Whiteman, Bian and Zhong, 1999). The observed seasonal disparities from the presented results are due to the seasonal contributions of the local sources, which contribute significantly to the measured surface NO_2 concentrations (Collett, Piketh and Ross, 2010; Laakso *et al.*, 2012). In winter, domestic burning for cooking and space heating is elevated and, therefore, increases the emissions of NO_2, contributing significantly to observed seasonal variations in surface NO_2 concentrations (Collett, Piketh and Ross, 2010; Laakso *et al.*, 2012). The design of power station tall stacks also plays a crucial role in pollutant dispersion and, therefore, the measured concentrations in an area. Emissions are often released above the surface inversion layer (typically around 300 metres). During winter, when the surface inversion layers are more pronounced, emissions are prevented from reaching the surface, particularly at night. Instead, the emissions are transported away from the source region by the low-level jet winds above the inversion layer. Biomass burning reaches a maximum during spring in southern Africa and significantly contributes to air pollution, particularly oxides of nitrogen and ozone. This aligns with the highest nitrogen dioxide concentrations observed in Wakkerstroom during spring. Figure 6.1 shows the active fires recorded in South Africa and surrounding regions in 2020, which confirms the high amount of biomass burning in southern Africa.

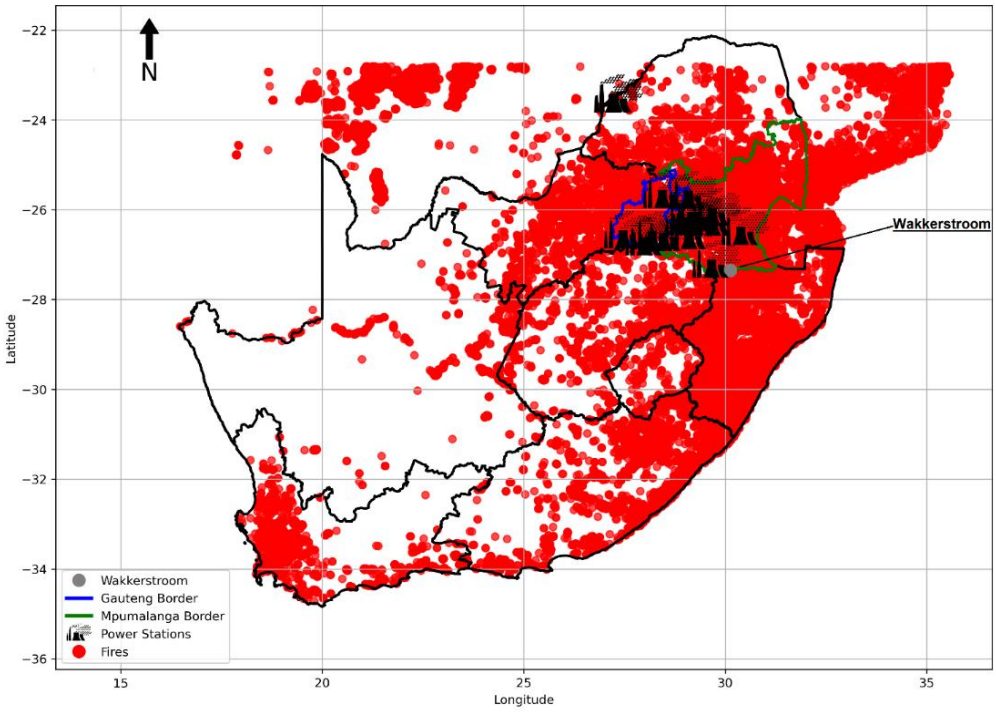

Figure 6. 1: Burnt fires in South Africa and surrounding regions during 2020.

The observed elevated spring surface NO_2 concentrations in Wakkerstroom also highlight the significant effect of atmospheric stability and air mass transport within and across regions, as shown by the main transport pathways to Wakkerstroom during 2020 in Figure 6.2.

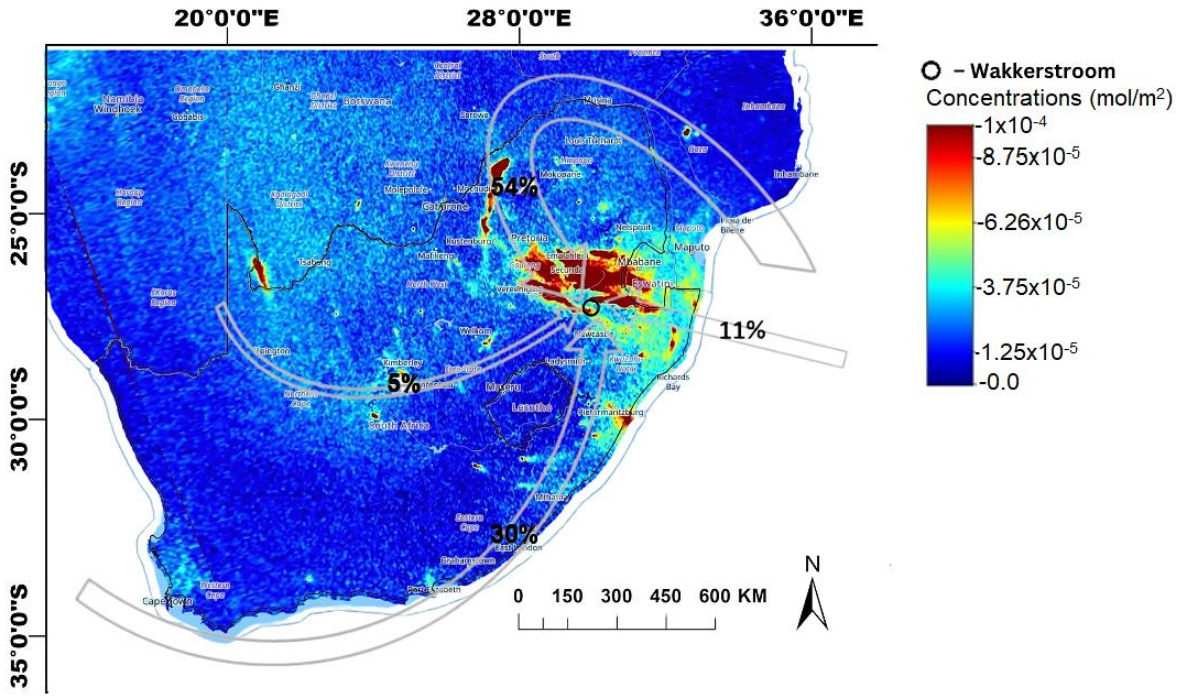

Figure 6. 2: A schematic showing the tropospheric vertical column NO_2 concentrations over the Highveld and the main transport pathways to Wakkerstroom in 2020.

Wakkerstroom's location makes it ideal for revealing various NO_2 sources in the Mpumalanga Highveld. Spring, characterised by higher wind speeds and more air mass transport (Adesina *et al.*, 2022), facilitates the contribution of emissions from surrounding areas. The Pandora-derived near-surface NO_2 concentrations in Wakkerstroom exhibit high temporal variability, similar to other Highveld areas. Peak concentrations in Wakkerstroom are approximately 4.5 times lower than those at Kendal, 3.7 times lower than those at Majuba, but only 1.7 times lower than those at Elandsfontein.

These findings emphasise the various contributors to NO_2 pollution in Wakkerstroom and potentially the entire Highveld region, highlighting the spatial variability of the observed NO_2 concentrations. To better understand the local and regional contributions of the many sources of NO_2 emissions in this area, long-term data analyses and source apportionment studies are essential.

6.2 Tropospheric Vertical Column NO_2 Concentrations in Wakkerstroom

Tropospheric vertical column (TVC) NO_2 concentrations were measured in Wakkerstroom using the ground-based Pandora-2s instrument and the TROPOMI satellite from January 2020 to December 2021. The Pandora instrument, operating in MAX-DOAS mode, provided the first TVC ground-based remote-sensed data for the Highveld region, with measurements taken approximately every 13 minutes. TROPOMI data were collected once daily. Both datasets were averaged weekly and annually over a 0.1° x 0.05° area around Wakkerstroom.

Annual mean Pandora-derived TVC-NO_2 concentrations were 5.1 x 10^{-5} mol/m^2 ± 9.0 x 10^{-5} mol/m^2 in 2020 and 5.03 × 10^{-5} mol/m^2 ± 9.40 × 10^{-5} mol/m^2 in 2021. TROPOMI-derived measurements exceeded Pandora-derived concentrations by ~ 21% in 2020 and ~ 40% in 2021. The expected ~1:3 ratio of Pandora to TROPOMI-derived concentrations was not observed. Weekly averaged concentrations showed different peak patterns: Pandora data peaked in summer 2020 and late winter/early spring 2021, while TROPOMI data peaked during winter 2020 and late winter/early spring 2021. Theil-Sen regression analyses of coincident data (±5 minutes and ±1 hour) revealed that TROPOMI overestimated Pandora-derived TVC-NO_2 concentrations by over 50%. This large discrepancy in the coincidence data was unexpected because of the improved spatial alignment of the Pandora-derived MAX-DOAS data with the satellite-derived data. It is worth noting that Pandora measurements in MAX-DOAS mode are primarily sensitive to lower tropospheric NO_2, while TROPOMI measures the entire tropospheric column (Hönninger, von Friedeburg and Platt, 2004). These findings verify Verhoelst *et al.* (2021) regarding TROPOMI's limitations in capturing boundary-layer NO_2 concentrations, emphasising the need for localised ground-based data. In addition, the observed overestimation by TROPOMI, although less pronounced, aligns with other validation studies (Verhoelst *et al.*, 2021).

In 2021, both instruments recorded peak concentrations in the same season. The seasonal patterns observed in this study partially contradict previous reports of consistently elevated NO_2 concentrations in winter over the Highveld (Lourens *et al.*, 2012; Matandirotya and Burger, 2021). However, other studies have shown that the relationship between seasons and TVC-NO_2 concentrations is not uniform across all locations (Matandirotya and Burger, 2021). The partial alignment of Pandora and TROPOMI-derived weekly averaged TVC concentrations in capturing seasonal patterns suggests that MAX-DOAS measurements could provide better spatial resolution than DS-DOAS measurements.

The integration of satellite and ground-based measurements offers a comprehensive approach to monitoring NO_2 patterns across various spatial scales. The enhanced spatial resolution of MAX-DOAS measurements provides insights into the relationship between emission sources, atmospheric chemistry, and local meteorology.

These results contribute to ongoing efforts to validate and enhance satellite measurements of atmospheric pollutants, particularly in data-scarce regions and heavily polluted areas such as South Africa's NO_2 emissions hotspot (Lourens *et al.*, 2012). The findings highlight the complexities involved in comparing ground-based and satellite measurements and emphasise the importance of integrating multiple measurement techniques for a more accurate understanding of air quality dynamics.

6.3 Major air mass transport pathways to Wakkerstroom

The seasonal patterns of near-surface and TVC-NO_2 concentrations measured in Wakkerstroom using the ground-based Pandora instrument contradict the patterns published in the literature for the Highveld region. While Wakkerstroom is downwind of major NO_2 sources in the Highveld, the Pandora-derived measurements do not show the same elevated winter NO_2 concentrations observed in other Highveld areas, such as Elandsfontein and the site downwind of the Majuba power station.

The atmosphere over the heavily industrialised Highveld is characterised by significant emissions of nitrogen oxides, sulfur dioxide, and aerosols (Freiman and Piketh, 2003; Collett, Piketh and Ross, 2010). These emissions are dispersed over the Highveld and exported to remote areas of the subcontinent through direct and recirculated air mass transport. Synoptic-scale and local meteorological processes influence pollutant transport, with anticyclonic circulation patterns trapping aerosols and trace gases below 700 or 500 hPa (Freiman and Piketh, 2003). Seasonal air mass transport patterns over the Highveld show distinct characteristics. Winter is dominated by stable atmospheric conditions and prevalent westerly and north-westerly airflow, directly transporting emissions from power station sources to nearby monitoring sites (Collett, Piketh and Ross, 2010). Summer experiences more dynamic atmospheric conditions with dispersive transport patterns.

To investigate the discrepancies between seasonal patterns reported in this study and the literature, air mass transport over Wakkerstroom was analysed using the HYSPLIT model. Daily

10-day back trajectories to Wakkerstroom at the near-surface level (~ 800 hPa) during 2020 revealed that 54% of air mass transport originated from the east of Wakkerstroom, over eSwatini and southern Mozambique, recirculating over the Highveld region (Figure 6.2). Only 11% of transport showed north-westerly airflow, which is reported as the most prevalent air mass transport over the Highveld. Five-day daily back trajectories at ~ 700 hPa and 500 hPa for weeks with the highest tropospheric NO_2 concentrations during 2020 and 2021 showed similar prevalent pathways from the east of Wakkerstroom, recirculating over the Highveld, with one exception.

These findings suggest that other sources influence the elevated NO_2 concentrations measured over Wakkerstroom in addition to power station emissions despite its downwind location from major emission sources (power stations). The Highveld's elevation (from 1500 to 2000 m a.s.l) may be the main driver of these contradictory findings, as topography-driven outflow plays a role in pollutant transport and dispersion. The spatial variability of NO_2 concentrations over the Highveld is further shown by peak winter surface concentrations measured at Majuba and Elandsfontein monitoring sites, indicating the major contribution of seasonal emissions from local sources. Significant influence from synoptic and local meteorological conditions also plays a role.

Figure 6.2 illustrates the four major transport pathways contributing to observed NO_2 concentrations in Wakkerstroom at the near-surface level. The transported air masses from the east of Wakkerstroom passed over areas showing evidence of biomass burning in September. This highlights the significant contribution of other sources, such as biomass burning from eSwatini, southern Mozambique, and the Highveld, to accumulated surface NO_2 concentrations in Wakkerstroom.

Figure 6.1 depicts the numerous fires that burned in South Africa and surrounding regions during 2020, providing compelling evidence that regional sources substantially influence NO_2 concentrations in Wakkerstroom due to inter-regional air mass transport (West *et al.*, 2009). The impact of biomass burning activities in neighbouring countries, particularly during the dry season, appears to contribute significantly to elevated NO_2 levels.

Previous studies (Rorich and Galpin, 1998; Lourens *et al.*, 2011; Lourens *et al.*, 2012; Matandirotya and Burger, 2021) have shown that coal-fired power stations and vehicular emissions contribute significantly to elevated surface NO_2 concentrations in the Highveld. However, this

study reveals that transboundary emissions from eSwatini and southern Mozambique also play a significant role in the measured concentrations over the Wakkerstroom atmosphere.

There is a notable difference in the transportation pathways of the highest concentrations of nitrogen dioxide at Wakkerstroom compared to the pathways in the Highveld region. While the Highveld generally experiences more stagnant, pollution-trapping conditions in winter and dispersive patterns in summer, Wakkerstroom's NO_2 concentrations are influenced by the relationship between regional sources and transport patterns, including significant contributions from biomass burning in neighbouring countries.

6.4 Conclusion and Further Research

This study has contributed to the understanding of the Highveld atmosphere by providing insights about the possible sources that contribute to the NO_2 concentrations and transport patterns in the South African Highveld region, particularly in Wakkerstroom. Peak NO_2 concentrations were observed in spring and summer, challenging the winter maximum typically reported by previous studies. The integration of ground-based Pandora-2s and satellite TROPOMI measurements revealed significant spatial and temporal variability in NO_2 concentrations across the Highveld. TROPOMI consistently overestimated NO_2 concentrations compared to Pandora measurements, highlighting the importance of ground-based validation for satellite data. Air mass transport analyses using the HYSPLIT model showed that the majority of air masses reaching Wakkerstroom originated from the east rather than the expected northwest, suggesting significant contributions from sources other than local power stations. The study emphasises the compound effect of industrial emissions, biomass burning, and transboundary pollution in shaping NO_2 concentrations in the region.

The findings from this thesis highlight the need for comprehensive, long-term monitoring and source apportionment studies to better understand and manage air quality in the South African Highveld. Future research would also benefit from further enquiry into vertical profiles of emissions in highly polluted areas and the integration of machine learning when analysing NO_2 concentrations in data-scarce regions.

Chapter 7

References

Abad, G.G., Souri, A.H., Bak, J., Chance, K., Flynn, L.E., Krotkov, N.A., Lamsal, L., Li, C., Liu, X., Miller, C.C., Nowlan, C.R., Suleiman, R., Wang, H., 2019. Five decades observing Earth's atmospheric trace gases using ultraviolet and visible backscatter solar radiation from space. Journal of Quantitative Spectroscopy and Radiative Transfer 238, 106478. https://doi.org/10.1016/j.jqsrt.2019.04.030

Adesina, J.A., Piketh, S.J., Burger, R.P., Mkhatshwa, G., 2022. Assessment of criteria pollutants contributions from coal-fired plants and domestic solid fuel combustion at the South African industrial highveld. Cleaner Engineering and Technology 6, 100358. https://doi.org/10.1016/j.clet.2021.100358

Adesina, J.A., Piketh, S.J., Qhekwana, M., Burger, R., Language, B., Mkhatshwa, G., 2020. Contrasting indoor and ambient particulate matter concentrations and thermal comfort in coal and non-coal burning households at South Africa Highveld. Science of The Total Environment 699, 134403. https://doi.org/10.1016/j.scitotenv.2019.134403

Ambus, P., Skiba, U., Butterbach-Bahl, K., Sutton, M.A., 2011. Reactive nitrogen and greenhouse gas flux interactions in terrestrial ecosystems. Plant Soil 343, 1–3. https://doi.org/10.1007/s11104-011-0777-z

Anenberg, S.C., Mohegh, A., Goldberg, D.L., Kerr, G.H., Brauer, M., Burkart, K., Hystad, P., Larkin, A., Wozniak, S., Lamsal, L., 2022. Long-term trends in urban NO_2 concentrations and associated paediatric asthma incidence: estimates from global datasets. The Lancet Planetary Health 6, e49–e58. https://doi.org/10.1016/S2542-5196(21)00255-2

Anttila, P., Tuovinen, J.-P., Niemi, J.V., 2011. Primary NO_2 emissions and their role in the development of NO_2 concentrations in a traffic environment. Atmospheric Environment 45, 986–992. https://doi.org/10.1016/j.atmosenv.2010.10.050

Azad, S., Ghandehari, M., 2022. Emissions of nitrogen dioxide in the northeast U.S. during the 2020 COVID-19 lockdown. Journal of Environmental Management 312, 114902. https://doi.org/10.1016/j.jenvman.2022.114902

Balashov, N.V., Thompson, A.M., Piketh, S.J., Langerman, K.E., 2014. Surface ozone variability and trends over the South African Highveld from 1990 to 2007. Journal of Geophysical Research: Atmospheres 119, 4323–4342. https://doi.org/10.1002/2013JD020555

Bergström, A.-K., Jansson, M., 2006. Atmospheric nitrogen deposition has caused nitrogen enrichment and eutrophication of lakes in the northern hemisphere. Global Change Biology 12, 635–643. https://doi.org/10.1111/j.1365-2486.2006.01129.x

Boersma, K.F., Brinksma, E.J., Eskes, H.J., 2004. Error analysis for tropospheric NO2 retrieval from space. Journal of Geophysical Research: Atmospheres 109. https://doi.org/10.1029/2003jd003962

Boersma, K.F., Eskes, H.J., Veefkind, J.P., Brinksma, E.J., van der A, R.J., Sneep, M., van den Oord, G.H.J., Levelt, P.F., Stammes, P., Gleason, J.F., Bucsela, E.J., 2007. Near-real time retrieval of tropospheric NO_2 from OMI. Atmospheric Chemistry and Physics 7, 2103–2118. https://doi.org/10.5194/acp-7-2103-2007

Brewer, A., Mcelroy, C., Kerr, J., 1973. Nitrogen-Dioxide Concentrations in Atmosphere. Nature 246, 129–133. https://doi.org/10.1038/246129a0

Brinksma, E., Pinardi, G., Volten, H., Braak, R., Richter, A., Schönhardt, A., Van Roozendael, M., Fayt, C., Hermans, C., Dirksen, R., Vlemmix, T., Berkhout, S., Swart, D., Oetjen, H., Wittrock, F., Wagner, T., Ibrahim, O., de Leeuw, G., Moerman, M., Levelt, P., 2008. The 2005 and 2006 DANDELIONS NO2 and aerosol intercomparison campaigns. Journal of Geophysical Research-Atmospheres, v.113 (2008) 113. https://doi.org/10.1029/2007JD008808

Burns, J.M., Collins, R.O. (Eds.), 2013. The peoples and states of southern Africa, in: A History of Sub-Saharan Africa. Cambridge University Press, Cambridge, pp. 159–172. https://doi.org/10.1017/CBO9781139795333.013

Burrows, J.P., Weber, M., Buchwitz, M., Rozanov, V., Ladstätter-Weißenmayer, A., Richter, A., DeBeek, R., Hoogen, R., Bramstedt, K., Eichmann, K.-U., Eisinger, M., Perner, D., 1999. The Global Ozone Monitoring Experiment (GOME): Mission Concept and First Scientific Results.

Cede, A., 2021. Manual for Blick Software Suite 1.8 199.

Cede, A., Herman, J., Richter, A., Krotkov, N., Burrows, J., 2006. Measurements of Nitrogen Dioxide total column amounts using a Brewer double spectrophotometer in direct Sun mode. Journal of Geophysical Research: Atmospheres 111. https://doi.org/10.1029/2005JD006585

Cede, A., Tiefengraber, M., Gebetsberger, M., Spinei Lind, E., 2021. Pandonia Global Network Data Products Readme Document (Manual No. 1.8-5).

Celarier, E.A., Brinksma, E.J., Gleason, J.F., Veefkind, J.P., Cede, A., Herman, J.R., Ionov, D., Goutail, F., Pommereau, J.-P., Lambert, J.-C., Roozendael, M. van, Pinardi, G., Wittrock, F., Schönhardt, A., Richter, A., Ibrahim, O.W., Wagner, T., Bojkov, B., Mount, G., Spinei, E., Chen, C.M., Pongetti, T.J., Sander, S.P., Bucsela, E.J., Wenig, M.O., Swart, D.P.J., Volten, H., Kroon, M., Levelt, P.F., 2008. Validation of Ozone Monitoring Instrument nitrogen dioxide columns. Journal of Geophysical Research: Atmospheres 113. https://doi.org/10.1029/2007JD008908

Chameides, W.L., Stedman, D.H., Dickerson, R.R., Rusch, D.W., Cicerone, R.J., 1977. NO_x Production in Lightning.

Choi, S., Joiner, J., Choi, Y., Duncan, B.N., Vasilkov, A., Krotkov, N., Bucsela, E., 2014. First estimates of global free-tropospheric NO_2 abundances derived using a cloud-slicing technique applied to satellite observations from the Aura Ozone Monitoring Instrument (OMI). Atmospheric Chemistry and Physics 14, 10565–10588. https://doi.org/10.5194/acp-14-10565-2014

Choi, S., Lamsal, L.N., Follette-Cook, M., Joiner, J., Krotkov, N.A., Swartz, W.H., Pickering, K.E., Loughner, C.P., Appel, W., Pfister, G., Saide, P.E., Cohen, R.C., Weinheimer, A.J., Herman, J.R., 2020. Assessment of NO_2 observations during DISCOVER-AQ and KORUS-AQ field campaigns. Atmospheric Measurement Techniques 13, 2523–2546. https://doi.org/10.5194/amt-13-2523-2020

Collett, K.S., Piketh, S.J., Ross, K.E., 2010. An assessment of the atmospheric nitrogen budget on the South African Highveld. South African Journal of Science 106, 35–43. https://doi.org/10.4102/sajs.v106i5/6.220

Connors, V., Swap, R., Garstang, M., Piketh, S., Mason, S., 1999. Carbon Monoxide Distributions and Atmospheric Transports over Southern Africa.

Conradie, E.H., Van Zyl, P.G., Pienaar, J.J., Beukes, J.P., Galy-Lacaux, C., Venter, A.D., Mkhatshwa, G.V., 2016. The chemical composition and fluxes of atmospheric wet deposition at four sites in South Africa. Atmos. Environ. 146, 113–131. https://doi.org/10.1016/j.atmosenv.2016.07.033

Cosijn, C., 1996. Stable discontinuities in the atmosphere over South Africa.

Crutzen, P., 1973. A discussion of the chemistry of some minor constituents in the stratosphere and troposphere. PAGEOPH 106, 1385–1399. https://doi.org/10.1007/BF00881092

Crutzen, P.J., 1979. The Role of NO and NO_2 in the Chemistry of the Troposphere and Stratosphere. Annual Review of Earth and Planetary Sciences 7, 443–472. https://doi.org/10.1146/annurev.ea.07.050179.002303

Cui, L., Song, X., Zhong, G., 2021. Comparative Analysis of Three Methods for HYSPLIT Atmospheric Trajectories Clustering. Atmosphere 12, 698. https://doi.org/10.3390/atmos12060698

Davidson, J.A., Cantrell, C.A., McDaniel, A.H., Shetter, R.E., Madronich, S., Calvert, J.G., 1988. Visible-ultraviolet absorption cross sections for NO2 as a function of temperature. Journal of Geophysical Research: Atmospheres 93, 7105–7112. https://doi.org/10.1029/JD093iD06p07105

Davis, T.C., Rutledge, S.A., Fuchs, B.R., 2019. Lightning Location, NO_x Production, and Transport by Anomalous and Normal Polarity Thunderstorms. Journal of Geophysical Research: Atmospheres 124, 8722–8742. https://doi.org/10.1029/2018JD029979

Dickerson, R.R., 1984. Measurements of reactive nitrogen compounds in the free troposphere. Atmospheric Environment (1967) 18, 2585–2593. https://doi.org/10.1016/0004-6981(84)90323-8

Dimitropoulou, E., Hendrick, F., Pinardi, G., Friedrich, M.M., Merlaud, A., Tack, F., De Longueville, H., Fayt, C., Hermans, C., Laffineur, Q., Fierens, F., Van Roozendael, M., 2020. Validation of TROPOMI tropospheric NO_2 columns using dual-scan multi-axis

differential optical absorption spectroscopy (MAX-DOAS) measurements in Uccle, Brussels. Atmospheric Measurement Techniques 13, 5165–5191. https://doi.org/10.5194/amt-13-5165-2020

Duncan, B.N., Lamsal, L.N., Thompson, A.M., Yoshida, Y., Lu, Z., Streets, D.G., Hurwitz, M.M., Pickering, K.E., 2016. A space-based, high-resolution view of notable changes in urban NO_x pollution around the world (2005–2014). Journal of Geophysical Research: Atmospheres 121, 976–996. https://doi.org/10.1002/2015JD024121

Eskes, H.J., Eichmann, K.-U., 2023. S5P Mission Performance Centre Nitrogen Dioxide Readme (Report S5P-MPC-KNMI-PRF-NO2 No. version 2.5).

Eskes, H.J., van Geffen, J.H.G.M., Boersma, K.F., Eichmann, K.-U., Pedergnana, M., Sneep, M., Veefkind, J.P., Loyola, D., 2023. S5P/TROPOMI Level-2 Product User Manual Nitrogen Dioxide.

Freiman, M.T., Piketh, S.J., 2003. Air Transport into and out of the Industrial Highveld Region of South Africa. Journal of Applied Meteorology and Climatology 42, 994–1002. https://doi.org/10.1175/1520-0450(2003)042<0994:ATIAOO>2.0.CO;2

Fuglestvedt, J.S., Berntsen, T.K., Isaksen, I.S.A., Mao, H., Liang, X.-Z., Wang, W.-C., 1999. Climatic forcing of nitrogen oxides through changes in tropospheric ozone and methane; global 3D model studies. Atmospheric Environment 33, 961–977. https://doi.org/10.1016/S1352-2310(98)00217-9

Galloway, J.N., Aber, J.D., Erisman, J.W., Seitzinger, S.P., Howarth, R.W., Cowling, E.B., Cosby, B.J., 2003. The Nitrogen Cascade. BioScience 53, 341.

Galloway, J.N., Dentener, F.J., Capone, D.G., Boyer, E.W., Howarth, R.W., Seitzinger, S.P., Asner, G.P., Cleveland, C.C., Green, P.A., Holland, E.A., 2004. Nitrogen Cycles: Past, Present, and Future. Biogeochemistry 70, 153.

Galy-Lacaux, C., Delon, C., Solmon, F., Adon, M., Yoboué, V., Mphepya, J., Pienaar, J.J., Diop, B., Sigha, L., Dungall, L., 2014. Dry and Wet Atmospheric Nitrogen Deposition in West Central Africa, in: Nitrogen Deposition, Critical Loads and Biodiversity. Springer, pp. 83–91.

Grange, S., 2014. Technical note: Averaging wind speeds and directions. https://doi.org/10.13140/RG.2.1.3349.2006

Griffin, D., Zhao, X., McLinden, C.A., Boersma, F., Bourassa, A., Dammers, E., Degenstein, D., Eskes, H., Fehr, L., Fioletov, V., Hayden, K., Kharol, S.K., Li, S.-M., Makar, P., Martin, R.V., Mihele, C., Mittermeier, R.L., Krotkov, N., Sneep, M., Lamsal, L.N., Linden, M. ter, Geffen, J. van, Veefkind, P., Wolde, M., 2019. High-Resolution Mapping of Nitrogen Dioxide With TROPOMI: First Results and Validation Over the Canadian Oil Sands. Geophysical Research Letters 46, 1049–1060. https://doi.org/10.1029/2018GL081095

Griffing, G.W., 1977. Ozone and oxides of nitrogen production during thunderstorms. Journal of Geophysical Research 82, 943–950. https://doi.org/10.1029/JC082i006p00943

Guicherit, R., 1972. Indirect determination of nitrogen oxides by a chemiluminescence technique. Atmospheric Environment (1967) 6, 807–814. https://doi.org/10.1016/0004-6981(72)90053-4

Guo, L., Chen, J., Luo, D., Liu, S., Lee, H.J., Motallebi, N., Fong, A., Deng, J., Rasool, Q.Z., Avise, J.C., Kuwayama, T., Croes, B.E., FitzGibbon, M., 2020. Assessment of Nitrogen Oxide Emissions and San Joaquin Valley PM2.5 Impacts From Soils in California. Journal of Geophysical Research: Atmospheres 125, e2020JD033304. https://doi.org/10.1029/2020JD033304

Guo, X., Zhang, Z., Cai, Z., Wang, L., Gu, Z., Xu, Y., Zhao, J., 2022. Analysis of the Spatial-Temporal Distribution Characteristics of NO2 and Their Influencing Factors in the Yangtze River Delta Based on Sentinel-5P Satellite Data. Atmosphere 13, 1923. https://doi.org/10.3390/atmos13111923

Haagen-Smit, A.J., 1964. The Control of Air Pollution. Scientific American 210, 24–31.

Harlass, T., Dischl, R., Kaufmann, S., Märkl, R., Sauer, D., Scheibe, M., Stock, P., Bräuer, T., Dörnbrack, A., Roiger, A., Schlager, H., Schumann, U., Pühl, M., Schripp, T., Grein, T., Bondorf, L., Renard, C., Gauthier, M., Johnson, M., Luff, D., Madden, P., Swann, P., Ahrens, D., Sallinen, R., Voigt, C., 2024. Measurement report: In-flight and ground-based measurements of nitrogen oxide emissions from latest-generation jet engines and

sustainable aviation fuel. Atmospheric Chemistry and Physics 24, 11807–11822. https://doi.org/10.5194/acp-24-11807-2024

Harris, G.W., Winer, A.M., Pitts, J.N., Platt, U., Perner, D., 1983. Measurements of HONO, NO_3, and NO_2 by Long-Path Differential Optical Absorption Spectroscopy in the Los Angeles Basin, in: Killinger, D.K., Mooradian, A. (Eds.), Optical and Laser Remote Sensing. Springer, Berlin, Heidelberg, pp. 106–113. https://doi.org/10.1007/978-3-540-39552-2_14

Heland, J., Schlager, H., Richter, A., Burrows, J.P., 2002. First comparison of tropospheric NO_2 column densities retrieved from GOME measurements and in situ aircraft profile measurements. Geophysical Research Letters 29, 44-1-44–4. https://doi.org/10.1029/2002GL015528

Held, G., 1996. Air pollution and its impacts on South African highveld. Environmental Scientific Association.

Herman, J., Cede, A., Spinei, E., Mount, G., Tzortziou, M., Abuhassan, N., 2009. NO_2 column amounts from ground-based Pandora and MFDOAS spectrometers using the direct-sun DOAS technique: Intercomparisons and application to OMI validation. Journal of Geophysical Research: Atmospheres 114. https://doi.org/10.1029/2009JD011848

Hilboll, A., Richter, A., Burrows, J.P., 2013. Long-term changes of tropospheric NO_2 over megacities derived from multiple satellite instruments. Atmospheric Chemistry and Physics 13, 4145–4169. https://doi.org/10.5194/acp-13-4145-2013

Hönninger, G., Platt, U., 2002. Observations of BrO and its vertical distribution during surface ozone depletion at Alert. Atmospheric Environment, Air/Snow/Ice Interactions in the Arctic: Results from ALERT 2000 and SUMMIT 2000 36, 2481–2489. https://doi.org/10.1016/S1352-2310(02)00104-8

Hönninger, G., von Friedeburg, C., Platt, U., 2004. Multi axis differential optical absorption spectroscopy (MAX-DOAS). Atmospheric Chemistry and Physics 4, 231–254. https://doi.org/10.5194/acp-4-231-2004

Ibebuchi, C.C., 2021. Circulation pattern controls of wet days and dry days in Free State, South Africa. Meteorol Atmos Phys 133, 1469–1480. https://doi.org/10.1007/s00703-021-00822-0

Igbafe, A.I., Jewell, L.L., Piketh, S.J., Dlamini, T.S., 2015. A Wintertime Impact of Dilution on Transformation Rate in the Planetary Boundary Layer. Journal of Environmental Informatics 8, 34-48–48.

Ionov, D.V., Timofeev, Yu.M., 2009. Regional space monitoring of nitrogen dioxide in the troposphere. Izvestiya - Atmospheric and Ocean Physics 45, 434–443. https://doi.org/10.1134/S0001433809040045

Ito, A., Nishina, K., Ishijima, K., Hashimoto, S., Inatomi, M., 2018. Emissions of Nitrous Oxide (N_2O) from soil surfaces and their historical changes in East Asia: a model-based assessment. Progress in Earth and Planetary Science 5, 55. https://doi.org/10.1186/s40645-018-0215-4

Jacob, D.J., Winner, D.A., 2009. Effect of climate change on air quality. Atmospheric Environment, Atmospheric Environment - Fifty Years of Endeavour 43, 51–63. https://doi.org/10.1016/j.atmosenv.2008.09.051

Jaworski, N.A., Howarth, R.W., Hetling, L.J., 1997. Atmospheric deposition of nitrogen oxides onto the landscape contributes to coastal eutrophication in the Northeast United States. Environmental Science and Technology 31, 1995–2004. https://doi.org/10.1021/es960803f

Josipovic, M., Annegarn, H.J., Kneen, M.A., Pienaar, J.J., Piketh, S.J., 2010. Concentrations, distributions and critical level exceedance assessment of SO_2, NO_2 and O_3 in South Africa. Environmental Monitoring and Assessment 171, 181–196. https://doi.org/10.1007/s10661-009-1270-5

Judd, L.M., Al-Saadi, J.A., Szykman, J.J., Valin, L.C., Janz, S.J., Kowalewski, M.G., Eskes, H.J., Veefkind, J.P., Cede, A., Mueller, M., Gebetsberger, M., Swap, R., Pierce, R.B., Nowlan, C.R., Abad, G.G., Nehrir, A., Williams, D., 2020. Evaluating Sentinel-5P

TROPOMI tropospheric NO_2 column densities with airborne and Pandora spectrometers near New York City and Long Island Sound. Atmospheric Measurement Techniques 13, 6113–6140. https://doi.org/10.5194/amt-13-6113-2020

Kalbarczyk, R., Kalbarczyk, E., 2020. Meteorological conditions of the winter-time distribution of nitrogen oxides in Poznań: A proposal for a catalog of the pollutants variation. Urban Climate 33. https://doi.org/10.1016/j.uclim.2020.100649

Keegan, T., 1983. The sharecropping economy on the South African Highveld in the early twentieth century. The Journal of Peasant Studies 10, 201–226. https://doi.org/10.1080/03066158308438205

Kerr, G.H., Goldberg, D.L., Anenberg, S.C., 2021. COVID-19 pandemic reveals persistent disparities in nitrogen dioxide pollution. Proceedings of the National Academy of Sciences 118, e2022409118. https://doi.org/10.1073/pnas.2022409118

Khodayari, A., Vitt, F., Phoenix, D., Wuebbles, D.J., 2018. The impact of NO_x emissions from lightning on the production of aviation-induced ozone. Atmospheric Environment 187, 410–416. https://doi.org/10.1016/j.atmosenv.2018.05.057

Köhler, M.O., Wild, O., Rogers, H.L., Pyle, J.A., Dessens, O., Shine, K.P., Rädel, G., 2008. Impact of perturbations to nitrogen oxide emissions from global aviation. Journal of Geophysical Research: Atmospheres 113. https://doi.org/10.1029/2007jd009140

Kollonige, D.E., Thompson, A.M., Josipovic, M., Tzortziou, M., Beukes, J.P., Burger, R., Martins, D.K., van Zyl, P.G., Vakkari, V., Laakso, L., 2018. OMI Satellite and Ground-Based Pandora Observations and Their Application to Surface NO_2 Estimations at Terrestrial and Marine Sites. Journal of Geophysical Research: Atmospheres 123, 1441–1459. https://doi.org/10.1002/2017JD026518

Laakso, L., Vakkari, V., Virkkula, A., Laakso, H., Backman, J., Kulmala, M., Beukes, J.P., van Zyl, P.G., Tiitta, P., Josipovic, M., Pienaar, J.J., Chiloane, K., Gilardoni, S., Vignati, E., Wiedensohler, A., Tuch, T., Birmili, W., Piketh, S., Collett, K., Fourie, G.D., Komppula, M., Lihavainen, H., de Leeuw, G., Kerminen, V.-M., 2012. South African EUCAARI measurements: seasonal variation of trace gases and aerosol optical properties.

Atmospheric Chemistry and Physics 12, 1847–1864. https://doi.org/10.5194/acp-12-1847-2012

Lange, K., Richter, A., Burrows, J.P., 2022. Variability of nitrogen oxide emission fluxes and lifetimes estimated from Sentinel-5P TROPOMI observations. Atmospheric Chemistry and Physics 22, 2745–2767. https://doi.org/10.5194/acp-22-2745-2022

Lazar, G., Capatina, C., Simonescu, C.M., 2014. Analysis of Nitrogen Oxides levels measured in Turceni area. Revista de Chimie 65, 1260–1265.

Lee, H., Kim, Y.J., Lee, C., 2009. Estimation of the rate of increase in nitrogen dioxide concentrations from power plant stacks using an imaging-DOAS. Environmental Monitoring and Assessment 152, 61–70. https://doi.org/10.1007/s10661-008-0296-4

Leser, H., Hönninger, G., Platt, U., 2003. MAX-DOAS measurements of BrO and NO_2 in the marine boundary layer. Geophysical Research Letters 30. https://doi.org/10.1029/2002GL015811

Levelt, P.F., Joiner, J., Tamminen, J., Veefkind, J.P., Bhartia, P.K., Stein Zweers, D.C., Duncan, B.N., Streets, D.G., Eskes, H., van der A, R., McLinden, C., Fioletov, V., Carn, S., de Laat, J., DeLand, M., Marchenko, S., McPeters, R., Ziemke, J., Fu, D., Liu, X., Pickering, K., Apituley, A., González Abad, G., Arola, A., Boersma, F., Chan Miller, C., Chance, K., de Graaf, M., Hakkarainen, J., Hassinen, S., Ialongo, I., Kleipool, Q., Krotkov, N., Li, C., Lamsal, L., Newman, P., Nowlan, C., Suleiman, R., Tilstra, L.G., Torres, O., Wang, H., Wargan, K., 2018. The Ozone Monitoring Instrument: overview of 14 years in space. Atmospheric Chemistry and Physics 18, 5699–5745. https://doi.org/10.5194/acp-18-5699-2018

Levelt, P.F., Van Den Oord, G.H.J., Dobber, M.R., Mälkki, A., Visser, H., De Vries, J., Stammes, P., Lundell, J.O.V., Saari, H., 2006. The ozone monitoring instrument. IEEE Transactions on Geoscience and Remote Sensing 44, 1093–1100. https://doi.org/10.1109/TGRS.2006.872333

Levy, H., 1972. Photochemistry of the lower troposphere. Planetary and Space Science 20, 919–935. https://doi.org/10.1016/0032-0633(72)90177-8

Likens, G.E., Bormann, F.H., Pierce, R.S., Eaton, J.S., Johnson, N.M., 1977. Biogeochemistry of a Forested Ecosystem. Springer US, New York, NY. https://doi.org/10.1007/978-1-4615-9993-7

Liu, C., Beirle, S., Butler, T., Hoor, P., Frankenberg, C., Jöckel, P., Penning de Vries, M., Platt, U., Pozzer, A., Lawrence, M.G., Lelieveld, J., Tost, H., Wagner, T., 2014. Profile information on CO from SCIAMACHY observations using cloud slicing and comparison with model simulations. Atmospheric Chemistry and Physics 14, 1717–1732. https://doi.org/10.5194/acp-14-1717-2014

Logan, J., Prather, M., Wofsy, S., McElroy, M., 1981. Tropospheric chemistry: A global perspective. Journal of Geophysical Research 86. https://doi.org/10.1029/JC086iC08p07210

Logan, J.A., 1983. Nitrogen oxides in the troposphere: Global and regional budgets. Journal of Geophysical Research: Oceans 88, 10785–10807. https://doi.org/10.1029/JC088iC15p10785

Lourens, A.S. M., Butler, T.M., Beukes, J.P., van Zyl, P.G., Beirle, S., Wagner, T.K., Heue, K.-P., Pienaar, J.J., Fourie, G.D., Lawrence, M.G., 2012. Re-evaluating the NO_2 hotspot over the South African Highveld. South African Journal of Science 108, 83–91.

Lourens, A.S., Beukes, J.P., Van Zyl, P.G., Fourie, G.D., Burger, J.W., Pienaar, J.J., Read, C.E., Jordaan, J.H., 2011. Spatial and temporal assessment of gaseous pollutants in the highveld of South Africa. South African Journal of Science 107. https://doi.org/10.4102/sajs.v107i1/2.269

Lynch, J., Cain, M., Frame, D., Pierrehumbert, R., 2021. Agriculture's Contribution to Climate Change and Role in Mitigation Is Distinct From Predominantly Fossil CO_2-Emitting Sectors. Frontiers in Sustainable Food Systems 4.

Manahan, Stanley.E., 2010. Environmental Chemistry, 9th ed. CRC Press.

Marais, E.A., Jacob, D.J., Choi, S., Joiner, J., Belmonte-Rivas, M., Cohen, R.C., Beirle, S., Murray, L.T., Schiferl, L.D., Shah, V., Jaeglé, L., 2018. Nitrogen oxides in the global upper troposphere: Interpreting cloud-sliced NO_2 observations from the OMI satellite

instrument. Atmospheric Chemistry and Physics 18, 17017–17027. https://doi.org/10.5194/acp-18-17017-2018

Maregele, B., 2014. The environmental legacy of mining on the Mpumalanga Highveld [WWW Document]. Centre for Environmental Rights. URL https://cer.org.za/news/the-environmental-legacy-of-mining-on-the-mpumalanga-highveld (accessed 10.30.22).

Martins, J.J., Dhammapala, R.S., Lachmann, G., Galy-Lacaux, C., Pienaar, J.J., 2007. Long-term measurements of sulphur dioxide, nitrogen dioxide, ammonia, nitric acid and ozone in southern Africa using passive samplers. South African Journal of Science 103, 336–342.

Matandirotya, N.R., Burger, R., 2022. An assessment of NO2 atmospheric air pollution over three cities in South Africa during 2020 COVID-19 pandemic. Air Qual Atmos Health 1–14. https://doi.org/10.1007/s11869-022-01271-3

Matandirotya, N.R., Burger, R.P., 2021. Spatiotemporal variability of tropospheric NO2 over four megacities in Southern Africa: Implications for transboundary regional air pollution. Environmental Challenges 5, 100271. https://doi.org/10.1016/j.envc.2021.100271

Maull, H.W., 1986. South Africa's Minerals: The Achilles Heel of Western Economic Security? International Affairs (Royal Institute of International Affairs 1944-) 62, 619–626. https://doi.org/10.2307/2618555

McGill, M.J., Swap, R.J., Yorks, J.E., Selmer, P.A., Piketh, S.J., 2020. Observation and quantification of aerosol outflow from southern Africa using spaceborne lidar. South African Journal of Science 116. https://doi.org/10.17159/sajs.2020/6398

Molina, M.J., Molina, L.T., 2004. Megacities and Atmospheric Pollution. Journal of the Air & Waste Management Association.

Moller, S.J., Lee, J.D., Commane, R., Edwards, P., Heard, D.E., Hopkins, J., Ingham, T., Mahajan, A.S., Oetjen, H., Plane, J., Roscoe, H., Lewis, A.C., Carpenter, L.J., 2010. Measurements of nitrogen oxides from Hudson Bay: Implications for NOx release from snow and ice covered surfaces. Atmospheric Environment 44, 2971–2979. https://doi.org/10.1016/j.atmosenv.2010.05.015

Mucina, L., Rutherford, M.C., 2006. The Vegetation of South Africa, Lesotho and Swaziland. South African National Biodiversity Institute.

Noxon, J.F., 1975. Nitrogen Dioxide in the Stratosphere and Troposphere Measured by Ground-Based Absorption Spectroscopy. Science 189, 547–549. https://doi.org/10.1126/science.189.4202.547

Ojelede, M.E., Annegarn, H.J., Price, C., Kneen, M.A., Goyns, P., 2008. Lightning-produced NO_x budget over the Highveld region of South Africa. Atmospheric Environment 42. https://doi.org/10.1016/j.atmosenv.2007.12.072

Piketh, S., Walton, N.M., 2004. Characteristics of Atmospheric Transport of Air Pollution for Africa. URL https://www.semanticscholar.org/paper/Characteristics-of-Atmospheric-Transport-of-Air-for-Piketh-Walton/9a03a92cc327858504f6d0d5966600b2aab638cc (accessed 1.22.24).

Pinardi, G., Hendrick, F., Clemer, K., Lambert, J.-C., Bai, J., Roozendael, M.V., 2008. On the use of the maxdoas technique for the validation of tropospheric NO2 column measurements from satellite. Presented at the EUMETSAT.

Pinardi, G., Van Roozendael, M., Hendrick, F., Theys, N., Abuhassan, N., Bais, A., Boersma, F., Cede, A., Chong, J., Donner, S., Drosoglou, T., Dzhola, A., Eskes, H., Frieß, U., Granville, J., Herman, J.R., Holla, R., Hovila, J., Irie, H., Kanaya, Y., Karagkiozidis, D., Kouremeti, N., Lambert, J.-C., Ma, J., Peters, E., Piters, A., Postylyakov, O., Richter, A., Remmers, J., Takashima, H., Tiefengraber, M., Valks, P., Vlemmix, T., Wagner, T., Wittrock, F., 2020. Validation of tropospheric NO_2 column measurements of GOME-2A and OMI using MAX-DOAS and direct sun network observations. Atmospheric Measurement Techniques 13, 6141–6174. https://doi.org/10.5194/amt-13-6141-2020

Platt, U., 1994. Differential optical absorption spectroscopy (DOAS), in: Air Monitoring by Spectroscopic Techniques. John Wiley & Sons, New York, pp. 27–84.

Platt, U., Perner, D., 1983. Measurements of Atmospheric Trace Gases by Long Path Differential UV/Visible Absorption Spectroscopy, in: Killinger, D.K., Mooradian, A. (Eds.),

Optical and Laser Remote Sensing. Springer, Berlin, Heidelberg, pp. 97–105. https://doi.org/10.1007/978-3-540-39552-2_13

Platt, U., Perner, D., Pätz, H.W., 1979. Simultaneous measurement of atmospheric CH_2O, O_3, and NO_2 by differential optical absorption. Journal of Geophysical Research: Oceans 84, 6329–6335. https://doi.org/10.1029/JC084iC10p06329

Prunet, P., Lezeaux, O., Camy-Peyret, C., Thevenon, H., 2020. Analysis of the NO_2 tropospheric product from S5P TROPOMI for monitoring pollution at city scale. City and Environment Interactions 8, 100051. https://doi.org/10.1016/j.cacint.2020.100051

Reidl-Leuthner, C., Ofner, J., Tomischko, W., Lohninger, H., Lendl, B., 2015. Simultaneous open-path determination of road side mono-nitrogen oxides employing mid-IR laser spectroscopy. Atmospheric Environment 112, 189–195. https://doi.org/10.1016/j.atmosenv.2015.04.010

Rogerson, C.M., 1996. Urban poverty and the informal economy in South Africa's economic heartland. Environment and Urbanization 8, 167–179. https://doi.org/10.1177/095624789600800115

Rolph, G., Stein, A., Stunder, B., 2017. Real-time Environmental Applications and Display sYstem: READY. Environmental Modelling & Software 95, 210–228. https://doi.org/10.1016/j.envsoft.2017.06.025

Rorich, R.P., Galpin, J.S., 1998. Air quality in the Mpumalanga Highveld region, South Africa 94.

Roscoe, H.K., Van Roozendael, M., Fayt, C., du Piesanie, A., Abuhassan, N., Adams, C., Akrami, M., Cede, A., Chong, J., Clémer, K., Friess, U., Gil Ojeda, M., Goutail, F., Graves, R., Griesfeller, A., Grossmann, K., Hemerijckx, G., Hendrick, F., Herman, J., Hermans, C., Irie, H., Johnston, P.V., Kanaya, Y., Kreher, K., Leigh, R., Merlaud, A., Mount, G.H., Navarro, M., Oetjen, H., Pazmino, A., Perez-Camacho, M., Peters, E., Pinardi, G., Puentedura, O., Richter, A., Schönhardt, A., Shaiganfar, R., Spinei, E., Strong, K., Takashima, H., Vlemmix, T., Vrekoussis, M., Wagner, T., Wittrock, F., Yela, M., Yilmaz, S., Boersma, F., Hains, J., Kroon, M., Piters, A., Kim, Y.J., 2010. Intercomparison of slant column measurements of NO_2 and O_4 by MAX-DOAS and

zenith-sky UV and visible spectrometers. Atmospheric Measurement Techniques 3, 1629–1646. https://doi.org/10.5194/amt-3-1629-2010

Ross, K., Broccardo, S., Heue, K.P., Ferguson, K., Piketh, S., 2007. Nitrogen Oxides on the South African Highveld. Clean Air Journal 16. https://doi.org/10.17159/caj/2007/16/2.7166

Saueprasearsit, P., Khummongkol, P., 2009. Evaluation of SO_2 dry deposition over a cassava plantation in Rayong, Thailand. International Journal of Environment and Pollution 36, 255–261. https://doi.org/10.1504/ijep.2009.021830

Schaub, D., Boersma, K.F., Kaiser, J.W., Weiss, A.K., Folini, D., Eskes, H.J., Buchmann, B., 2006. Comparison of GOME tropospheric NO_2 columns with NO_2 profiles deduced from ground-based in situ measurements. Atmospheric Chemistry and Physics 6, 3211–3229. https://doi.org/10.5194/acp-6-3211-2006

Seinfeld, J.H., 1986. ES&T Books: Atmospheric Chemistry and Physics of Air Pollution. Environ. Sci. Technol. 20, 863–863. https://doi.org/10.1021/es00151a602

Seinfeld, J.H., Pandis, S.N., 2016. Atmospheric Chemistry and Physics: From Air Pollution to Climate Change. John Wiley & Sons.

Seinfeld, J.H., Pandis, S.N., Noone, K., 1998. Atmospheric Chemistry and Physics: From Air Pollution to Climate Change. Physics Today 51, 88–90. https://doi.org/10.1063/1.882420

Shah, V., Jacob, D.J., Dang, R., Lamsal, L.N., Strode, S.A., Steenrod, S.D., Boersma, K.F., Eastham, S.D., Fritz, T.M., Thompson, C., Peischl, J., Bourgeois, I., Pollack, I.B., Nault, B.A., Cohen, R.C., Campuzano-Jost, P., Jimenez, J.L., Andersen, S.T., Carpenter, L.J., Sherwen, T., Evans, M.J., 2023. Nitrogen oxides in the free troposphere: implications for tropospheric oxidants and the interpretation of satellite NO_2 measurements. Atmospheric Chemistry and Physics 23, 1227–1257. https://doi.org/10.5194/acp-23-1227-2023

Shah, V., Jacob, D.J., Li, K., Silvern, R.F., Zhai, S., Liu, M., Lin, J., Zhang, Q., 2020. Effect of changing NOx lifetime on the seasonality and long-term trends of satellite-observed

tropospheric NO_2 columns over China. Atmospheric Chemistry and Physics 20, 1483–1495. https://doi.org/10.5194/acp-20-1483-2020

Shaw, S., Van Heyst, B., 2022. Nitrogen Oxide (NOx) emissions as an indicator for sustainability. Environmental and Sustainability Indicators 15, 100188. https://doi.org/10.1016/j.indic.2022.100188.

Shikwambana, L., Mhangara, P., Mbatha, N., 2020. Trend analysis and first time observations of sulphur dioxide and nitrogen dioxide in South Africa using TROPOMI/Sentinel-5 P data. International Journal of Applied Earth Observation and Geoinformation 91, 102130. https://doi.org/10.1016/j.jag.2020.102130

Shon, Z.-H., Kim, K.-H., Song, S.-K., 2011. Long-term trend in NO_2 and NO_x levels and their emission ratio in relation to road traffic activities in East Asia. Atmospheric Environment 45, 3120–3131. https://doi.org/10.1016/j.atmosenv.2011.03.009

Sillman, S., 1999. The relation between ozone, NOx and hydrocarbons in urban and polluted rural environments. Atmospheric Environment 33, 1821–1845. https://doi.org/10.1016/S1352-2310(98)00345-8

Smith, R.A., 1872. Air and rain : the beginnings of a chemical climatology / by Robert Angus Smith. Longmans, Green and Co., London.

Solomon, S., Portmann, R.W., Sanders, R.W., Daniel, J.S., Madsen, W., Bartram, B., Dutton, E.G., 1999. On the role of nitrogen dioxide in the absorption of solar radiation. Journal of Geophysical Research: Atmospheres 104, 12047–12058. https://doi.org/10.1029/1999JD900035

Solomon, S., Schmeltekopf, A.L., Sanders, R.W., 1987. On the interpretation of zenith sky absorption measurements. Journal of Geophysical Research: Atmospheres 92, 8311–8319. https://doi.org/10.1029/JD092iD07p08311

Stein, A.F., Draxler, R.R., Rolph, G.D., Stunder, B.J.B., Cohen, M.D., Ngan, F., 2015. NOAA'S HYSPLIT ATMOSPHERIC TRANSPORT AND DISPERSION MODELING SYSTEM. Bulletin of the American Meteorological Society 96, 2059–2078.

Steinbacher, M., Zellweger, C., Schwarzenbach, B., Bugmann, S., Buchmann, B., Ordóñez, C., Prevot, A.S.H., Hueglin, C., 2007. Nitrogen oxide measurements at rural sites in Switzer-land: Bias of conventional measurement techniques. Journal of Geophysical Research: At-mospheres 112. https://doi.org/10.1029/2006JD007971

Sturman, A.P., Tyson, P.D., D'Abreton, P.C., 1997. A preliminary study of the transport of air from Africa and Australia to New Zealand. Journal of the Royal Society of New Zea-land 27, 485–498. https://doi.org/10.1080/03014223.1997.9517550

Tyson, P.D., 1969. Towards a regional model of local topographically induced wind systems in Natal. South African Journal of Science 65, 201. https://doi.org/10.10520/AJA00382353_3816

Tyson, P.D., 1997. Atmospheric transport of aerosols and trace gases over southern Africa. Progress in Physical Geography: Earth and Environment 21, 79–101. https://doi.org/10.1177/030913339702100105

Tyson, P.D., Garstang, M., Swap, R., 1996. Large-Scale Recirculation of Air over Southern Africa. Journal of Applied Meteorology (1988-2005) 35, 2218–2236.

Tyson, P.D., Preston-Whyte, R.A., 2000. The Weather and Climate of Southern Africa, second edition. ed. Oxford University Press Southern Africa.

van Geffen, J., Eskes, H., Compernolle, S., Pinardi, G., Verhoelst, T., Lambert, J.-C., Sneep, M., ter Linden, M., Ludewig, A., Boersma, K.F., Veefkind, J.P., 2022. Sentinel-5P TROPOMI NO2 retrieval: impact of version v2.2 improvements and comparisons with OMI and ground-based data. Atmospheric Measurement Techniques 15, 2037–2060. https://doi.org/10.5194/amt-15-2037-2022

Veefkind, J.P., Aben, I., McMullan, K., Förster, H., de Vries, J., Otter, G., Claas, J., Eskes, H.J., de Haan, J.F., Kleipool, Q., van Weele, M., Hasekamp, O., Hoogeveen, R., Land-graf, J., Snel, R., Tol, P., Ingmann, P., Voors, R., Kruizinga, B., Vink, R., Visser, H., Levelt, P.F., 2012. TROPOMI on the ESA Sentinel-5 Precursor: A GMES mission for global observations of the atmospheric composition for climate, air quality and ozone layer applications. Remote Sensing of Environment, The Sentinel Missions - New Op-portunities for Science 120, 70–83. https://doi.org/10.1016/j.rse.2011.09.027

Verhoelst, T., Compernolle, S., Pinardi, G., Lambert, J.-C., Eskes, H.J., Eichmann, K.-U., Fjæraa, A.M., Granville, J., Niemeijer, S., Cede, A., Tiefengraber, M., Hendrick, F., Pazmiño, A., Bais, A., Bazureau, A., Boersma, K.F., Bognar, K., Dehn, A., Donner, S., Elokhov, A., Gebetsberger, M., Goutail, F., Grutter de la Mora, M., Gruzdev, A., Gratsea, M., Hansen, G.H., Irie, H., Jepsen, N., Kanaya, Y., Karagkiozidis, D., Kivi, R., Kreher, K., Levelt, P.F., Liu, C., Müller, M., Navarro Comas, M., Piters, A.J.M., Pommereau, J.-P., Portafaix, T., Prados-Roman, C., Puentedura, O., Querel, R., Remmers, J., Richter, A., Rimmer, J., Rivera Cárdenas, C., Saavedra de Miguel, L., Sinyakov, V.P., Stremme, W., Strong, K., Van Roozendael, M., Veefkind, J.P., Wagner, T., Wittrock, F., Yela González, M., Zehner, C., 2021. Ground-based validation of the Copernicus Sentinel-5P TROPOMI NO_2 measurements with the NDACC ZSL-DOAS, MAX-DOAS and Pandonia global networks. Atmospheric Measurement Techniques 14, 481–510. https://doi.org/10.5194/amt-14-481-2021

Vlemmix, T., Piters, A.J.M., Stammes, P., Wang, P., Levelt, P.F., 2010. Retrieval of tropospheric NO₂ using the MAX-DOAS method combined with relative intensity measurements for aerosol correction. Atmos. Meas. Tech. 3, 1287–1305. https://doi.org/10.5194/amt-3-1287-2010

Weiss, R.F., Craig, H., 1976. Production of atmospheric nitrous oxide by combustion. Geophysical Research Letters 3, 751–753. https://doi.org/10.1029/GL003i012p00751

Wenig, M., Spichtinger, N., Stohl, A., Held, G., Beirle, S., Wagner, T., Jähne, B., Platt, U., 2003. Intercontinental transport of nitrogen oxide pollution plumes. Atmospheric Chemistry and Physics 3, 387–393. https://doi.org/10.5194/acp-3-387-2003

West, J.J., Fiore, A.M., Horowitz, L.W., Naik, V., 2009. Effect of regional precursor emission controls on long-range ozone transport – Part 1: Short-term changes in ozone air quality. Atmospheric Chemistry and Physics 9. https://doi.org/10.5194/acp-9-6077-2009

Whiteman, C.D., 1990. Observations of Thermally Developed Wind Systems in Mountainous Terrain, in: Banta, R.M., Berri, G., Blumen, W., Carruthers, D.J., Dalu, G.A., Durran, D.R., Egger, J., Garratt, J.R., Hanna, S.R., Hunt, J.C.R., Meroney, R.N., Miller, W., Neff, W.D., Nicolini, M., Paegle, J., Pielke, R.A., Smith, R.B., Strimaitis, D.G.,

Vukicevic, T., Whiteman, C.D., Blumen, W. (Eds.), Atmospheric Processes over Complex Terrain. American Meteorological Society, Boston, MA, pp. 5–42. https://doi.org/10.1007/978-1-935704-25-6_2

Whiteman, C.D., Bian, X., Zhong, S., 1999. Wintertime Evolution of the Temperature Inversion in the Colorado Plateau Basin. Journal of Applied Meteorology 38. https://doi.org/10.1175/1520-0450(1999)038<1103:weotti>2.0.co;2

WHO, 2003. Health aspects of air pollution with particulate matter, ozone and nitrogen dioxide : report on a WHO working group, Bonn, Germany 13-15 January 2003 (No. EUR/03/5042688). WHO Regional Office for Europe, Copenhagen.

Williams, J.E., Boersma, K.F., Le Sager, P., Verstraeten, W.W., 2017. The high-resolution version of TM5-MP for optimized satellite retrievals: description and validation. Geoscientific Model Development 10, 721–750. https://doi.org/10.5194/gmd-10-721-2017

Wright, C.Y., Oosthuizen, R., John, J., Garland, R.M., Albers, P., Pauw, C., 2011. Air Quality and Human Health among a Low Income Community in the Highveld Priority Area. Clean Air Journal 20. https://doi.org/10.17159/caj/2011/20/1.7180

Yang, J., Kang, S., Ji, Z., Yin, X., Tripathee, L., 2020. Investigating air pollutant concentrations, impact factors, and emission control strategies in western China by using a regional climate-chemistry model. Chemosphere 246. https://doi.org/10.1016/j.chemosphere.2019.125767

Zeldovich, Y., 1947. Oxidation of Nitrogen in Combustion. Publishing House of the Academy of Sciences of USSR.

Zhang, C., Liu, C., Chan, K.L., Hu, Q., Liu, H., Li, B., Xing, C., Tan, W., Zhou, H., Si, F., Liu, J., 2020. First observation of tropospheric nitrogen dioxide from the Environmental Trace Gases Monitoring Instrument onboard the GaoFen-5 satellite. Light: Science and Applications 9. https://doi.org/10.1038/s41377-020-0306-z

Zhang, Q., Streets, D.G., He, K., Wang, Y., Richter, A., Burrows, J.P., Uno, I., Jang, C.J., Chen, D., Yao, Z., Lei, Y., 2007. NO_x emission trends for China, 1995–2004: The view from the ground and the view from space. Journal of Geophysical Research: Atmospheres 112. https://doi.org/10.1029/2007JD008684

Zhao, X., Griffin, D., Fioletov, V., McLinden, C., Cede, A., Tiefengraber, M., Müller, M., Bognar, K., Strong, K., Boersma, F., Eskes, H., Davies, J., Ogyu, A., Lee, S.C., 2020. Assessment of the quality of TROPOMI high-spatial-resolution NO_2 data products in the Greater Toronto Area. Atmospheric Measurement Techniques 13, 2131–2159. https://doi.org/10.5194/amt-13-2131-2020